



A11103 520627

NIST
PUBLICATIONS

NISTIR 5752

**SUMMARY REPORT:
Second Workshop on Industrial
Applications of Scanned Probe
Microscopy**

**A Workshop co-sponsored by
NIST, SEMATECH, ASTM E42.14,
and the American Vacuum Society**

**held at
NIST
Gaithersburg, MD 20899**

**on
May 2 - 3, 1995**

Report prepared by:

J. A. Dagata
National Institute of Standards
and Technology

A. C. Diebold
SEMATECH

C. K. Shih
University of Texas-Austin

R. J. Colton
Naval Research Laboratory

U.S. DEPARTMENT OF COMMERCE
Technology Administration
National Institute of Standards
and Technology
Manufacturing Engineering Laboratory
Gaithersburg, MD 20899

QC
100
.U56
NO.5752
1995

NIST

**SUMMARY REPORT:
Second Workshop on Industrial
Applications of Scanned Probe
Microscopy**

**A Workshop co-sponsored by
NIST, SEMATECH, ASTM E42.14,
and the American Vacuum Society**

**held at
NIST
Gaithersburg, MD 20899**

**on
May 2 - 3, 1995**

Report prepared by:

J. A. Dagata
National Institute of Standards
and Technology

A. C. Diebold
SEMATECH

C. K. Shih
University of Texas-Austin

R. J. Colton
Naval Research Laboratory

U.S. DEPARTMENT OF COMMERCE
Technology Administration
National Institute of Standards
and Technology
Manufacturing Engineering Laboratory
Gaithersburg, MD 20899

November 1995



U.S. DEPARTMENT OF COMMERCE
Ronald H. Brown, Secretary
TECHNOLOGY ADMINISTRATION
Mary L. Good, Under Secretary for Technology
NATIONAL INSTITUTE OF STANDARDS
AND TECHNOLOGY
Arati Prabhakar, Director

EXECUTIVE SUMMARY

The Second Workshop on Industrial Applications of Scanned Probe Microscopy (IASPM) was held at the National Institute of Standards and Technology (NIST) Gaithersburg on May 2-3 1995. The meeting, co-sponsored by NIST, SEMATECH, the American Society for Testing and Materials (ASTM) E42.14 Subcommittee, and the Manufacturing Science and Technology Group of the American Vacuum Society (AVS), was attended by approximately one hundred scanned probe microscopy (SPM) users, suppliers, and researchers from industry, government, and academia.

SPM-based methods represent an attractive opportunity as measurement tools for process development and process control in a variety of advanced manufacturing applications. Quantitative measurement represents a foundation upon which commercial acceptance of SPM-based process control and development is based. As industrial experience increases, driven by the need for decreasing dimensional tolerances and higher performance of parts and materials, new applications are expected to take SPM from the research and development (R&D) laboratory into the production environment. The aim of the IASPM workshops is to foster effective standards and tool development as a means of achieving widespread industrial acceptance of SPM-based methods.

This Report presents a concise summary of the major themes which emerged during the workshop sessions. Over fifty industry overviews and technical presentations of SPM-based R&D activities were arranged into three oral focus sessions and poster presentations. Industrial applications of SPM in the areas of **Magnetic Recording Technology, Polymers and Coatings, and Semiconductors** were reviewed. A fourth session was devoted to **Progress on SPM Measurement Standardization and Tool Development** issues which have occurred since the previous workshop. Extended Abstracts for all oral and poster presentations are included with this Report.

A number of conclusions were extracted from a discussion of the topics presented at the workshop. These conclusions highlight technical trends, revealing how SPMs are being used successfully in a broad range of industrial applications, as well as suggest issues which future workshop programs need to address. The following were noted:

- **The simultaneous collection of SPM topographic data with other surface properties, e.g., capacitance, electrical potential, magnetic, optical, chemical, mechanical, friction, etc., provides a strong value-added element for industrial applications, particularly in process development and off-line defect review.**
- **SPM topography issues, specifically tip characterization and dimensional calibration of roughness and step height, remain high-priority standardization needs. Although the SPM requirements for process development tools differ from those required for high-throughput in-line metrology, performance standards which quantify topographic measurements are common to both applications.**

- **Without a concerted effort on the part of the applied SPM community, documents which establish standards and standard practices for SPM use will be developed in a very slow manner despite the importance of these documents for the advancement of SPM methods in industry.**

In response to the continuing interest in standards development on the part of the applied SPM community, a **Third IASPM Workshop is being planned for May 2-3 1996**. The workshop will again be held at NIST-Gaithersburg and it will feature a comprehensive tutorial on SPM standardization needs and activities. Some of the topics under consideration include: Understanding the relationship between standards documents, practices, artifacts, and calibration; accounting for the unique challenges involved in defining nanometer-scale standards and procedures; explanation of how standards documents are written and a consensus established; overview of standards organizations actively involved in SPM-related projects; discussion of the overlap which future SPM standards may have with existing optical- and stylus-based measurements of surface roughness and step-height measurements; and, the relevance of ISO 9000 conformance. Formal discussion periods following the tutorial will allow participants to lay the groundwork for formal SPM standard document activity.

Additional copies of this report are available as NIST Interagency Report #5752 from the National Technical Information Service (NTIS, Springfield VA 22161), or by contacting the authors directly:

John A. Dagata, NIST, 220-A117, Gaithersburg MD 20899

ph: 301-975-3597, fax: 301-869-0822, email: john.dagata@nist.gov

Alain C. Diebold, SEMATECH, 2703 Montopolis Road, Austin TX 78714

ph: 512-356-3146, fax: 512-356-3083, email: alain_diebold@sematech.org

C. K. Ken Shih, Department of Physics, University of Texas, RLM 5.208, Austin TX 78712

ph: 512-471-6603, fax: 512-471-1005, email: shih@utaphy.ph.utexas.edu

Richard J. Colton, Code 6177, Naval Research Laboratory, Washington DC 20375

ph: 202-767-0801, fax: 202-7673321, email: rcolton@stm2.nrl.navy.mil

ABSTRACT

The Second Workshop on Industrial Applications of Scanned Probe Microscopy (IASPM) was held at the National Institute of Standards and Technology (NIST) Gaithersburg on May 2-3 1995. The meeting, co-sponsored by NIST, SEMATECH, the American Society for Testing and Materials (ASTM) E42.14 Subcommittee, and the Manufacturing Science and Technology Group of the American Vacuum Society, was attended by approximately one hundred scanned probe microscopy (SPM) users, suppliers, and researchers from industry, government, and academia. This Summary Report presents an overview of current industrial applications of SPM in the areas of magnetic recording technology, polymers and coatings, and semiconductors. This report also reviews recent progress on SPM standardization and tool development issues. The main conclusions which emerged from the workshop are that: SPM topographic imaging, with simultaneously measurement of other surface properties, e.g., electrical potential, magnetic, optical, chemical, mechanical, and friction, is now recognized as a powerful approach to industrial applications in such areas as process development and product inspection; SPM tip characterization and calibration of roughness and step height remain high-priority standardization needs; and, without a concerted effort on the part of the applied SPM community, SPM standards documents and practices will develop only slowly.

TABLE OF CONTENTS

EXECUTIVE SUMMARY	p. iii
ABSTRACT	p. v
PART I: WORKSHOP SUMMARY REPORT	
A. INTRODUCTION	p. 3
1. Workshop Motivation	
2. Workshop Objectives	
3. Purpose of this Report	
B. OVERVIEW OF THE WORKSHOP PRESENTATIONS	p. 5
1. Magnetic Recording Technology Session	
2. Polymers and Coatings Session	
3. Semiconductors Session	
4. Progress on SPM Standardization and Development Needs	
C. DISCUSSION	P. 10
D. RECOMMENDATIONS FOR A THIRD WORKSHOP	p. 13
E. ACKNOWLEDGMENTS	p. 14
PART II: TECHNICAL PROGRAM	
A. AGENDA	p. 17
B. EXTENDED ABSTRACTS	p. 23
C. LIST OF PARTICIPANTS	p. 111

PART I: WORKSHOP SUMMARY REPORT

A. INTRODUCTION

The Second Workshop on Industrial Applications of Scanned Probe Microscopy (IASPM) was held at the National Institute of Standards and Technology (NIST) Gaithersburg on May 2-3 1995. The meeting, co-sponsored by NIST, SEMATECH, the American Society for Testing and Materials (ASTM) E42.14 Subcommittee, and the Manufacturing Science and Technology Group of the American Vacuum Society (AVS), was attended by approximately one hundred scanned probe microscopy (SPM) users, suppliers, and researchers from industry, government, and academia.

The workshop featured over fifty industry overviews and technical presentations of SPM-based research and development (R&D) activities arranged into three oral focus sessions and poster presentations. A fourth session was devoted to progress on SPM measurement standardization and tool development issues which have occurred since the previous workshop.

1. Workshop Motivation

SPM-based methods, because of their inherent electro-mechanical simplicity and their capability for making highly localized measurements of surface topography and other properties, represent an attractive opportunity for nonincremental improvements in measurement technology for process development and process control in a variety of advanced manufacturing applications. This has created a very dynamic situation where the deployment of SPMs for a number of critical applications is now underway in US industrial R&D labs. Growth in SPM sales has increased dramatically in the past few years, from only a few units in 1989, to numbers approaching or exceeding a thousand in 1995. A substantial portion of this growth is industrially based, and SPM vendors are shifting their market focus accordingly. As industrial experience with this tool is gained, additional applications, driven by the need for decreasing dimensional tolerances and higher performance of parts and materials, are expected to bring SPM from the R&D laboratory into the production environment.¹

Quantitative measurements represent a foundation upon which commercial acceptance of SPM-based process control and development is based. The IASPM workshop aims to foster effective development of standards documents and tool development as a means of achieving widespread industrial acceptance of SPM-based methods. Acceptance of these methods within individual operating units of a company or between firms demands that these tools meet performance standards specific to the application. While it would be preferable that standards development proceed in parallel with the introduction of this new industrial measurement technology, history shows that this is not the case and, in fact, there is a substantial lag time between the initial application of a new technique and the adoption of standard practices associated with its use.

Preparing the applied SPM community for such consensus, the IASPM workshops promote the formation of a network for improved communication among members of the applied SPM

¹ D. A. Swyt, "Metrological Issues in Precision Tolerance Manufacturing: A Report of a NIST Industry-needs Workshop", *J. Res. NIST* **98** 245 (1993).

community. Passage of new technology from the basic research laboratory to the production facility is difficult today because of the high level of investment required on the part of individual firms to channel basic research results into their R&D pipeline. Current SPM applications are limited to one or a few steps of a complex manufacturing stream, making it unlikely that a single industrial firms will be willing to invest in development efforts thought to be premature. An informed view of the SPM development path, shared by SPM vendors, industry users, and research personnel in university and government laboratories, is critical for widespread industrial acceptance of SPM methods.

The workshops are an effort to identify the roles and responsibilities of each of these member groups of the applied SPM community. The ultimate benefits of widespread industrial acceptance are to be shared by SPM manufacturers and their industrial customer base. It is only as a consequence of bringing about a clear understanding of their roles in the SPM standards and tool development processes, supported by government and university involvement whenever appropriate, that the efforts of the IASPM workshops and standards organizations will be worthwhile.

2. Workshop Objectives

The objectives of this workshop were:

- **To assess progress which had occurred in the past year on SPM standardization and development needs identified in the Summary Report of the first IASPM workshop.²**
- **To conduct Focus Sessions limited to Industrial Applications of SPMs in the areas of Magnetic Data Storage Technology, Polymers and Coatings, and Semiconductors.**

3. Purpose of this Report

Part I of this Report presents a summary of the major themes which emerged during the technical workshop presentations and discussions. Generic issues transcending individual industrial applications form the basis for an evaluation of overall progress on SPM standardization and instrument development. These are identified and discussed in this Report. During the past year, for example, NIST has responded to the needs identified at the first IASPM workshop by carrying out highly regarded standardization efforts on tip deconvolution and step-height calibration. SPM vendors have implemented, or are in the process of implementing, many of the critically needed instrument and software features. Part I concludes with a recommendation for a third workshop. Part II of this Report reprints the workshop Program, Extended Abstracts for all oral and poster presentations, and a Participants List.

²J. A. Dagata *et al.*, **Workshop Summary Report: Industrial Applications of Scanned Probe Microscopy**, NIST Interagency Report #5550, December 1994. (Available from NTIS, Springfield VA, 22161.)

B. OVERVIEW OF THE WORKSHOP PRESENTATIONS

1. Magnetic Recording Technology Session

The workshop program began with a session on Magnetic Data Storage Technology, organized by **John Moreland of NIST - Boulder**. An overview of SPM applications in this industry was given by **Allan Schultz of Seagate Technologies**. As bit densities exceed 1 Gbit-in², new techniques are needed for imaging the fields very near media surfaces and the airbearing surfaces (ABS). Bit transitions separated by less than 500 nm and head flying heights of less than 20 nm will be typical of disk drives in the next five years. The industry needs for nanometer-scale tolerances during component fabrication and testing critical components of a disk drive include pole tip recession of the read/write head, the domain structure of the magneto-resistive (MR) sensor, the relationship of grain size and surface roughness on the magnetic bit patterns, especially the fringe fields at the edges, and the wear properties of lubricants coating the disk surface which mediate the contact between the ABS and disk surfaces.

SPM topographic measurements of pole tip recession during quality assurance and acceptance testing were discussed in a talk by **Jim Potter of Maxtor**, the potential of magnetic force microscopy coupled with topographic imaging was discussed by **Dan Dahlberg and Yansheng Luo of the University of Minnesota** and **Ken Babcock of Digital Instruments**, and use of the SPM for determining the normal and lateral interaction forces which influence tribology in disk drives in a talk given by **Mathew Mate of IBM Almaden**.

The following themes emerged during the session:

First, there was significant interest noted in SPMs for performing not only topographic imaging, but other measurements simultaneously. In topographic mode, SPM is being used for critical dimensioning of the ABS, and allows for direct observation of media roughness at wavelengths as low as a few nanometers. Specific manufacturing issues are that polishing of hard disk substrates can be monitored with high spatial resolution, zone-texturing of disks can be optimized to minimize head wear, and grain morphology and size can be estimated.

In addition to topographic information, Magnetic Force Microscopy (MFM) is used to image the stray fields near bits recorded in media and near the ABS. It can also be used to image the domains in thin-film permalloy MR sensors, permanent magnetic films used to bias the MR sensors, and the soft magnetic films used to shield the MR sensors. Currently, measurements with the MFM are limited to relative comparisons typically between different samples with the same tip. Examples include, fringing fields above bits written in different media with the same head to determine relative media recording parameters, or fringing fields near the ABS of heads energized at different current levels to determine head saturation levels.

Lateral Force Microscopy (LFM) is being used to study the properties and performance of the lubricating layer deposited on media surfaces to minimize damage during head-media contact. Lubrication coverage uniformity can be imaged directly with LFM. Friction creates a lateral force acting on the SPM cantilever and media lubricant which can be resolved with nanometer spatial

resolution. Some knowledge of the chemical nature of the tip surface is required before LFM images can be related to molecular frictional processes; however, a qualitative picture of contact processes between an SPM tip and surface lubricants can be developed. Hysteresis of the force associated with dipping the SPM cantilever into the lubricant, pushing lubricant out of the way, and subsequently pulling free of the lubricant, can be measured in this way with a sensitivity of better than 10^{-10} N.

Second, there is a divergence in the way industry uses SPMs for production quality control and in process control and development. Research applications include fundamental studies of new kinds of storage media and thin-film recording heads. Specifically, SPM has been used to correlate magnetic media noise and grain morphology, as well as domain structure, in as-deposited films and films patterned into simple devices. Product development applications include studying the recording process in various head-media combinations and testing of component wear. Quality assurance applications include spot-testing of individual components from batches manufactured for assembly and testing of components shipped for assembly from other companies.

Third, industry needs relative as well as absolute calibration for MFM calibration standards. In addition to the general needs of the community for topographic standards and tip de-convolution, an artifact standard for MFM measurements would be useful for testing instrument sensitivity and resolution. It would be helpful if the standard was flat, thereby avoiding imaging artifacts such as topographic influences on the MFM image. The standard would require rapid field gradient changes at a period of $1\mu\text{m}$, or smaller. As in the case of comparing SPM to other profiling and roughness measurement techniques, the advantages and disadvantage of MFM relative to other magnetic imaging techniques needs to be clarified.

2. Polymers and Coatings Session

The second session of the workshop was entitled Polymers and Coatings, organized by **Andy Gilicinski of Air Products and Chemicals**. An overview of SPM applications in the polymer and coatings industry was given by **Greg Blackman of DuPont**. The issue has gone from 'is it possible to image the surfaces of soft materials' such as polymers to the more significant one of using SPM-based methods to better understand how the micromechanical properties of (complex) polymers systems affect the performance of films and coatings with respect to their intended purpose.

The main focus of current efforts in the applications concerned new methods for achieving high resolution chemical contrast by **Don Chernoff of Advanced Surface Microscopy**, obtaining and understanding of the relationship between SPM image and polymer structure presented by **Gerry Zajac of Amoco**, using the SPM to understand the control of particle film morphology during growth by **Cynthia Goh of the University of Toronto**, quantitative measurements of adhesion by **Howard Mizes of Xerox**, indentation by **Greg Meyers of Dow Chemical**, and the use of force modulation measurements for distinguishing between different phases in polymer blends by **Andy Gilicinski**.

There were several common themes which emerged during the session:

First, it is clear that topographic imaging, coupled with other modes which can provide

chemical and mechanical information about the film properties, is considered to be a critical aspect for process development. The widespread availability now of noncontact modes of operation for AFM which provide high resolution imaging without damage to the sample surface are combined in commercial instruments with friction, lateral force, and force modulation modes. Although it may be impossible to obtain data from all modes simultaneously, sequential scanning over a single region of the sample surface following a change of hardware or software is now generally possible with the current generation of SPMs.

The significance of multiple mode sampling was evident from several of the session presentations. Key criteria for evaluating the performance of coatings and polymer additives included: adhesion, wettability, friction, wear, stiffness, scratch damage, and appearance. Interpretation of these criteria requires direct and systematic correlation of molecular weight, film forming properties, and solvent content during process control and optimization.

Second, quantifying this information, particularly the correlation of micro-mechanical properties is becoming a serious concern in industry. Some of the current effort is devoted to model systems which are amenable to quantitative analysis. Investigations of real commercial systems, as in the use of SPM imaging to reveal blends of co-polymer coating systems, suggest the range of SPM applications for predicting wear, adhesion, and film thickness properties.

Third, standards for characterizing tip shape and determining its effect on image resolution remain an important issue, not only for topographic data related to polymer systems, but for the realization of quantitative lateral force imaging in the near future.

3. Semiconductor Session

The first IASPM workshop focused largely on the needs of the semiconductor industry for topographical inspection. These needs involve microroughness for wafer acceptance testing and critical dimension (CD) measurement in lithography. The present workshop emphasized using SPMs for in-line and off-line defect review and CD control. It is significant that only during the past year has it become possible to hear about actual user experience. **Neal Sullivan of Digital Equipment Corporation** discussed acceptance and qualification of an in-line tool for particle review, defect inspection, 1-D and 2-D CD metrology, grain-size evaluation of metallization layers, and planarization. **Henry Luftman of AT&T Bell Labs** discussed the use of SPM for off-line analysis of materials problems and planarization.

The major themes which emerged from this session were:

First, SPM systems are now being offered commercially which may be integrated with in-line optical inspection stations, data exchange of x and y coordinates, and particle size. Automation of system calibration and pattern recognition sequences, as well as topographical measurement, analysis, and data transfer, are available or close to being offered on the latest high-end systems. **Yale Strausser of Digital Instruments (DI)** described strategies which DI considers promising in this regard.

Second, the development of SPM methods for electrical characterization, topic of the first

workshop, was revisited in terms of the scanning Kelvin probe microscopy (SKPM), as reported by **Martin O'Boyle of IBM**. The SKPM methods provide information on the presence of contaminants which alter the electrical properties of metallization layers, or change the interfacial properties at ohmic, Schottky, or insulator regions. This probe makes it possible to correlate device failure or abnormal device performance with a localized difference in potential, thereby narrowing the problem down to a specific process step.

Third, Near-field Scanning Optical Microscopy (NSOM) reached the status of a commercial instrument during the past year. This provides an alternative to the mechanical capability of SPM techniques, relying rather on optical techniques. **Herschel Marchman and Walter Duncan of Texas Instruments** described the needs and directions which the semiconductor industry is investigating for using NSOM as an *in-situ* litho-metrology tool. In particular, the NSOM technique may have a significant role to play in process development by providing critical dimension information on exposure parameters in the latent resist image, process parameters during bake and etch steps, as well as on dimensional control of the final patterned resist. The NSOM is also promising for defect identification of sub 0.1- μm particles by using it in a spectroscopic mode, i.e., photoluminescence, fluorescence, or Raman. **Grover Wetsel of the University of Texas-Dallas and Paul West of Topometrix** discussed some aspects of instrument evolution in this rapidly developing field.

Despite the progress on in-line instrumentation, SPM techniques must prove their value to industry first in off-line process control applications. The instrumentation must be flexible, yet the routine tasks such as system calibration and tip exchange must become increasingly more rapid, if not automated, allowing R&D personnel to concentrate on developing the appropriate methodology rapidly and systematically. Tip calibration and standards for roughness and step height clearly represent a fundamental step towards this end. Again, there remains a entire spectrum of opportunities between in-line and off-line applications.

4. Progress on SPM Standardization and Development Needs

A fourth session organized by **Jason Schneir of NIST and Joe Griffith of AT&T Bell Labs**, provided an opportunity for the Workshop participants to assess the responsiveness of the standards community and SPM vendors towards meeting the needs expressed at the first IASPM workshop.

The major themes discussed at this session were:

First, probe tip deconvolution algorithms and their integration into SPM software is being actively pursued by researchers and vendors. At this time, detailed model calculations need to be done to give validity to more approximate methods which would be faster and more amenable to commercial applications. **John Villarrubia of NIST** discussed progress on tip modeling. The SPM tip is fairly well recognized as one of the greatest potential sources of variability in measurements.

This is certainly true in the simplest case of purely geometric considerations, but it was noted that variations in the orientation and quality of the magnetic thin film coating on MFM tips, for

example, might be responsible for large variations in signal intensity observed experimentally. Since microfabrication techniques seem to produce fairly uniform tip geometries on the wafer, either better process control of the deposition process is necessary or an identification of the cause based on careful modeling of the interaction of the MFM tip with a 'known' standard must be pursued.

Second, another probe-related issue which arose during this workshop was the use of spherically shaped objects for micromechanical experiments since for this geometry contact experiments measuring indentation or adhesion are more amenable to calculation. Given the recognized importance of mechanical information for the polymer and coatings industry, these probes must be considered as part of the ongoing interests of this Workshop. Likewise, NSOM probes were discussed. The exciting, although early, progress on using photoluminescence, fluorescence, and Raman techniques for spectroscopic evaluation of sub 0.1- μm defects and mapping strain in device structures will also require probes with sufficient light throughput to achieve reasonable signal-to-noise ratios using these techniques. In general, the developments suggest that for many industrial applications sharper tips may not be so important as one which can be used quantitatively or which yield more reproducible characteristics on a tip-to-tip basis.

Third, the development and widespread availability of suitable standardized roughness and step-height calibration samples is needed. Industry requirements were addressed by **Mark Lagerquist of IBM**. Progress on step-height standards was reported by **Jason Schneir of NIST**. It is clear that future workshops must provide the participants with a formal program which outlines the various aspects of standards development. NIST, in particular its Precision Engineering Division (PED), has expressed its intent to support SPM standards activities. In addition, there is much to be learned from existing profilometer and scattering step height and roughness standards. However, the point was made several times during the workshop that often an 'in-house' reference which is deemed 'good' is used for relative comparisons of SPM signal calibration. For many applications this will be good enough.

Fourth, the timely publication of standard methods and practices for obtaining and reporting experimental data. **Dennis Swyt, Chief of PED**, gave an overview of how PED performs its role in providing for SPM calibration and standardization needs. **Alain Diebold of SEMATECH**, chair of the ASTM E42.14 subcommittee reported on the status of activities for which that body is responsible.

C. DISCUSSION

The first IASPM workshop identified several areas of SPM performance where advances were needed: the universal availability of linearized piezo-scanners over the entire SPM product line, automated sampling for statistical process control, improved probe characteristics including tip-shape and wear properties, and a more complete understanding of the underlying physical and chemical interactions which affect sensitivity and image contrast.

The goal of the first Workshop was aimed at identifying developments which would impact on the quantitative aspects of topographic SPM-based measurement. Recall that the facilitated discussions following each of the three focus sessions were concerned with Microroughness, Critical Dimension Metrology, and Electrical Characterization. The discussions focused on specific targets given in the 1992 Semiconductor Industry Association (SIA) Roadmap, and some information from the draft 1994 SIA Roadmap, in order to define the standard of performance required by the semiconductor industry for SPM tools over the next decade.³

The second Workshop examined a broader range of applications than the first. Friction, lateral force, optical, magnetic force, nanomechanical, and nanoindentation measurements, often recorded simultaneously in conjunction with a topographic image, is an extremely valuable, perhaps essential, aspect of SPM strategies for process development. Enhanced functionality, and the information made possible by it, is a significant value-added feature of SPMs. These features are most significant for process development applications.

Experience with dedicated tools for high-throughput inspection for semiconductor industry applications is accumulating. Critical dimension and defect review represent the primary measurements which these tools will perform. Topographic AFM data and its quantification therefore remain the most immediate and generic SPM needs.

The most general use for SPMs will continue to be for gathering topographic information. Quantification of surface microroughness and texture as well as dimensional measurements such as step height and pitch, remains the key standardization issue for the SPM community. There has been sustained progress in this area and in SPM tip characterization as well. This progress has emerged from considerable activity at NIST and elsewhere on tip and sample calibration and understanding tip shape and wear, for example.

A common theme which several of the workshop speakers emphasized at all three focus sessions was the importance of simultaneous collection of topographic SPM data together with additional surface properties. Electrical potential, magnetic, chemical, friction, lateral force, index of refraction, nanohardness are examples of such properties. A map of surface, or near-surface, variations in physical structure or composition may be the primary goal of a measurement, as in

³ Semiconductor Industry Association, **The National Technology Roadmap for Semiconductors**, 4300 Stevens Creek Blvd, Suite 271, San Jose CA 95129.

magnetic force measurements. It may provide a means of detecting unexpected problems in materials processing of polymer blends or sources of contamination during quality control testing. The interplay of such complementary information proves advantageous, if not necessary, under these circumstances.

In the first case, a topographic map may be needed to subtract out variations in the MFM image due to the convolution of surface topographic structure intermixed with the magnetic signal map. Alternatively, chemical-phase or contaminant identification by friction, in the case of lateral force microscopy, or electrical potential variations in the case of SKPM, may be performed during failure analysis making this an extremely valuable feature for process development or defect inspection. The increasing flexibility of commercially available general-purpose SPMs to operate in a variety of simultaneous modes is unique among surface analytical instruments. As all speakers mentioned, however, these strategies, still largely under development, require additional correlation with other techniques before they can be used with confidence. Future workshops may consider the need and development path for other quantitative standards, e.g., magnetic or nano-hardness standards.

The lab to fab transition is now underway. From the time of the first IASPM workshop to the time of the second workshop, several semiconductor companies have taken delivery of in-fab SPM tools. Additional SPM vendors are now also offering highly automated tools for dedicated wafer inspection. These systems offer features such as coordinate transfer between current generation online optical inspection stations and the SPM tool, automated operation, and pattern recognition software.

R&D on model systems is proceeding in industrial labs and at universities. Specific examples discussed at the workshop were MFM on magneto-bacteria and adhesion studies in the polymer area. Model systems are critical for the development of analytical data treatment and for quantification. This is an area where communication between industry researchers and university/government researchers can result in fruitful collaborative efforts.

A grasp of these technological factors alone is not sufficient for evaluating the progress and acceptance of SPM-based methods by industry. R&D-driven innovation has become more difficult because of the high level of investment required on the part of individual companies to perform a meaningful level of basic research within their own laboratories and a decreasing capacity for purely technological advantages to offer significant returns on investment. As the focus of most current corporate R&D has moved towards short-term goals, it has become more difficult for industry to perform the kind of R&D required to ensure that SPM-based tools meet the performance standards demanded by advanced manufacturing over the next decade.

Furthermore, there is a sense that traditional methods for creating standards documents may be less effective in the present environment of industry restructuring and government downsizing. Progress depends on the sustained volunteer activity of many individuals who take on the responsibility of identifying the consensus areas and patiently writing and shepherding the documents through the organizations. While this approach has worked in the past, industrial researchers have little time available to devote to such altruistic efforts. Government personnel also have difficulty

committing to this process. Without a substantial push from the applied SPM community as a whole, a consensus on standards and standard practices will materialize slowly, despite the acknowledged interest in and importance of these issues. With few people able to assume a leadership position in standards activities and with the pressure on industry performance, there may be few opportunities to achieve a consensus on standards documentation for SPM applications.

Finally, SPM development is occurring at a very early stage in the life of these instruments. It is well known that when technological needs drive developments in a new field, the scientific understanding underlying the technique generally lag behind the use of the technique as long as its use provides a meaningful advantage in manufacturing. At the same time there are several manufacturers of SPMs which have entered this market beginning for the most part as suppliers to a research-oriented clientele. As these suppliers introduce products into industrial settings, standards of performance begin to become crucial. The US, as the home of the major suppliers of industrially oriented SPMs, is in a position to benefit in a significant way from the early and successful introduction of SPM-based technology into advanced manufacturing.

D. RECOMMENDATION FOR A THIRD IASPM WORKSHOP

The foregoing section discussed some of the implications of current standards and tool development efforts which emerged during the second IASPM workshop. To summarize:

- **The simultaneous collection of SPM topographic data with other surface properties, e.g., electrical potential, magnetic, optical, chemical, mechanical, friction, etc., provides a strong value-added element for industrial applications, particularly in process development and off-line defect review.**
- **SPM topography issues, specifically tip characterization and dimensional calibration of roughness and step height, remain high-priority standardization needs. Although the SPM requirements for process development tools differ from those required for high-throughput in-line metrology, performance standards which quantify topographic measurements are common to both applications.**
- **Without a concerted effort on the part of the applied SPM community, documents which establish standards and standard practices for SPM use will be developed in a very slow manner despite the importance of these documents for the advancement of SPM methods in industry.**

Based on these observations, we recommend that a third workshop be held at NIST-Gaithersburg in 1996. The workshop format will focus on two well-defined objectives: First, a substantial part of the meeting time will be devoted to an in-depth tutorial on standardization activities. Some of the topics under consideration include: Understanding the relationship between standards documents, practices, artifacts, and calibration; accounting for the unique challenges involved in defining nanometer-scale standards and procedures; explanation of how standards documents are written and a consensus established; overview of standards organizations actively involved in SPM-related projects; discussion of the overlap which future SPM standards may have with existing optical- and stylus-based measurements of surface roughness and step-height measurements; and, the relevance of ISO 9000 conformance. Formal discussion periods following the tutorial will allow participants to lay the groundwork for formal SPM standard document activity.

A second objective of this workshop will be to again present progress reports in the applications areas which have been covered in previous focus sessions, semiconductors, data storage, and polymers, as well as in other areas where there is a significant industrial interest. The workshop format will continue to serve as a filter for recent advances and development issues in both in-line metrology and process development applications. Efforts are underway to form an industry user - SPM vendor advisory committee to help identify emerging and novel SPM-based strategies and methods in industrial applications for presentation during the workshop.

E. ACKNOWLEDGMENTS

The authors/organizers wish to thank **Clayton Teague (NIST)** and the members of the Program Committee, **Jason Schneir and John Moreland (NIST)**, **Andy Gilicinski (Air Products)**, **Herschel Marchman (Texas Instruments)**, and **Joe Griffith (AT&T Bell Labs)** for reading this Summary Report and suggesting improvements in the text. The workshop would not have been possible without organizational and financial support from NIST management, in particular, **Dennis Swyt, Division Chief of the Precision Engineering Division**, for providing secretarial and financial support. We also acknowledge contributions from the following SPM vendors for refreshments during the Poster Presentations: **Digital Instruments, Park Scientific, Topometrix, and Veeco Instruments**. Finally, we thank the staff of the **NIST Conference Planning Office** for considerable assistance and advice with arrangements.

PART II: TECHNICAL PROGRAM

SECOND WORKSHOP ON
INDUSTRIAL APPLICATIONS OF SCANNED PROBE MICROSCOPY

Sponsored by
NIST, SEMATECH, ASTM E-42, and the American Vacuum Society

To be held at the
NATIONAL INSTITUTE OF STANDARDS AND TECHNOLOGY
Gaithersburg MD 20899
May 2-3 1995

AGENDA

TUESDAY MAY 2 1995

7:30-8:00 AM *WORKSHOP REGISTRATION/SIGN-IN*

8:00-8:10 AM *OPENING REMARKS AND WELCOME*

Session I: MAGNETIC DATA STORAGE TECHNOLOGY

Session Organizer and Chair: **John Moreland, NIST-Boulder**

Overview

8:10-8:50 Needs of the Recording Industry Related to Scanned Probe Microscopies

Allan Schultz, Seagate Technologies

8:50-9:20 The Power and Promise of Magnetic Force Microscopy

E. Dan Dahlberg, Univ of Minnesota

Applications of Magnetic Force Microscopy

9:20-9:40 MFM Study of Recording on Ultra-high Density Disk Media

Jian-Gang Zhu and Yansheng Luo, Univ of Minnesota

9:40-10:10 Magnetic Force Microscopy in Data Storage: Recent Advances and Applications

Ken Babcock, Digital Instruments

10:10-11:30 BREAK and POSTER PRESENTATIONS

Critical Dimension and Wear

11:30-12:00 Critical Dimensioning of Heads-Pole Tip Recession Measurements and Wear

Jim Potter, Maxtor

12:00-12:30 Disk Texture and Lubrication

Mathew Mate, IBM Almaden

12:30 DISCUSSION

12:45-1:30 LUNCH

Session II: POLYMERS AND COATINGS

Session Organizer: **Andy Gilicinski, Air Products & Chemicals**

Session Chair: **Rich Colton, Naval Research Laboratory**

Overview

1:30-2:10 PM Survey of Industrial SPM Needs and Opportunities

Greg Blackman, DuPont

Polymer Surface Imaging

2:10-2:40 Imaging Polymers using Topographic and Chemical Contrast

Don Chernoff, Advanced Surface Microscopy

2:40-3:10 Imaging of Cryo-ultramicrotomed Sections of Isotactic/Atactic Polypropylene by STM

Gerry Zajac, Amoco

Adhesion Studies using SPM

3:10-3:40 Adhesion Interaction of Latex Particles

M. Cynthia Goh, Univ of Toronto

3:40-4:10 Adhesion of Small Particles

Howard Mizes, Xerox

4:10-5:00 BREAK and POSTER PRESENTATION

Mechanical Measurements

5:00-5:30 Force Modulation AFM of Polymer Coatings

Andy Gilicinski, Air Products and Chemicals

5:30- 6:00 AFM-based Mechanical Property Measurements on Polystyrene Surfaces

Gregory Meyers, Dow Chemical

7:30-10:00 ASTM E42.14 Meeting

Bethesda Room, Gaithersburg Hilton

WEDNESDAY MORNING MAY 3 1995

Session III: SEMICONDUCTORS

Session Organizer: **Herschel Marchman, AT&T Bell Labs**

Session Chair: **Ken Shih, Univ of Texas - Austin**

In-fab Applications

8:00-8:40 Current Applications and Future Needs for In-line Atomic Force Microscopy

Neal Sullivan, Digital Equipment Corporation

8:40-9:10 In-line Defect Inspection

Yale Strausser, Digital Instruments

9:10- 9:40 Kelvin Probe Microscopy for Defect Analysis

Martin O'Boyle, IBM Yorktown Heights

9:40-10:10 AFM Analysis for Planarization, Defects, and Other Applications in an Off-line Laboratory

Henry Luftman, AT&T Bell Labs

10:10-10:45 BREAK and POSTER PRESENTATIONS

Applications of Near-field Optical Techniques in the Semiconductor Industry

10:45-11:15 A Near-field Optical Latent Image Sensor for Linewidth Metrology

Herschel Marchman, AT&T Bell Labs

11:15-11:45 Near Field Optical Microscopy of Electronic Materials and Devices

Walter Duncan, Texas Instruments

11:45-12:15 Measurement Issues in Lateral Force Microscopy

Grover Wetsel, Univ of Texas - Dallas

12:15-12:45 Progress on Applications in Near Field Scanning Optical Microscopy

Paul West, Topometrix

12:45-1:30 LUNCH

WEDNESDAY AFTERNOON MAY 3 1995

Session IV: SPM STANDARDIZATION AND DEVELOPMENT NEEDS

Session Organizers: **Jason Schneir, NIST, and Joe Griffith, AT&T Bell Labs**

Session Chair: **Joe Griffith, AT&T Bell Labs**

Meeting Industry's Needs for SPM Standards

1:30-1:50 Industry Needs for SPM Standards: The View from NIST

Dennis Swyt, NIST

1:50-2:10 Update on ASTM E42.14 Activities

Alain Diebold, Sematech

Progress in Defining and Delivering Standards/Standard Practices

2:10-2:30 Steps towards Accuracy in Linewidth Measurements by Two-dimensional Scanning Force Microscopy

Mark Lagerquist, IBM Essex Junction

2:30-2:50 Progress in Tip Modeling

John Villarrubia, NIST

2:50-3:10 Calibration and Use of a Waffle-pattern Step Height SPM Artifact

Jason Schneir, NIST

3:10-3:30 BREAK

The View from the Vendors

3:30-3:45 **Mike Young, Veeco**

3:45-4:00 **Yale Strausser, Digital Instruments**

4:00-4:15 **Sang-il Park, Park Scientific**

4:15-4:30 **Paul West, Topometrix**

4:30-5:00 DISCUSSION AND ADJOURN

POSTER PRESENTATIONS

1. Advances of SPM Lithography with New Resist Material
S-w. Park, M. Kirk, and S-i. Park, Park Scientific Instruments
2. AFM Analysis of Photoresist Test Structures for use in SEM as in-house Linewidth Standards
Donald Chernoff, Advanced Surface Microscopy
3. Study of VLSI Step Height Standards on the Veeco AFM
R. Raheem and M. Young, AMD/Sloan Technology
4. Dimensional Metrology with AFM
T. McWaid, J. Schneir, R. Dixon, V. W. Tsai, N. Sullivan, S. H. Zaidi, S. R. J. Brueck, E. D. Williams, and E. Fu, NIST
5. Precision Nanometer-scale 3-D and Z-only Calibration Standards
Douglas Hansen, James Thorne, and Wang Qui, MOXTEK
6. Effect of Interface Roughness on Mobility of Si/SiGe Heterostructures
Martin Lutz and R. M. Feenstra, IBM
7. Scanned Probe Microscopy of Mixed Chain Length Langmuir-Blodgett Films
D. D. Koleske, W. R. Barger, and R. J. Colton, NRL
8. Characterization of Metallic Thin Film Growth by STM
A. Davies, J. A. Stroscio, D. T. Pierce, J. Unguris, M. D. Stiles, and R. J. Celotta, NIST
9. Surface Studies with the Scanning Kelvin Force Probe
Todd Hochwitz, A. K. Henning, C. Levey, and C. Daghlín, Dartmouth College
J. Slinkman, J. Never, P. Kaszuba, R. Gluck, R. Wells, R. Bolam, and P. Coutu, IBM
10. Measurement of the Absolute Nanoscale Mechanical Properties of Polymer Surfaces using the AFM
D. M. Shaeffer, C. F. Draper, R. J. Colton, B. M. DeKoven, G. F. Meyers, T. Ho, K. J. Wynne, S. C. Webb, and S. M. Hues, NRL
11. Pneumatic Scanning Force Microscopy - A Methodic Approach of Membrane Characterization
H. Kamusewitz, M. Keller, and D. Paul, GKSS Research Centre
12. NIST Industrial Fellows Program: Magnetic Force Microscopy at Maxtor Corp.
P. Rice and J. Potter, NIST/Maxtor

13. Automated Calibration of Scanning Probe Microscopes by Image Processing
J. Jorgensen, Danish Institute of Fundamental Metrology/NIST
14. Magnetic Force Microscopy using Fe-SiO₂ Coated Tips, **P. F. Hopkins**, J. Moreland, S. S. Malhotra, and S. H. Liou, NIST-Boulder/University of Nebraska
15. An Atomic Force-Scanning Tunneling-Scanning Electron Microscope with a Novel Electron Beam Cantilever Deflection Sensor, **A. V. Ermakov** and E. L. Garfunkel, Rutgers University

PART IIB: EXTENDED ABSTRACTS

Oral Presentations pages 25-75

Poster Presentations pages 77-110

NEEDS OF THE RECORDING INDUSTRY RELATED TO SCANNED PROBE MICROSCOPIES

Dr. ALLAN SCHULTZ SEAGATE TECHNOLOGY

ATOMIC FORCE MICROSCOPY IN THE RECORDING INDUSTRY

Atomic Force Microscopy and its subspecialty, Magnetic Force Microscopy, already play crucial roles in the development of advanced magnetic recording heads. In addition, AFM and MFM, are being increasingly relied upon in the production of recording heads, particularly magnetoresistive (MR) heads. AFM measurements are being instituted in all phases of recording head operations, from the earliest steps in the wafer fabrication process, through the analysis of finished heads at the air bearing surface, to testing the performance of heads in drives by examining the written tracks with MFM.

Among the more common wafer and head level measurements utilizing AFM are:

1. Film Thickness

The AFM has become the tool of choice for measuring the very thin films(500 Å) used in making MR heads.

2. Grain Size and Structure

Because the AFM is an imaging tool, as well as a measurement tool, it provides both sizes and shapes of grains at very high resolutions. An 8 μm scan of a device is typically at 16,000X magnification; while a scan area of 1 μm yields over 120,000X magnification, enough to resolve a grain size on the order of 100 Å with a precision of +/- 50 Å.

Figure 1 shows an AFM image of a 1000 Å thick Mo film. The magnification is approximately 250,000 X and the grains are ~800 Å across. The rounding of the grains is an artifact of the AFM

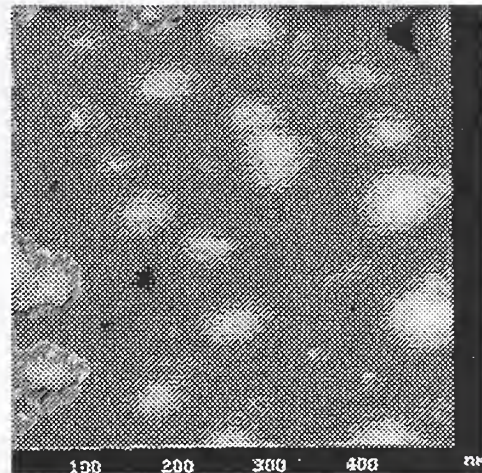


Figure 1 AFM of Mo Grains

3. Roughness

The AFM provides direct roughness measurements of film samples at levels exceeding that of the best profilometers. AFM also provides a quantitative way to measure the surface finish after bar lapping during the machining of recording heads.

4. Line or Trackwidths

The AFM is widely used to measure line and trackwidths in both the magnetic recording and semiconductor industries. However, the AFM's technology and measuring strategy is very different from a typical photolithography system, such as a KLA. The user gets the entire line or trench profile, including the width at both the bottom and top of trenches, as well as wall angles. On a sloped line or trench, photolithography and SEM-based systems must estimate where the track ends, thus giving an average. Recent AFM based systems, such as the Veeco system marketed by IBM, actually allow the measurement of reentrant topography, because

the point of the tip is offset from its body. However, all AFM based systems used for linewidths suffer the serious drawback of being very slow. As a result of this, AFM is used more in conjunction with photolithography measurements, rather than in place of them.

5. Pole and Sensor Recession at the Air-Bearing Surface

The extreme vertical-sensitivity of the AFM, along with the sharpness of the tip, are well matched for examining the recession of very small recording head features. Typical examples would be a $3\ \mu\text{m} \times 3\ \mu\text{m}$ pole tip recessed 200 Å or a diamond-like carbon protective film less than 80 Å thick.

DIFFERENT TYPES OF TIPS AND SOME TIP RELATED ISSUES

The variety of special purpose tips is a key ingredient in the versatility of the AFM. Some examples of special purpose tips are discussed below:

Special geometry tips, such as FIB (focused ion beam) and reentrant, allow physical measurements previously impossible. Figure 2 on the right shows a FIB tip that is $6\ \mu\text{m}$ high with a tip radius of approximately 1000 Å.

Specially coated tips, such as MFM tips, use a variety of different magnetic film coating to image and measure the fields coming off of magnetic samples. These include hard magnetic tips, usually of a Co-based alloy that image the bit patterns on magnetic disks, and Fe-based tips that are useful for domain studies in magnetically soft films, such as permalloy

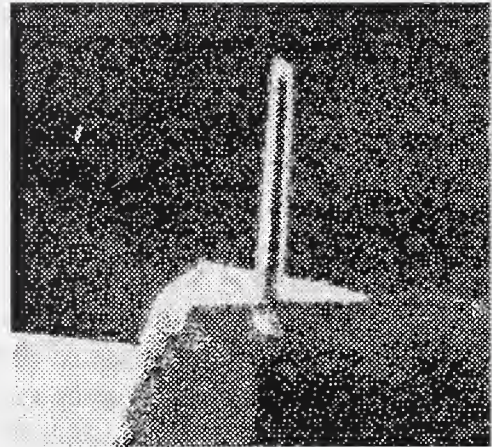


Figure 2 FIB Tip

Both the image and the measurements obtained by AFM and other force microscopy techniques are very dependent upon tip quality and shape. While the role of tip geometry in measurements has long been recognized, and been the subject of work at NIST and elsewhere, workers in the field of force microscopy have only recently recognized the susceptibility of AFM tips to electrostatic damage and debris build-up.

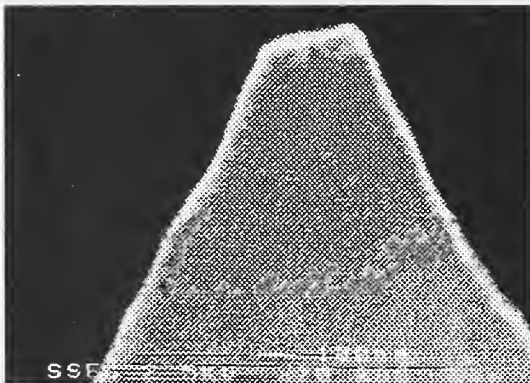


Figure 3 ESD Damaged MFM Tip



Figure 4 Debris Build-up on Tip

Figure 3 shows how ESD can damage an MFM tip, resulting in blurry images for both AFM and MFM. Figure 4 shows an intact MFM tip, but with a metallic whisker, the result of operating an ungrounded sample for a lengthy period of time. With this tip, both the AFM and MFM images started out with good resolution, but the AFM image clarity actually improved, while the MFM image faded. Consistent, high quality AFM and MFM work require both careful handling and ESD precautions.

USING MFM IN THE RECORDING INDUSTRY

One of the first uses of Magnetic Force Microscopy was the imaging of magnetic bits. Previous imaging techniques, such as SEMPA or bitter patterns, required the destruction of the disk. With MFM the imaging is non-destructive, and the disk can be remounted for further experiments. Figures 5 and 6 below are examples of MFM images from recorded tracks on a hard drive disk.

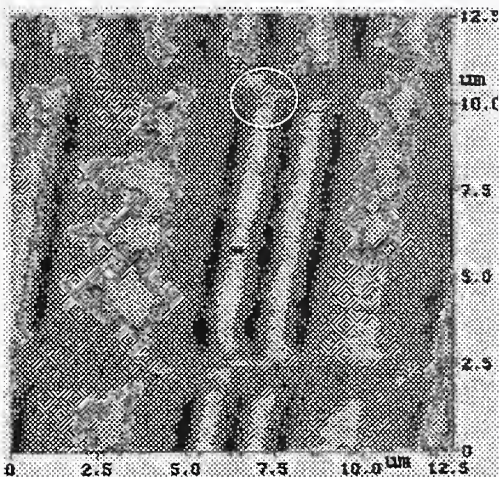


Figure 5 MFM of Magnetic Disk Showing Bit Pattern

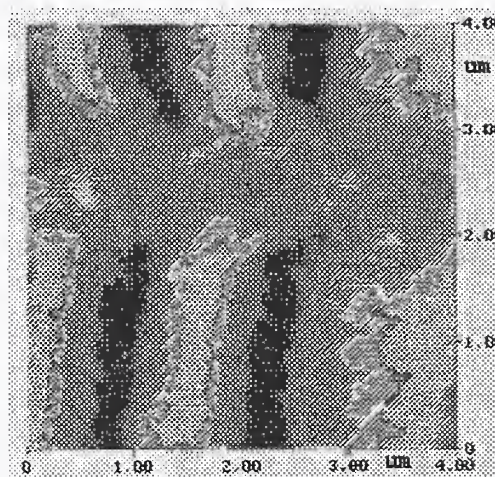


Figure 6 Circled Area of Fig. 5 Showing Bit Edge and Erase Band

Another major area of activity is the use of MFM to study the domain state of magnetoresistive read heads. The MR head employs a thin strip of permalloy that must be maintained in a single domain state in order for the head to operate noise-free. As the need for greater bit density in hard drives increases, the area of the MR sensor continues to shrink. The domain patterns in a $2 \times 3 \mu\text{m}$ MR sensor can no longer be imaged by bitter patterns or Kerr microscopy, but are easily seen in an MFM scan. In addition, the non-destructive nature of MFM allows it to be used on actual parts, that can be further processed. Figure 7 is an image of a multi-domain permalloy sensor, and figure 8 is an enlarged area of figure 7 that shows some finer magnetic detail:

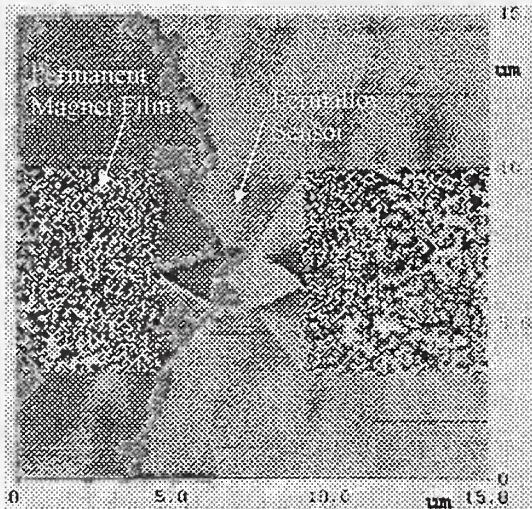


Figure 7 Multi-domain MR Sensor

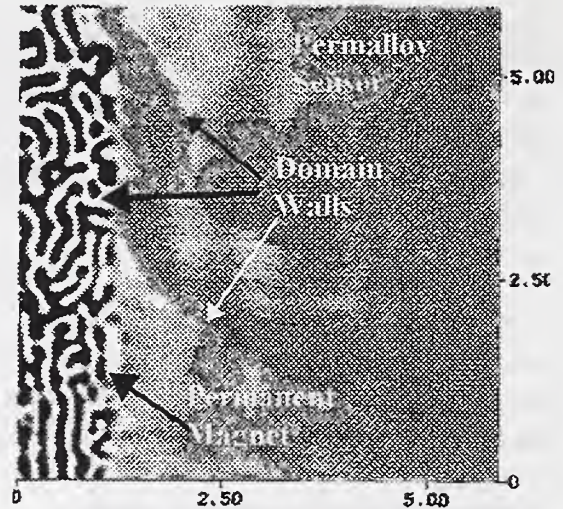


Figure 8 Close-up of MR and Permanent Magnet Domains

FUTURE PROBE MICROSCOPY NEEDS IN THE RECORDING INDUSTRY

The extraordinary usefulness of scanning probe microscopy has been described in the preceding pages. However, there are a number of issues that still need to be addressed in order for scanning probe microscopy to achieve universal acceptance similar to SEM.

The most pressing need is for **speed**--scanning probe microscopy is simply too slow for most production uses. Another problem is the influence of the tip shape upon the image and measurements. For narrow ($2\ \mu\text{m}$) trenches the error caused by the finite size of the tip can be as high as several percent. The work being done by several groups on tip deconvolution needs to be incorporated into the operation of commercial AFMs, so that the removal of tip shape from an AFM scan involves little more than a mouse click.

MFM has a different set of needs. MFM is much slower than AFM, because the scan must be taken twice (on most commercial machines). Since a better quality image is usually desired, the number of pixels required is also greater, further increasing scan time. However, speed is not the major roadblock, since MFM is not a normal production operation. The major problem in MFM is the **variability of the tips**. The MFM signal arises from the interaction from the tip and the sample, so it can be very difficult to tell whether the variation in the magnetic image is the result of the process or the tip. Also, MFM images depict the second or third derivative (depending upon the technique used) of the magnetic field arising from the sample, not the field itself. There is, at present, no simple way to calculate the field from a sample from MFM data.

Given the rapid rate of progress in scanning probe microscopy, it is very likely that substantial progress towards meeting these needs will be made in the coming year.

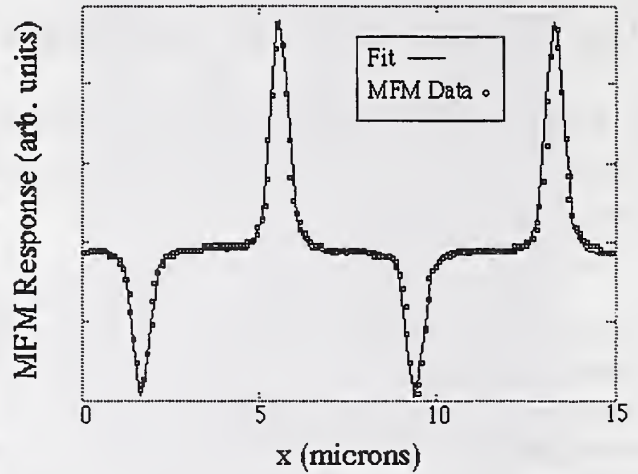
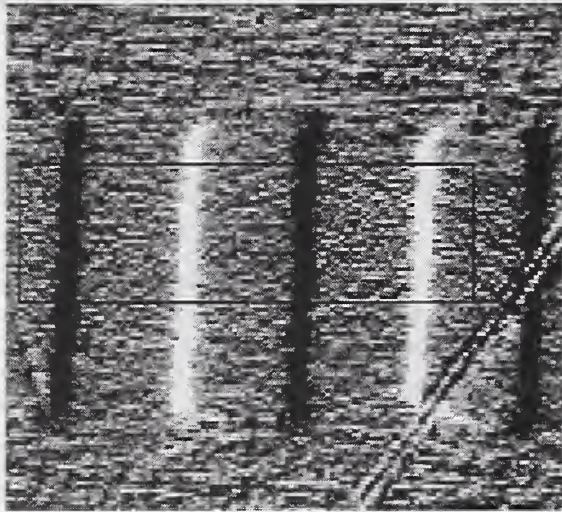
The Power and Promise of Magnetic Force Microscopy *

E. Dan Dahlberg, Sheryl Foss and Roger Proksch, Magnetic Microscopy Center and School of Physics and Astronomy, University of Minnesota, Minneapolis, Minnesota, 55455

Developments in scanning probe microscopy (SPM) [1] for both fundamental research and industrial applications have proceeded at a phenomenal rate over the past decade or so. One of the most important of these techniques is magnetic force microscopy (MFM) which allows one to image the magnetic force gradient above a surface with lateral resolution on the order of 10 nm [see ref. 2 for overview of magnetic microscopies]. MFM images may provide useful but simple information such as the existence of a domain wall or the magnetic state of a single domain particle. However, for more quantitative information about the specimen's magnetization, its utility has been more restrained. Improved quantification of MFM images is being advanced largely by the needs in fundamental research programs, where accurate interpretation of the data is necessary. For example, in order to critically test a micromagnetic model of a domain wall, one must obtain a measure of the width of the wall or the spin configuration within the wall. MFM can provide such information, but not directly. This has been a continuing evolution with the most recent advances coming from the quantification of the MFM images of the single crystal magnetite particles in magnetotactic bacteria [3].

A direct result of this research is a more sophisticated understanding of both the magnetic properties of MFM cantilever probes and the MFM imaging process. This allows MFM images of microscopic magnetic structures to provide the information to directly test micromagnetic models of them. On the applied side, a consequence of the research is the ability to fit micromagnetic models to MFM images of industrially important magnetic structures and devices. One example is bit transitions in magnetic recording media. In the first figure on the next page, the left hand part is a MFM image of magnetic recording bits in a hard disk. On the right is the profile of the MFM data across the bits. With the measured MFM response profile, is a fitted profile calculated using a micromagnetic model of the bit transitions and an accurate model of the MFM cantilever tip used for the experiment. Although the purpose of this work was not to critically test the micromagnetics of bit transitions, it does indicate the MFM is becoming a useful, quantitative tool.

Although substantial progress has been made, there is still considerable untapped potential remaining in MFM. To tap this underdeveloped resource requires continuation of both our understanding of the magnetic tips and the imaging process in general. An example of both image interpretation (related to process) and MFM potential are illustrated with the figure on the bottom of the next page. On the left hand side is a MFM image of bits recorded in a commercial magneto-optic (MO) disk. Note that the bits appear with a single contrast, white in this case, against the background of neutral gray. Because the MFM detects magnetic field gradients, one might expect to see the edge of a bit distinctly from the rest of the bit. (Within a bit, the magnetization is uniform and opposite that of the background.) The resolution of this apparent dilemma is that with the aluminum reflector coating on the MO disk, the MFM tip is far above the



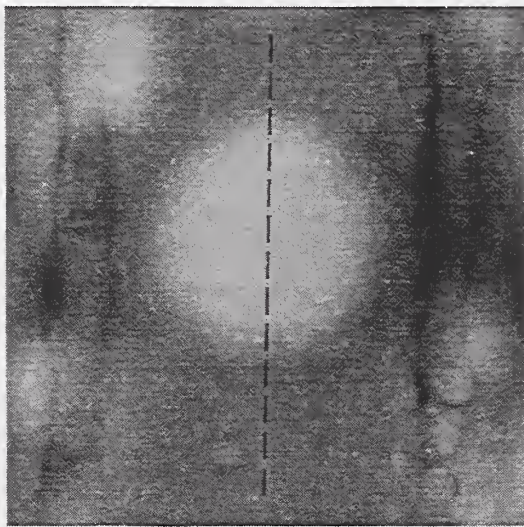
recorded bits and the image is that of a distant dipole consisting of the entire bit. On the right hand side of the figure is MFM data profiles measured at different heights across the center of a MO bit with the reflector layer removed. The top scan is the far field, at a distance similar to the scans with the reflector, whereas the bottom is the closest and shows the domain wall transition surrounding the bit. An understanding of such domain boundaries is crucial to controlling edge transition noise in MO media.

* Research funded by ONR grants N/N00014-94-1-0123 and N/N00014-89-J-1355

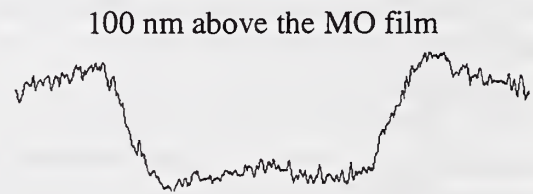
[1] "Atomic Force Microscope," G. Binnig, C.F. Quate, and R. Gerber, Phys. Rev. Lett. 56, 930 (1986)

[2] "Micromagnetic modeling and magnetic microscopy," E. Dan Dahlberg and Jian-Gang Zhu, Physics Today, April 1995 issue.

[3] "Magnetic force microscopy of the submicron magnetic assembly in a magnetotactic bacterium," R. B. Proksch, B. M. Moskowitz, E. D. Dahlberg, T. Schaeffer, D. A. Bazylinski and R. B. Frankel, accepted for pub. in Appl. Phys. Lett.



2 μm



25 nm above the MO film



2.2 μm

MFM Study of Ultra-high Density Magnetic Recording on Particulate and Thin film Media

Jian-Gang Zhu and Yansheng Luo

MINT, Department of Electrical Engineering, University of Minnesota, MN55455

Introduction

We present the applications of Magnetic Force Microscopy(MFM) in field of magnetic recording. First, we present the MFM study of the switching properties of individual iron particles used in particulate media[1]. Second, we describe an experimental method which allows us to measure the edge erase band in thin film recording and study the phase and density dependence of the edge erasure.

Part I: Switching Properties of individual recording particles

Understanding the magnetic properties of the recording particles is crucial for making high density particulate recording media. However, it has been very difficult to directly measure the magnetic properties of individual particles. The interaction among particles can not be eliminated using conventional techniques. To overcome this barrier, we have developed a technique using MFM as an ultra sensitive sensor to measure individual particles.

Iron recording particle were used for the study. First, an array of 39x39 distinct patterns were fabricated on Si wafers using E-beam lithography. Commercial iron recording particles were then dispersed on patterned Si substrates[2]. A vacuum MFM system operated in non-contact mode was used to measure the direction of their magnetization. After the sample is magnetized in an magnetic field, the particles were located using the pattern array and the magnetization direction is measured. The switching field is just the field threshold at which the particle switch its magnetization.

Fig. 1 shows the 0 degree switching fields of six iron particles vs. particle diameters. Fig. 2 shows the switching of particle B and F vs. applied field angle. Surprisingly, a multidomain state was observed in particle C after a 10K Oe field had been applied along 90 degree angle. This state is illustrated in Fig. 3.

Micromagnetic calculation were performed to simulate the particle switching mode. The particle is modeled by a chain of magnetic spheres. The calculated switching fields at 0 degree angle for particles with aspect ratios equal 4 and 9 are plotted in Fig. 1. The simulated angular dependence of the switching field of particle B is plotted in Fig. 2. As shown in these figures, the calculation agrees very well with the experimental. The simulation reveals that the switching mode is fanning-like at small angles and approaches coherent rotation at larger angles.

Part II: Phase and Density Dependence of Edge erase band

MFM can be an excellent tool for study recorded patterns in thin film disk for high density storage applications. Here, we present a a study on track edge overwrite characteristics at high recording densities.

Previous studies indicate the track edge erasure are very media and head dependent[3]. For the same head media combination, there are phase and density dependences. A method is developed to accurately measure the edge erase band width(EBW) from MFM images of overwrite tracks.

To get rid of track edge noise and electronic noise in the MFM images, the same overwrite tracks were imaged at different locations. The images were then averaged. Alignment of these images were achieved utilizing the cross-correlation of two images. When the features in two images were matched, the cross-correlation of the two images was at its maximum. Fig. 4(a) shows an example of an averaged MFM image. The signal power at each cross-track position was then calculated from the image. The cross-track signal power profile is plotted in Fig. 4(b). It clearly shows the profile of the erase band, We define the EBW as the width of the region where the signal power is below 50% of the on-track value.

Fig. 5(a) shows a series of cross-track signal power profile of the overwrite tracks with various phases at relatively low density: $B=2.2\mu\text{m}$. At this recording density, the EBW exhibits strong phase dependence: EBW is the largest at 180 and 270 degrees and is smallest at 0 degree. However, this strong EBW phase dependence diminishes at high recording densities. Fig. 5(b) shows the cross-track profile for $B=0.22\mu\text{m}$. The EBW is almost constant over all the phases. The phase and density dependences of EBW have important implication for future high track density magnetic recording.

REFERENCES

- [1] Y. -S. Luo and J. -G. Zhu, "Switching Field Characteristics of Individual Iron Particles by MFM," *IEEE Trans. Magn.*, Vol. 30, November 1994.
- [2] T. Chang, J.-G. Zhu, and J. Judy, "Direct Measurement of the Switching Field of Isolated Barium Ferrite Fine Particles Utilizing Magnetic Force Microscopy," *J. Appl. Phys.*, 73, pp. 6716, 1993.
- [3] J. -G. Zhu, Y. -S. Luo and J. Ding, "Magnetic Force Microscopy Study of Edge Overwrite Characteristics," *IEEE Trans. Magn.*, Vol. 30, pp. 4242-4244, November 1994.

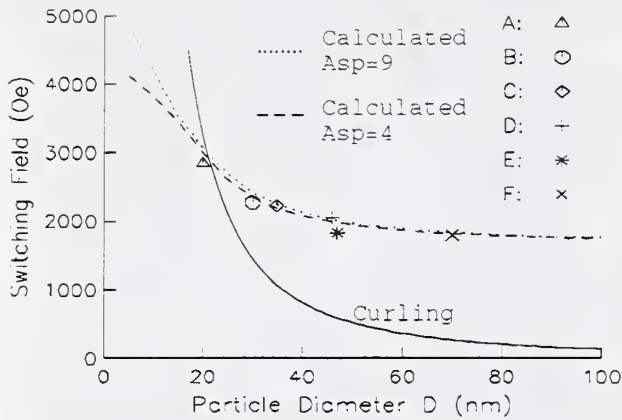


Fig. 1 Switching field as a function of particle diameter. Symbols: measured values; dotted line: calculated values with particle aspect ratio=9; dash line: calculated values with particle aspect ratio=4; solid line: curling mode for an infinite cylinder.

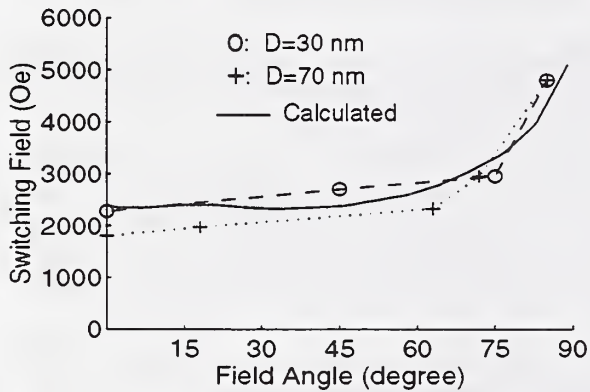


Fig. 2 Switching field as a function of applied field angle. Dash line: measured values for particle B; Dotted line: measured values for particle F; solid line: calculated values for particle B.

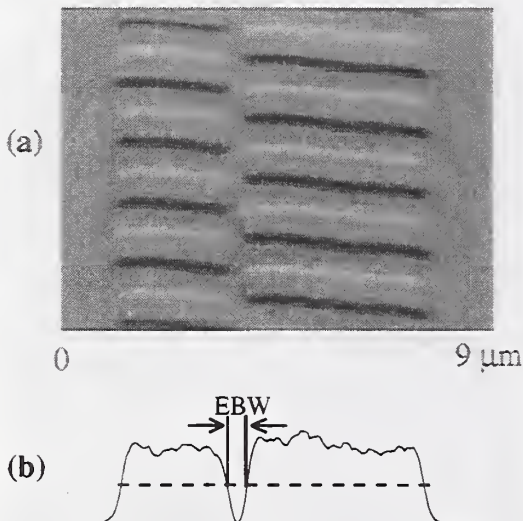


Fig. 4. (a) Averaged MFM image of an overwrite track: $B=0.57 \mu\text{m}$, phase= 180° . (b) The cross-track signal power profile of the tracks in 1(a), the erase band width is indicated by EBW.

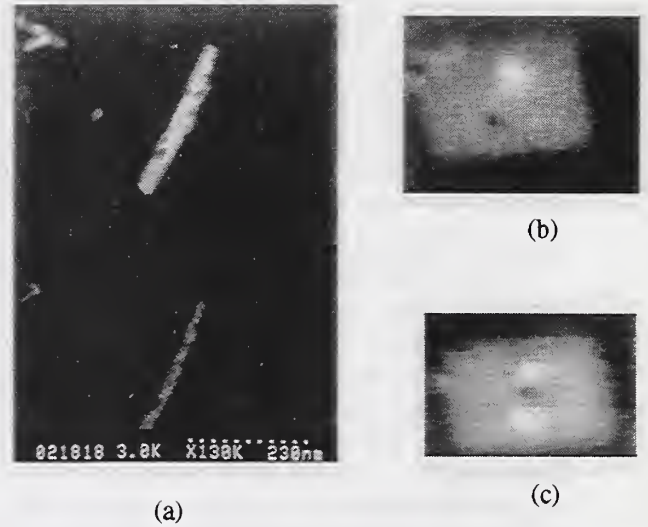


Fig. 3 (a) SEM images of particle C, the upper half is the secondary electron image, the lower half is the backscattered electron image; (b) MFM image of particle C in a single domain state; (c) MFM image of particle C in a multidomain state.

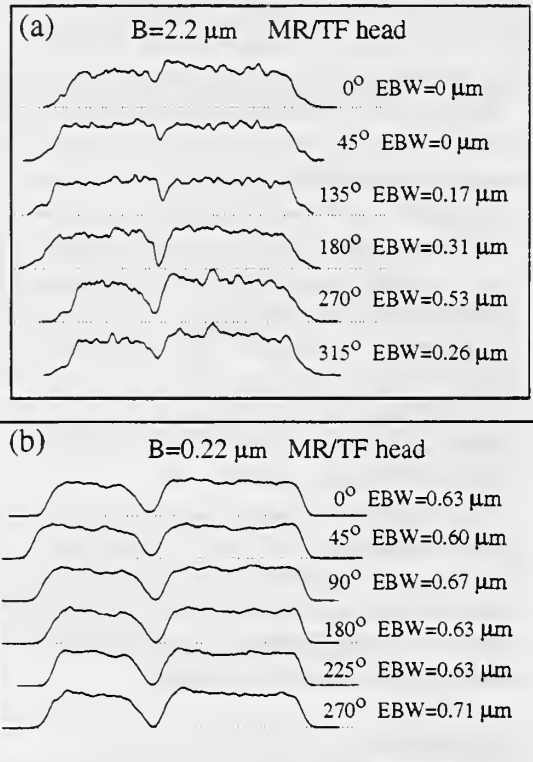


Fig. 5. The cross-track signal power profile for overwrite tracks at different phases, recording head is a MR/TF head. (a) $B=2.2 \mu\text{m}$, (b) $B=0.22 \mu\text{m}$.

Magnetic Force Microscopy in Data Storage: Recent Advances and Applications

Ken Babcock and Virgil Elings

Digital Instruments, Inc., Santa Barbara, CA 93103

The past year has seen a dramatic increase in the use of magnetic force microscopy (MFM) in real-world data storage applications. There are now upwards of 50 MFMs in use, their convenient, high-resolution imaging of surface magnetic fields utilized to evaluate the performance of media and head components. Much of this growth can be traced to significant improvements in reliability and ease-of-use, without sacrificing any of the power of earlier MFMs that required SPM experts for their operation. Specific advances include:

- the development of batch-fabricated scanning probes,^{1,2} sputter-coated with a magnetic alloy. Tip properties such as moment and coercivity can be altered by changing the sputtered magnetic material or its deposition. The result has been wide availability of reliable MFM probes, with properties tailored to specific applications; see Fig. 1.
- the development of a robust, two-pass scanning technique to acquire separate topographic and magnetic data.³ Using LiftMode,⁴ these data types are measured independently for each SPM raster scan line. This renders the technique immune to tip crashes, and allows even rough samples to be scanned reliably, giving the robust performance required for industrial applications. Comparison of topographic and magnetic data gives valuable information about the effects of morphology (eg., media roughness) on magnetization. See Fig. 2.

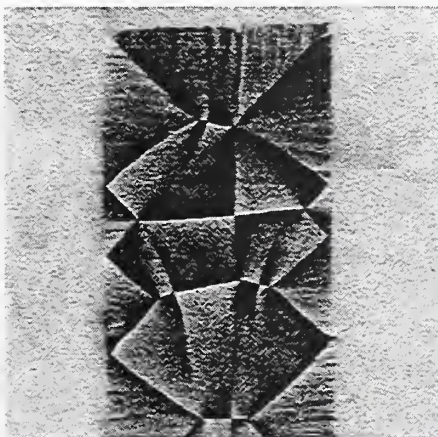


Fig. 1 Magnetic force gradient image of CoZrNb film, used in emerging thin-film heads. A low-moment MFM tip was used to prevent perturbation of the domains in this low-coercivity film.

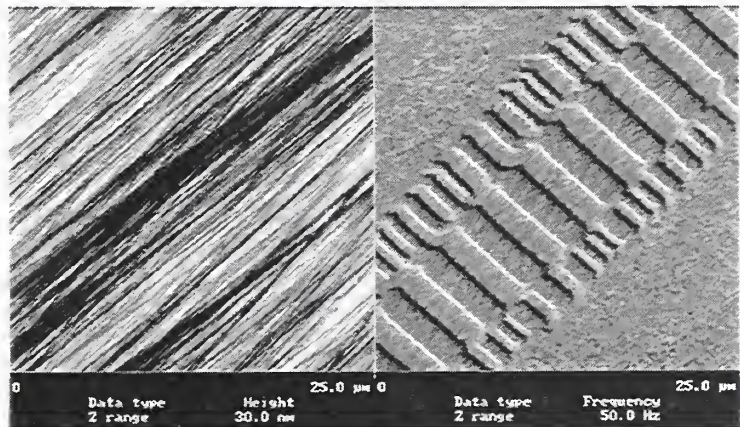


Fig. 2. TappingMode AFM image of hard disk surface texture (left), and magnetic force gradient image (right) of the same area. High frequency data tracks were overwritten with a low frequency periodic signal. Visible are track width, ripple, fringing fields, transition irregularities, and the difference between erased and virgin areas. Such images allow direct, detailed evaluation of head and media performance. Note the complete separation of topographic and magnetic data produced by LiftMode.

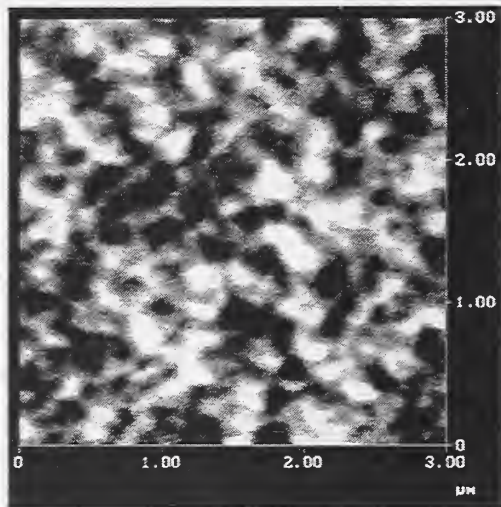


Fig. 3. High-resolution magnetic force gradient image of demagnetized hard disk media, showing random magnetic "clusters" thought to determine media noise and set limits on storage density.

This talk will also give an overview of current and proposed data storage applications, including media development and characterization (Fig. 3), imaging of thin-film head elements, and evaluation of head performance. Time permitting, we will also address issues concerning the use of MFM as a quantitative tool (as discussed by E. Dan Dahlberg in this session), focusing on what MFM, in its current form, can and cannot do in a data storage context. Finally, describe recent work⁵ using MFM probes, in conjunction with an external field H_{ext} , to write "bits" on perpendicular media, and evaluate media coercivity on a submicron scale (Figs. 4,5).

References

1. P. Grütter, D. Rugar, H.J. Martin, G. Castillo, S.E. Lambert, C.J. Lin, O. Wolter, T. Bayer, and J. Greschner, *Appl. Phys. Lett* 57, 1820 (1990).
2. K. Babcock, M. Dugas, V. Elings, and S. Loper, *IEEE Transactions on Magnetics*, 30, 4503 (1994).
3. K. Babcock, M. Dugas, S. Manalis, and V. Elings, "*Magnetic Force Microscopy: Recent Advances and Applications (Invited)*", to appear in proceedings of the MRS Meeting, Boston, November 1994.
4. LiftMode are trademarks of Digital Instruments. TappingMode and LiftMode, V. Elings and J. Gurley, U.S. Patent Nos. 5,266,801 and 5,308,974, Digital Instruments, Santa Barbara, CA.
5. S. Manalis, K. Babcock, M. Dugas, J. Massie, and V. Elings, *Appl. Phys. Lett.*, May 1995.

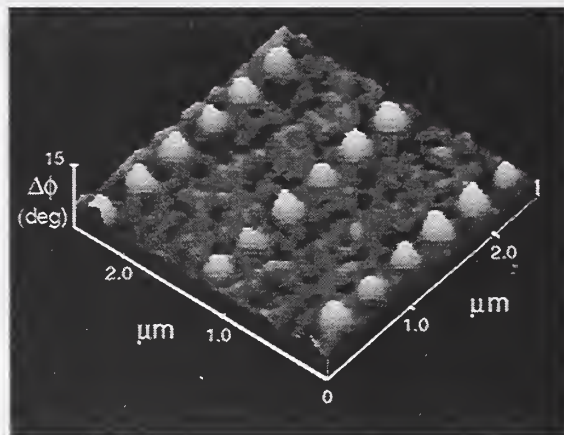


Fig. 4. Magnetic force gradient image of bits written on CoCr/NiFe bilayer perpendicular media (Censtor Corp.). The same tip was used to write and image. The 180 nm bits are spaced 370 nm apart.

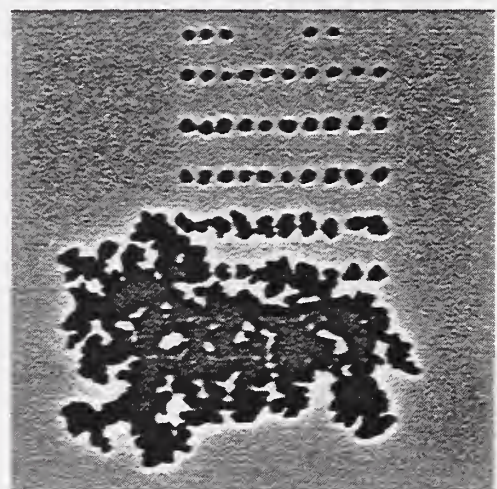


Fig. 5. 25 μm MFM scan of bits written on TbFeCo media (3M Corp.) with H_{ext} decreasing from bottom to top. For the lowermost bits, H_{ext} was strong enough to cause the bits to grow, producing large-scale magnetization reversal.

Critical Dimensioning of Heads - Pole Tip Recession Measurements and Wear

Jim Potter
Maxtor Corporation

In today's ever expanding PC world, the need for storage devices with high capacity extremely fast access time and smaller dimension is always pushing the disk drive manufactures toward high density media and micro geometry in the heads. The small geometry requires tools like the scanning probe microscopy instruments. In the recent past and even currently, optical tools like the WYCO's PTR (Pole Tip Recession) systems, have been used for these measurements. With the ever shrinking technologies, the limitation of the optical systems becomes a problem. The AFM instruments are better suited for the small geometry. Pixel counts of thousands in an AFM image compared to tens or hundred in an optical system seems to make the AFM the instrument of choice. However, the AFM is slow by comparison and not very well suited for a high rate production environment. However, the instrument is becoming an indispensable tool in the laboratory. An issue that came up during a head wear study was the negative effect of an instrument attribute on PTR measurements.

AFM instruments with the movable scanner configuration may cause significant systematic error. Instruments that have the piezo scanner integrated into the sample positioning system are the problem. Most of the instruments commercially available today have routines to subtract the characteristic piezo curvature from data sets. The routine subtracts a best fit polynomial. With the Park Scientific LS, the stage position causes a perturbation in the curvature of the piezo. Thereby, significant error is introduced into the measurement. To make things worse, head have an intrinsic curvature creating another perturbation in the data set. Adding the potential error from the sample positioning issue to the intrinsic head curvature, produces unreliable and often non-reproducible data. The mathematical routines built into the software packages for flattening can not separate the individual contributors, consequently the flattening routines fall short.

The method we have to overcome these issues turned out to be quite laborious and tedious. The instrument has an automated stage, which can only use for the initial sample insertion. A known flat, WYKO standard, was used to characterize the piezo's curvature. Once this is accomplished, the stage or more precisely, the position of the piezo can not be changed. Utilizing this method we were able to characterize a series of heads.

The main thrust of the analysis was to determine the cause of signal degradation in a specific head/media combination. Using AFM, it became obvious very quickly that the source of the signal degradation was not classical wear of the head or of the media, but rather a deposit on the surface of the head.

Characterizing the deposit became more complicated than first expected. The material was on the order of twenty nanometers thick and discontinuous on the surface of the head. Several analytical methods were used in the attempt to identify the source of the material much less obtaining information on the material at all. Auger spectroscopy, XPS, EDS, SEM, and FTIR were all used in attempting to identify this mystery material. Auger spectroscopy found carbon but no traces of the constituents of the lubricant. There was not enough material for the EDS or FTIR. The only instrument that reliably, reproducibly, and easily confirmed the presence of the material was the AFM.

Disk Texture and Lubrication

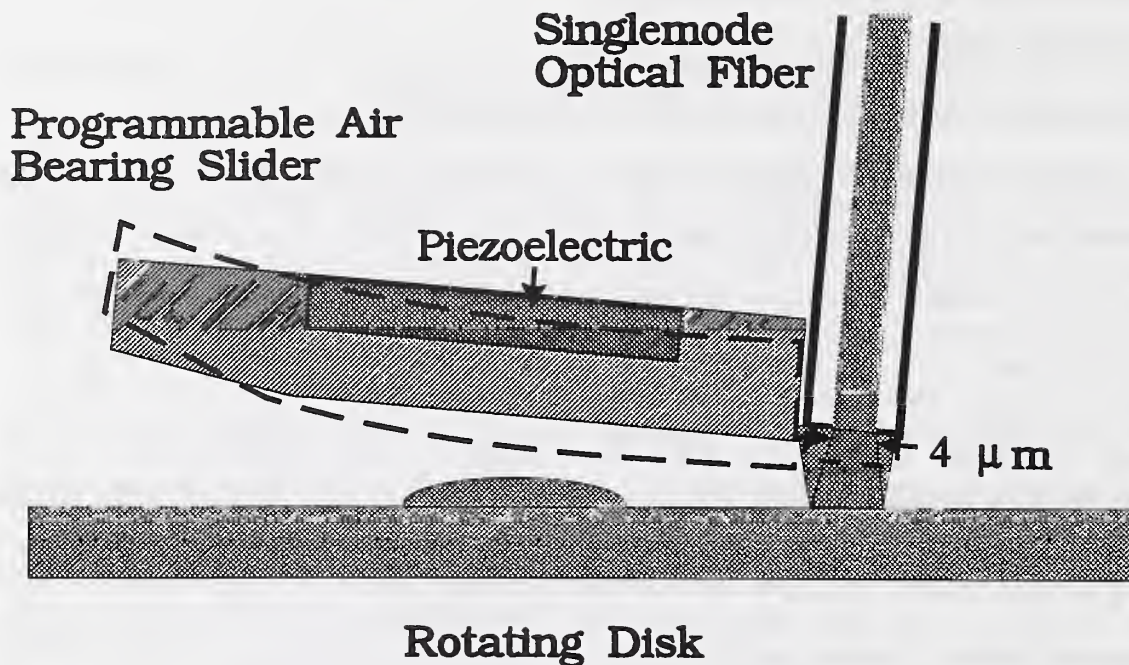
C. Mathew Mate

IBM Almaden Research Center, San Jose, California 95120

Since its invention in 1986 [1], force microscopy has been used extensively to study tribological interfaces important to the magnetic recording industry. Many of the tribological applications of force microscopy were pioneered in our laboratory at IBM Almaden. For example, in 1987 we built the first friction force microscope and reported the first observation of atomic scale friction for a tungsten tip sliding on the basal plane of graphite surface [2]. A few years later, we invented a version of the force microscopy called dipstick microscopy capable of mapping the thickness of lubricant films on surfaces with submicron lateral resolution [3,4]. Since then much of our research with force microscopy has concentrated on understanding how lubricants work at the molecular level to lubricate disk surfaces [5-8]. For example, in 1992 we demonstrated that a simple alcohol endgroup at the end of a perfluoropolyether polymer chain can dramatically increase the load bearing capacity of a molecularly thin film of lubricant [7]. We have also used force microscopy to show that bonding an otherwise liquid polymer to a surface reduces, but does not eliminate, the liquid character of the polymer film [5]. Recently, it has been demonstrated that friction force microscopy can distinguish between different chemical species on a surfaces [9,10]. For example, we observed that different types of carbon surfaces have dramatically different coefficients of friction, μ , at ultra low loads ($<1\mu\text{N}$) [10]: i.e., for graphite, $\mu=0.01$; for diamond, $\mu=0.05$ to 0.3 ; for hydrogenated amorphous carbon, $\mu=0.33$; and for C_{60} , $\mu=0.8$. Information from these AFM tribology experiments have provided valuable insights into the tribological processes occurring at the head-disk interface of the disk drives and is aiding the development of future generations of these products.

The use of force microscopy in disk technology research and development has increased dramatically in recent years due to the commercial availability of force microscopes that can measure both topography and friction properties of disk surfaces. The main application of commercial force microscopes by the disk drive industry is to aid in the development of new texturing processes for disk surfaces that allow the recording head-disk spacing to be reduced while maintaining good friction and wear properties. The main shortcoming of force microscopy for measuring disk morphologies is that it can only map a very small fraction of the disk surface in a reasonable period of time. To get around this shortcoming, we have developed a new type of scanning probe that we call the flying interferometer, which is shown schematically in the figure.

In flying interferometry a single mode optical fiber is attached to the back of a slider that flies over a rotating disk surface. The laser light that exits from the end of the optical fiber reflects off the disk surface and a fraction of the reflected light reenters the optical fiber where it interferes with light internally reflected off the end of the optical fiber. Attaching the optical fiber on a flying slider provides a mechanical feedback system so that the end of the fiber maintains a fairly constant flying height over the disk surface. By varying the voltage applied to the piezoelectric material on the back of a programmable air bearing slider [11], the fly height can be adjusted so that the interference cavity length is at the most sensitive part of the interference fringe for measuring vertical variations in disk morphology. Using a single mode optical fiber provides for a very small laser spot size, as small as $4\mu\text{m}$ in diameter for a 633 nm wavelength laser. The amount



of noise from the optical system is very small and mainly comes from photon shot noise. For $50 \mu\text{W}$ of interference intensity the rms photon shot noise is about an Angstrom for a 100 MHz bandwidth. We have used this technique to scan an entire disk surface in a few minutes with $5 \mu\text{m}$ lateral resolution to map out the important features of the disk topography such as texture, defects, and wear.

References

1. G. Binnig, C.F. Quate, Ch. Gerber, *Phys. Rev. Lett.* 56 (1986) 930.
2. C.M. Mate, G.M. McClelland, R. Erlandsson, and S. Chiang, *Phys. Rev. Lett.* 59, (1987) 1942.
3. C.M. Mate, M.R. Lorenz, and V.J. Novotny, *J. Chem. Phys.* 90, (1989) 7550.
4. C.M. Mate, M.R. Lorenz, and V.J. Novotny, *IEEE Trans. on Magnetics* 26, (1990) 1225.
5. G.S. Blackman, C.M. Mate, and M.R. Philpott, *Phys. Rev. Lett.* 65, (1990) 2270.
6. C.M. Mate and V.J. Novotny, *J. Chem. Phys.* 94, (1991) 8420.
7. C.M. Mate, *Phys. Rev. Lett.* 68 (1992) 3323.
8. M. Binggeli and C.M. Mate, *Appl. Phys. Lett.* 65 (1994) 415.
9. R.M. Overney, E. Meyer, J. Frommer, D. Brodbeck, R. Luthi, L. Howald, H.-J. Guntherodt, M. Fujihira, H. Takano, and Y. Gotoh, *Nature* 359 (1992) 133.
10. C.M. Mate, *Wear* 168 (1993) 17.
11. U.S. Patent 5,021,906.

Survey of Industrial SPM Needs and Opportunities

G.S. Blackman and S.A. Riggs
Central Research and Development
E. I. Dupont de Nemours Inc.
Wilmington DE

Scanning probe microscopy (SPM) has changed rapidly over the last few years as reflected in the burgeoning list of acronyms associated with the field. Improved instrument and cantilever fabrication have allowed researchers to focus less attention on instrumentation and more attention towards application issues. There are many challenging areas in the polymer and coatings industry where SPM's provide novel information that is not available through any other technique. I will address three broad areas of application of scanning probe microscopy to problems of industrial relevance: high resolution three dimensional imaging of polymers, microtribological imaging where the SPM is used not only as a imaging device but also as a micromechanical probe, and finally I will discuss the newest area utilizing a modified SPM to probe chemical differences at surfaces.

The most straitforward and by far the most exploited aspect of the AFM (Atomic Force Microscope) is its use as a high resolution microscope. The primary advantage of the AFM is that it provides complete three dimensional images of a surface. In some cases, subtle but important changes in surface morphology are difficult to detect with other techniques. I will discuss the use of the AFM to analyze defect structure in coatings on polymer films, and to image the surface morphology in non-contact mode of very soft polymers. Many coatings perform a dual role of protecting the underlying substrate from the environment and of providing a pleasant high gloss appearance. We have used the AFM to investigate both aspects on automotive coatings. I will present some recent results on wear of automotive coatings and the relation of real surface topography to appearance. Despite numerous efforts there are few successful examples of molecular resolution of polymers. A challenge for the future will be to improve the resolution in contact, noncontact, and tapping mode imaging by better control and measurement of tip geometry.

Another promising area of research is to use the AFM cantilever as a micromechanical probe of surfaces. Much of what we know of tribology comes from macroscopic measurements, but with the new techniques we have an opportunity to measure friction, wear and lubricant properties on a nanometers scale. Non-contact microscopy and the so-called dipstick microscopy (Mate et al.) enable the study of thickness and distribution of liquid films and lubricants on surfaces. Nanowear of thin protective films, nano hardness and elastic moduli can all be measured with high spatial resolution. I will describe experiments using the AFM to investigate nanometer scale wear processes in thin films.

The major weakness in all of the scanning probe techniques has been the lack of chemical sensitivity, one atom or molecule or bump looks much like any other. One of the most exciting recent developments in the SPM literature is the ability to map chemically distinct domains on the surface

of phase segregated materials. A promising probe of chemistry at surfaces is force modulation microscopy which has been used by Maivald et al., Overney et al., and Motomatsu et al. to image phase segregated organic films. The early work by Meyer et al. demonstrated the power of lateral or friction force microscopy to distinguish hydrocarbon from fluorocarbon domains in mixed Langmuir-Blodgett films. The recent work by Frisbie et al. extends the LFM technique by chemically modifying the cantilever tip to probe specific interactions between chemically distinct regions of the surface. In the years to come the chemical probes of surface structure will have an impact in the polymer and coatings industry.

Imaging Polymers using Topographic and Chemical Contrast

Donald A. Chernoff, Advanced Surface Microscopy, Inc.,
6009 Knyghton Rd., Indianapolis, IN 46220

Topographic imaging of polymers has been a powerful tool for several years. Using the extraordinary height sensitivity and wide scan capability of the AFM, we are often able to answer simple (but important) questions about surfaces and surface features, including:

- Is a contaminant present?
- Is a coating discontinuous?
- Is a feature a pit or a peak?
- How tall is it?
- What is the particle or molecular size?

The following table outlines a number of applications which have practical importance in a diverse group of industries.

<u>Performance issue</u>	<u>Example</u>	<u>AFM approach</u>
Defect analysis	Food can coatings	Pit or peak, particle size and shape
Appearance (haze, sheen)	Packaging	Pit or peak, height of texture features
Data Storage	Compact discs	Coating thickness of master Bump and pit dimensions on stamper and replica
Wettability	Chemically- treated textiles, implants Medical diagnostic reagent coatings	Coating continuity Detect contaminant
Adhesion failure	Coatings, Joints	Determine failure mode (adhesive or cohesive) by distinguishing substrate from residue
Materials processing	Polymer blends Wood pulp refining Molecular size distribution	Phase distribution Distinguish lignin from cellulose Image molecules directly

In many instances, topographic information alone is not sufficient. We are using the TappingMode™ AFM in a new way to get chemical contrast based on adhesion. This rapid imaging technique provides high lateral resolution (10-20 nm) using standard probes. We will show examples in several different material systems, as well as a correlation of adhesion with lateral force contrast.



Figure 1. Height (left) and adhesion (right) images of a wood pulp fiber. The adhesion image shows fine structure which is difficult to see in the height image, due to the rough topography. Thin patches of lignin (bright areas in the adhesion image) cover the cellulose microfibrils.

Imaging of Cryo-Ultramicrotomed Sections of Isotactic/Atactic Polypropylene by Scanning Tunneling Microscopy

G. W. Zajac

Amoco Research Center, Amoco Corporation

P O Box 3011

Naperville, IL 60566-7011

Imaging of polymeric materials by scanning probe microscopy is problematic although success has been achieved at the molecular scale by atomic force microscopy in specially prepared thin films. A novel approach to molecular scale imaging of bulk polymers (1) has permitted near molecular resolution imaging of polyethylene. The technique involves cryo-ultramicrotomed sections of bulk polymer samples which are amorphous carbon coated to provide the needed surface conductivity for tunneling microscopy to be performed. Our previous efforts at scanning tunneling microscopy (2) of such sections of isotactic polypropylene permitted observation of the lamellar structure with dimensions of order 100-250 Angstrom. Within ordered regions of these lamellae we often found characteristic separation of features which we have associated with the pendant methyl groups between adjacent propylene monomer units in the isotactic form. Molecular modeling of the 3-sub1 helix of the isotactic form of polypropylene indicates that the methyl-methyl separation is 6.6 Angstrom. In this presentation we extend the selection of polypropylene materials imaged by STM to include highly crystalline polypropylene where x-ray diffraction measurements indicate over 60 % volume percent crystallinity. The lower limit of crystallinity observed by XRD is obtained in isotactic/atactic polypropylene materials where < 20% crystallinity is found. The STM imaging of this wide range of crystalline polypropylene materials will be presented. The correlation of ordered domain dimension as measured by STM imaging with percent crystallinity from XRD is demonstrated. Among the least crystalline polypropylene materials (<20% crystalline) the STM imaging provides a measure of the relatively small ordered domain dimension (50-100 Angstrom) and a glimpse into the nature of the macromolecular organization at the nanometer scale within these ordered regions. From a hard-segment soft-segment perspective in copolymers the nature of the elastic interactions of these materials can be obtained by consideration of the uniquely folded structure glimpsed by the STM imaging. An attempt to heuristically understand the elastic properties of this wide range of crystalline polypropylene materials is presented in the context of the observed STM crystalline ordered dimensions.

- 1) D. H. Reneker, J. Schneir, B. Howell, H. Harary, *Polymer Commun.* 31, 167 (1990).
- 2) G. W. Zajac, M. Q. Patterson, P. M. Burrell and C. Metaxas, *Ultramicroscopy* 42-44, 998 (1992).

Adhesion Interactions in Latex Films

M. Cynthia Goh

Department of Chemistry, University of Toronto, Toronto, Ontario M5S 1A1

In this presentation, I would like to discuss interactions in soft latex leading to film formation, and how we have utilized the AFM to investigate the quantitative aspects of such. For these studies, as well as for others in which sample features are of comparable dimensions with the AFM probe tip, it is important to address the issue of tip-sample convolution effects, which I will also discuss.

Annealing of latex

Film formation from soft latex of polybutyl methacrylate (PBMA) begins with the evaporation of the solvent which compresses the individual particles isotropically producing an arrangement into rhombic dodecahedra in the bulk [1]. A robust film is obtained by drying above the minimum film forming temperature (MFFT), and by annealing to allow interparticle diffusion. Figure 1 shows the surface of such a film. Below the MFFT, one can see micro-cracks developing in the nascent film.

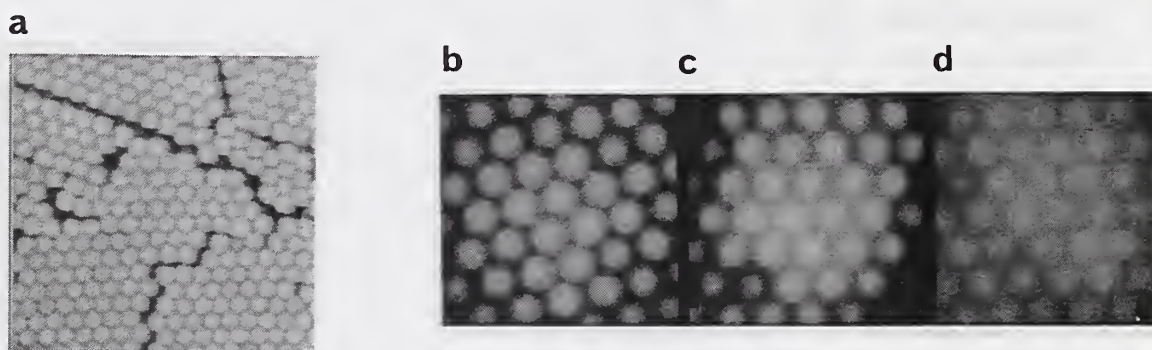


Figure 1. Films made from PBMA latex with 337 nm particle diameters. (a) solvent cast and dried below the MFFT. Solvent cast film dried above the MFFT for 4 hours, and annealed at 70 °C for (b) 2 h, (c) 12 h, (d) 55 h. (b), (c) and (d) are on the same grey scale.

Since the AFM is a relatively non-destructive probe, we are able to follow the evolution of the same film as after various annealing times at high temperature [2]. The films we studied were carefully prepared to show a high degree of order and flatness; this enabled us to quantify the changes in surface corrugations as a function of annealing time (Figure 2). These changes in corrugations are due to particle

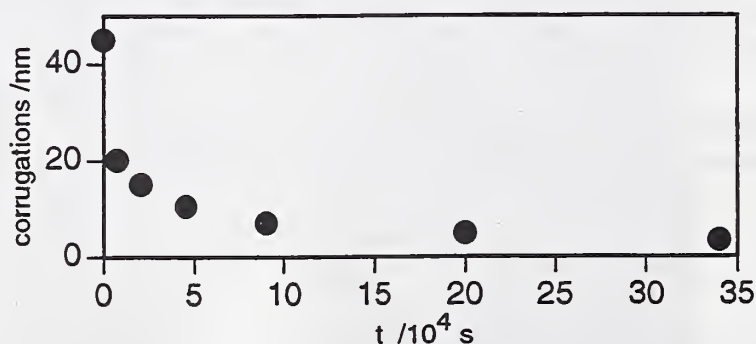


Figure 2. Change in corrugations with increasing annealing time.

interpenetration by migration of polymers across the interfaces. A simple model of spreading by Brownian diffusion provides an estimate of a diffusion time of 10^{-13} cm²/sec for these surface particles, which is 4 orders of magnitude faster than the measured value for bulk latex.

Tip inspection and image reconstruction

In our studies of non-crystalline materials, especially polymers and biopolymers, one important issue that arises is the presence of tip artifacts that may produce misleading images. It has been pointed out by numerous authors that the AFM image is a convolution of the tip and sample geometry, and is thus necessarily distorted. At the very least, the sample will appear broad, but in the case of a deformed tip, the picture obtained may have very little qualitative resemblance to the sample, but rather mirror the tip imperfections.

To address this issue and enable us to distinguish between artifacts and real data, we developed numerical algorithms that for in situ tip inspection and removal of tip geometry from AFM images [3], utilizing the principle that the tip and sample cannot both occupy the same location in space, and that the AFM topographic information is collected with the assumption that the apex of the tip is in contact with the sample. This procedure, sketched in Figure 2, is simple to implement since the AFM image is a two-dimensional array of height information, and the tip geometry can thus be processed out of the picture.

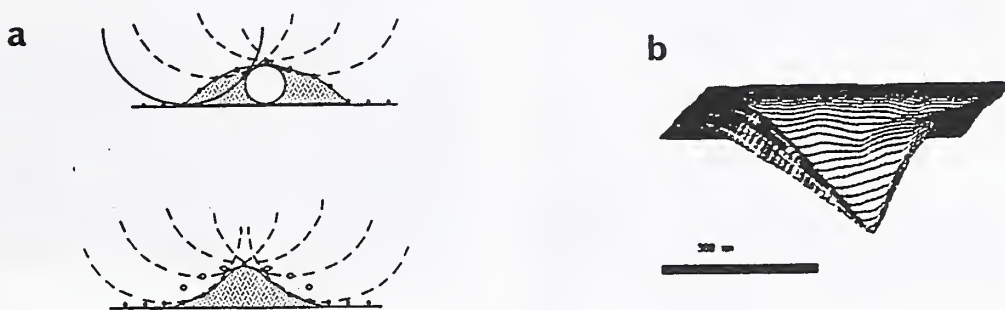


Figure 3. (a) Schematic of the numerical procedure for processing to remove the tip geometry. (b) Picture of the probe tip visualized in situ using polystyrene spheres and (a).

This process is reciprocal: that is, given a known sample geometry, it can be processed out of the AFM image, leaving behind a picture of the tip (Figure 3b). This procedure thus provides a systematic way of evaluating whether a particular tip is of reasonable quality; if not, it must be replaced prior to actual studies. Furthermore, with this tip information, we can process it out of the subsequently obtained images to produce a more accurate representation, which can sometimes be dramatically different from the original [3,4]

Conclusions

We have utilized the AFM for qualitative and quantitative studies of latex film formation. At these mesoscopic length scales, the capability for in situ tip inspection and image processing for removal of tip artifacts is important in producing reliable results.

References

1. Y Wang, et al. *Langmuir* **8**, 1435 (1992).
2. MC Goh, et al. *Langmuir* **9**, 1319 (1993)
3. P Markiewicz, MC Goh *Langmuir*, **10**, 5 (1994); *Rev Sci Instrum* **66**, 3186 (1995).
4. MS Pollanen, P Markiewicz, C Bergeron, MC Goh, *Am J Pathology* **144**, 869 (1994)

ADHESION OF SMALL PARTICLES

H. A. Mizes

Wilson Center for Research and Technology
Xerox Corporation
800 Phillips Rd. 114-23D
Webster, NY 14580

INTRODUCTION

Toner particles used in xerographic printing are roughly 10 μm polymer particles that must be moved controllably from one surface to another.[1] Improvements in the technology to enable this movement are made easier with a better understanding of the fundamentals of particle adhesion. AFM techniques can lead to this understanding by probing the adhesion of single particles. More generally, an understanding of particle-substrate adhesion also impacts other industrial applications such as particle contamination in semiconductor or optical processing

Particle-substrate adhesion depends on many physical and chemical characteristics of both the particle and the substrate. The work we performed with AFM focuses on three of these: the relationship between the roughness of the surfaces and variations in the adhesion, material inhomogeneities on the scale of the particle, and changes in adhesion that occur in an electric field.

Adhesion measurements are extracted from AFM loading curves.[2] The particles are attached to commercial silicon nitride microfabricated cantilevers.

SURFACE ROUGHNESS DEPENDENCE

If the adhesion between two curved surfaces is dominated by long range forces such as the Van der Waals interaction, then the Derjaguin approximation[3] gives the geometric dependence of adhesion F_A as

$$F_A = W \left(\frac{R_p R_s}{R_p + R_s} \right)$$

where R_p and R_s are the radii of curvature of the particle and the surface at the point of contact. For rough surfaces and particles, the radii at the point of contact depend on where the contact is made. In fig. 1 are shown AFM data from topographic and adhesion measurements from which the Derjaguin approximation can be quantified. From the

topography scan, the distribution of curvatures can be determined. From the adhesion map[4], which is extracted from a series of force curves taken over a grid pattern on the surface, the variations in the local adhesion can be determined. This kind of measurement has been taken on a series of surfaces of different roughnesses, and the data is observed to agree quite well with the Derjaguin approximation.

The adhesion of a rough particle to a surface depends on how the particle orientates on the surface and which protrusion makes contact. AFM and other techniques have been used to quantify the particle roughness and through simulated contacts a distribution of adhesions for a particle rough particle to a surface can be determined.[5] It has been found that the adhesion of the polymer particles used in xerography are much less than that for a perfect sphere of the same diameter.

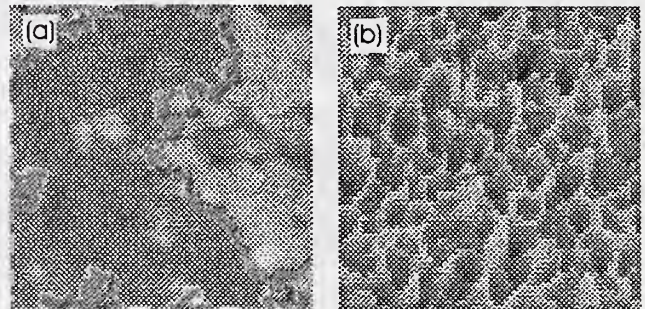


Figure 1: (a) topographic image of polysilicon. (b) adhesion map to the same surface. Whiter areas correspond to higher local adhesion.

MATERIAL DEPENDENCE

Material inhomogeneities in either the substrate or the particle can affect adhesion. Two materials may have a different surface energy, polarizability, or something else that gives rise to a different local adhesion. These may be caused by nonuniformly adsorbed contaminants on the surface, phase separation of blended polymers, or a

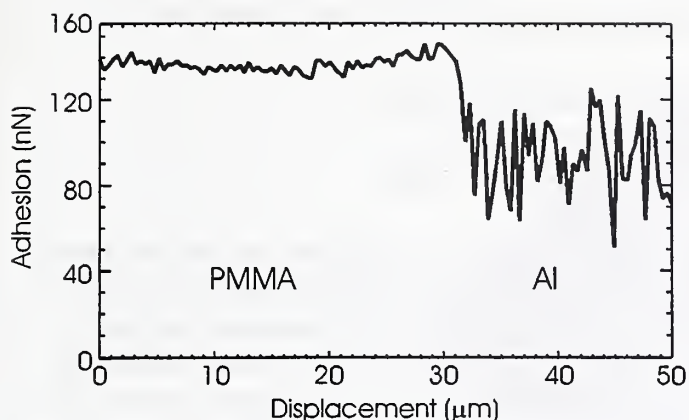


Figure 2: Adhesion near the interface between PMMA and Aluminum. The fluctuations in the aluminum adhesion are due to surface roughness.

multitude of other reasons depending on the system. Adhesion measurements can identify these inhomogeneous regions on a local scale. This is illustrated in fig. 2, where adhesion was extracted from a series of loading curves taken across the interface between an PMMA film and an aluminum surface. The resolution of the local adhesion measurement is on the order of the area of contact between the particle and surface. This measurement has been used to quantify how particle-substrate adhesion changes when the particle surface is intentionally modified to lower adhesion.[6]

ELECTRIC FIELD DEPENDENCE

In xerography, the particles are moved by applying an electric field. In an electric field, the force of adhesion becomes

$$F_A = F_0 + \alpha q^2 - \beta qE + \gamma E^2$$

where F_0 are all the nonelectrostatic contributions to adhesion, q is the charge on the particle, E is the electric field, and α , β , and γ are terms that depend on the particle geometry. The second and fourth terms on the right hand side increase the adhesion and are due to the attraction of the particle to its image charge and image dipole. The third term lowers adhesion and is the force on the particle's charge in the electric field.

We have looked the fourth term by applying an electric field across an uncharged glass sphere. The glass

sphere is held just above the surface, and in the electric field the attractive force generated will bend the cantilever downward. The attraction as a function of applied field is shown in fig. 3. This attractive force adds to the nonelectrostatic adhesion forces when the particle is in contact. The adhesion increases quadratically with field, as expected. The rate of increase is much larger than expected from theory however, and the sensitivity of surface conductivity due to adsorbed water is explored.[7]

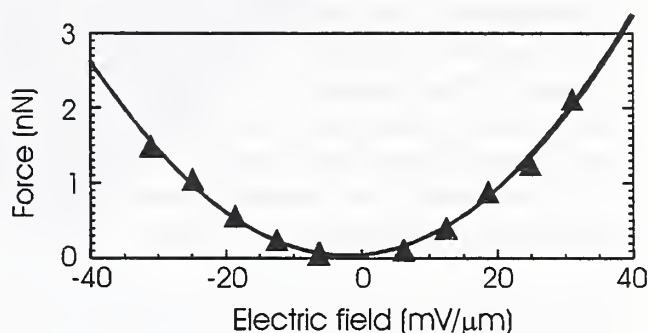


Figure 3: Additional attractive force acting on a particle in an electric field.

CONCLUSIONS

The sensitivity of the AFM to small forces provides a unique tool to probe the physical characteristics of the adhesion of small particles. We have illustrated here how surface roughness, material inhomogeneities, and electric fields modify particle adhesion.

REFERENCES

1. L. B. Schein, *Electrophotography and Development Physics*. Springer, New York (1988).
2. N. A. Burnham and R. J. Colton, *J. Vac. Sci. Technol. A* 7, 2906 (1989).
3. J. N. Israelachvili *Intermolecular and Surface Forces*, 2nd edition, Academic Press, London, 1981, p. 161-164.
4. H. A. Mizes, K.-G. Loh, R. J. D. Miller, S. K. Ahuja and E. F. Grabowski, *Appl. Phys. Lett.* 59, 2901 (1991).
5. H. A. Mizes, to be published in the *Journal of Adhesion*, 1995.
6. M. L. Ott and H. A. Mizes, *Colloids and Surfaces A* 87, 245 (1994).
7. H. A. Mizes, *J. Adhesion Sci. Technol* 8, 937 (1994).

Force Modulation Atomic Force Microscopy of Polymer Coatings

Andrew G. Gilicinski and Charles R. Hegedus -
Air Products and Chemicals, Inc.
7201 Hamilton Blvd. Allentown, PA 18195

Modern coatings development is being driven by environmental regulations and worker safety concerns regarding volatile organic content in paints and coatings. A resulting trend is the development of waterborne coatings. A key challenge is promoting film formation to obtain good barrier properties in waterborne systems. Few analysis tools exist to directly probe the extent of film formation. In earlier work, surface imaging by tapping mode atomic force microscopy was shown to be such a probe for coatings prepared from aqueous dispersions of 40-60 nm particles of acrylic/polyurethane hybrid polymers.¹ Film formation was ranked based on number density and extent of protrusion of uncoalesced polymer particles. The use of tip characterizers improved accuracy in identifying particles protruding from the coating surface.²

One limitation of AFM is the inability to identify the chemical nature of topographic features. This limited the ability to study polymer blends and to investigate the mechanisms responsible for extent of film formation. The recent development of force modulation AFM (FM-AFM) promises mechanical information to complement topographic data.³ FM-AFM is a modified contact-mode AFM with a small, rapid vertical (z) modulation applied during the scan. Stiff areas deform less than softer areas and therefore deflect the cantilever more during the modulation. Variation in cantilever deflection amplitude can thus be used to measure the relative stiffness of the surface. Average dc deflection provides topographic information.

FM-AFM was used to image topography and modulus of latex coatings. Single component coatings yielded topographic images of smooth surfaces for a good film former and bumpy surfaces of uncoalesced particles for a poor film former. Modulus images showed relatively uniform behavior for both single component coatings. FM-AFM was also used to analyze coatings from a 1:1 blend of the polymers. Topography was midway between that of single component coatings. Modulus images showed dramatic differences, with uncoalesced particles clearly showing higher stiffness (due to higher acrylic Tg) than surrounding coalesced regions.

Coating blends were generated with a range of added solvent and low heat bake treatments, both of which are thought to promote film formation by allowing polymer chains to expand and become mobile. The effect is especially pronounced for the higher Tg acrylic. FM-AFM results showed improved coalescence for the higher Tg polymer and appear to provide direct evidence for the effect of low heat baking and solvent addition on film formation in this latex system.

¹ Poster, R. M. Rynders, J. R. Stets, A. G. Gilicinski, "Use of Tip Standards in AFM Studies of Silicon Surface Roughness and Polymer Coating Morphology," First Industrial Applications of SPM Workshop, March 24-25, 1994, NIST, Gaithersburg, MD.

² R. M. Rynders, C. R. Hegedus, A. G. Gilicinski, "Characterization of Particle Coalescence in Waterborne Coatings Using Atomic Force Microscopy" *J. Coatings Technology*, in press (June 1995).

³ M. Radmacher, R. W. Tillman, H. E. Gaub, "Imaging Viscoelasticity by Force Modulation with the Atomic Force Microscope" *Biophysical J.* 64 (1993) p. 735-742.

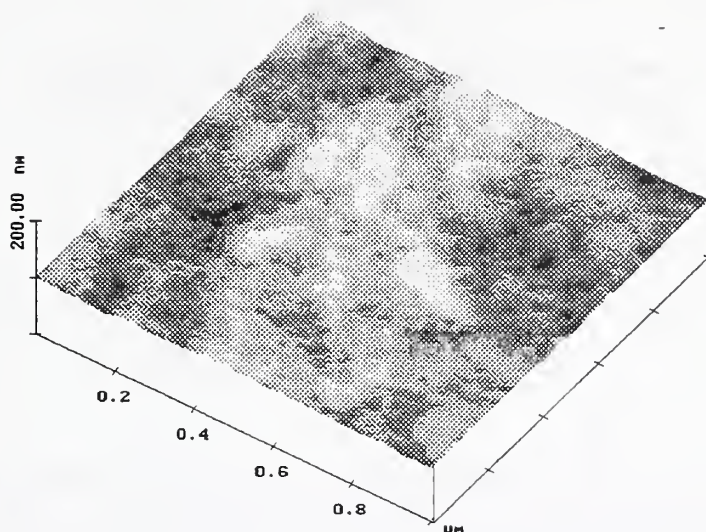


Figure 1. Coating formed from an aqueous dispersion of 40-60 nm particles of an acrylic/polyurethane hybrid polymer (acrylic with a low acrylic T_g) imaged by atomic force microscopy. Good film formation is reflected in the relatively smooth surface topography.

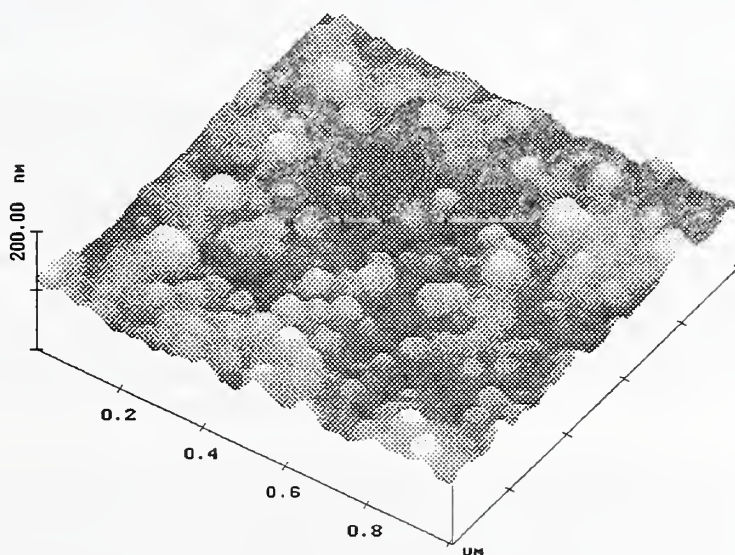


Figure 2. Coating formed from an aqueous dispersion of 40-60 nm particles of an acrylic/polyurethane hybrid polymer (acrylic with a high acrylic T_g) imaged by atomic force microscopy. Uncoalesced polymer particles are observed protruding from the surface.

AFM-Based Mechanical Property Measurements on Polystyrene Surfaces

Gregory F. Meyers and Benjamin M. DeKoven
The Dow Chemical Company, Midland MI 48667

and

Steven M. Hues and Richard J. Colton
Code 6170
Naval Research Laboratory
Washington, D.C. 20375-5342

The atomic force microscope (AFM) has been used to probe the surface of glassy polystyrene (PS) surfaces. The focus of this work has been to understand the mechanical response of PS surface layers to the AFM tip in both scanning (shear) and indentation (compression/tension) modes. For our initial work we have prepared a series of atactic, monodisperse PS thin films (~2 μm thick on silicon wafers) ranging in molecular weight (MW) from 12,000 to 1,000,000 amu.

The interaction of the AFM tip with the PS surface while scanning under constant load leads to the production of unique nanoscale morphologies [1,2]. We have found for the first time that this morphology is dependent upon the PS molecular weight, producing *abrasion* patterns for MWs less than 24,000 amu and a fully developed *oriented* pattern for MWs above 100,000 amu. The marked transitions in the patterning and the evolution of the patterning as a function of time are indications of the elastic nature of the PS surface [2].

Nanoindentation experiments using an AFM [3] were performed at the Naval Research Laboratory on the PS films described above and have produced quantitative measurements of the absolute elastic modulus of the PS surfaces [4]. Using a 2000 μm spherical glass indenter to penetrate to depths of less than 50 nm, a surface elastic modulus may be calculated from the initial unloading portion of the force vs. penetration depth curve. Values for the surface modulus are found to decrease with decreasing molecular weight (mean values of 540 MPa for a 1,000,000 MW; 380 MPa for a 215,000 MW; and 190 MPa for a 35,000 MW). The MW dependent mechanical behavior of the PS surfaces in both shear and compression/tension is best explained by either a change in chain entanglement density or a change in free chain-end density.

The behavior of the PS surfaces during scanning (under shear) suggests that the elastic modulus of surface layers of PS may be substantially different than the bulk. The nanoindentation studies are currently being continued in order to examine how the elastic modulus changes as one probes deeper into the bulk. Among the important developments which have made this work possible are: consideration of the sample stiffness relative to the cantilever [5,6]; detailed study of the error introduced by hysteresis and creep in actuators used for surface or tip movement [7]; and the use of spherical indenters in nanoindentation [3,8].

-
- [1] Leung, M.; Goh, M. C. *Science* 1992, 255, 64.
- [2] Meyers, G.; DeKoven, B.; Seitz, J. *Langmuir* 1992, 8, 2330.
- [3] Draper, C. F.; Schaefer, D.M.; Colton, R.J.; Webb, S.C.; Hues, S.M. submitted to *J. Mater. Res.*
- [4] Schaefer, C.; Draper, C.; Colton, R.; DeKoven, B.; Meyers, G.; Ho, T.; Wynne to be presented at STM '95, July 23-28, 1995, Snowmass Village, CO.
- [5] Radmacher, M. ; Tillmann, R.; Fritz, M.; Gaub, H. *Science* 1992, 257,1900.
- [6] DeKoven, B.; Meyers, G. in preparation for *Tribology Letters*
- [7] Hues, S.; Draper, C.; Lee, K.; Colton, R. *Review of Scientific Instruments* 1994, 65(5), 1561.
- [8] Field, J. S.; Swain, M.V. *J. Mater. Res.* 1993,8, 297.

Current and future applications of In-line Atomic Force Microscopy for Semiconductor Wafer Processing.

Neal T. Sullivan
Digital Semiconductor
Hudson, MA
nsullivan@enet.asdg.dec.com

The AFM has begun a migration from the strict laboratory (off-line) usage to an in-line usage with the successful system implementation of; “non-contact” (or low contact) imaging modes, large sample imaging capabilities and fully automated wafer handling. Essential to this migration is the level of automation and robustness required for successful integration into the semiconductor fab environment. User friendliness, often neglected in order to achieve a high level of functionality in the lab, will many times be one of the most critical factors for a successful wafer fab implementation. Current areas of research into tip-sample interactions, tip characterization (including wear and shape extraction), and quantitative data extraction and analysis move from a secondary status in the lab environment, where greater emphasis is often placed upon qualitative image information, to that of a primary output attribute in the fab environment where numerical output is the dominant currency for the exchange of information.

The current state of integration of an in-line AFM into the process environment at Digital Semiconductor’s Fab6 facility is discussed. Several z dimension measurement applications examples, where in-line implementation has resulted in significant savings of time and money in a development / manufacturing environment, will be presented. The first of these, shown in Figure 1, demonstrates the capability of the AFM to perform etch micro-loading measurements.

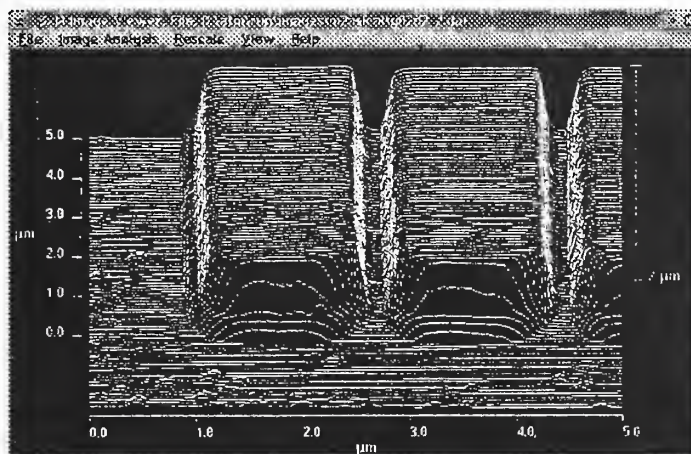


Figure 1: Example of etch micro-loading

The measurement of interest here is the difference in the oxide height between the dense packed lines and the open area (Figure 1). Traditionally this information is collected from a destructive cross-section measurement in an SEM. The information obtained in this way is not easily converted into quantitative results without a subjective measurement. With the AFM the height difference is easily obtained and, being a relative measure, is highly accurate.

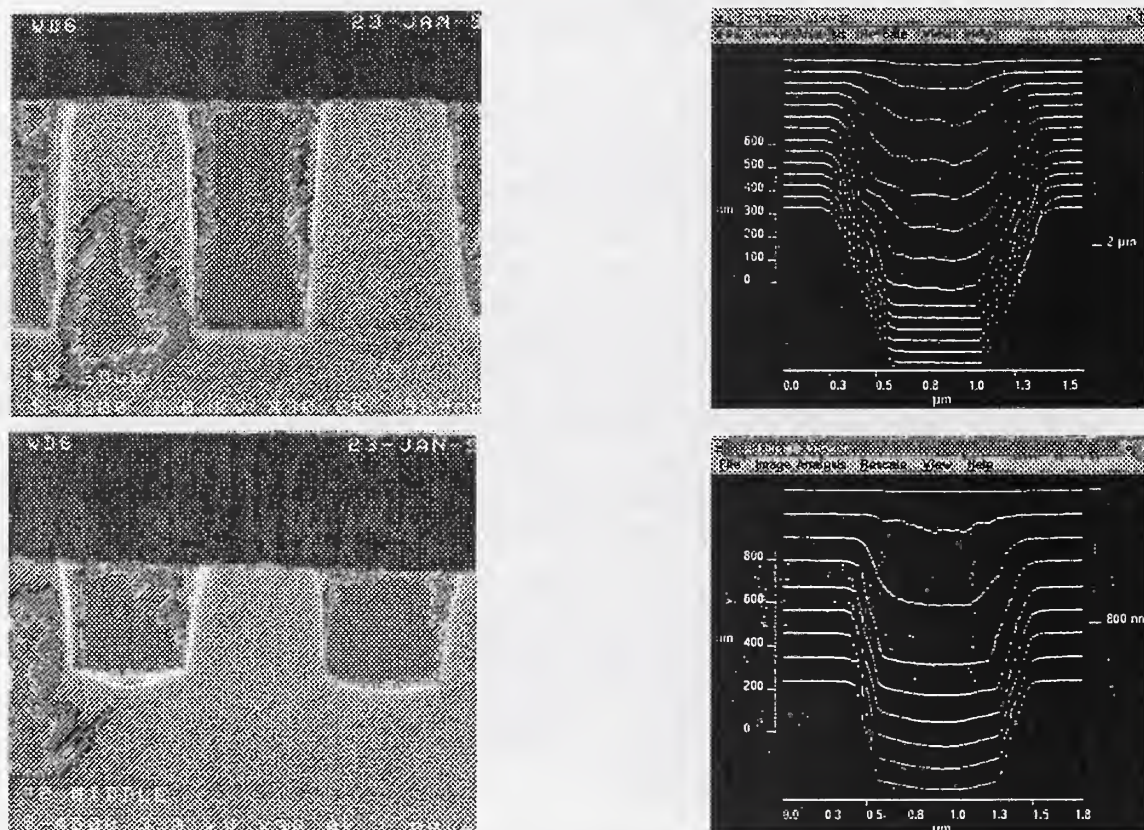


Figure 2: Example of contact etch depth measurement

The second example of a z dimension measurement is that of the contact depth measurement and is shown in Figure 2. A top down SEM image does not provide the information required to determine the depth of the contact. Here again, the data is typically obtained from an off-line destructive cross-section SEM measurement. The cross-section brings with it the associated subjective measurement errors and a delay in obtaining the data associated with the transport of the sample to the lab area, lab queue time and sample preparation, which is in many cases measured in days. As can be seen from the left portion of Figure 2, it is clear that the lower SEM image portrays a contact of shallower depth than the contact of the upper image. The information contained in the SEM images is not readily translated to numerical data without human intervention (ruler, calipers and etc.). The corresponding AFM images however, (Figure 2 - right), are merely graphical representations of the height (z dimension) information at each of the x and y coordinate locations, and as such easily yield quantitative results.

Of prime importance when interpreting AFM data is the interaction of the sample with the tip. Ignorance of this interaction is at the user's peril. It is absolutely essential that the impact to the measurement data from the tip-sample interaction be understood for each of the samples imaged, for this impact will always be present and will be vastly different for a given sample or measurement. In order to understand the tip - sample interaction, it is critical to know the tip shape. One of the simplest, and perhaps most effective methods for understanding the tip shape is to scan a sample of known geometry. Figure 3 depicts the evolution of a single tip, using a standard sample, over several hundred scans in a production environment (. As can be seen from the figure the scan of the standard appears to broaden over time, indicating that the tip itself is becoming dull.

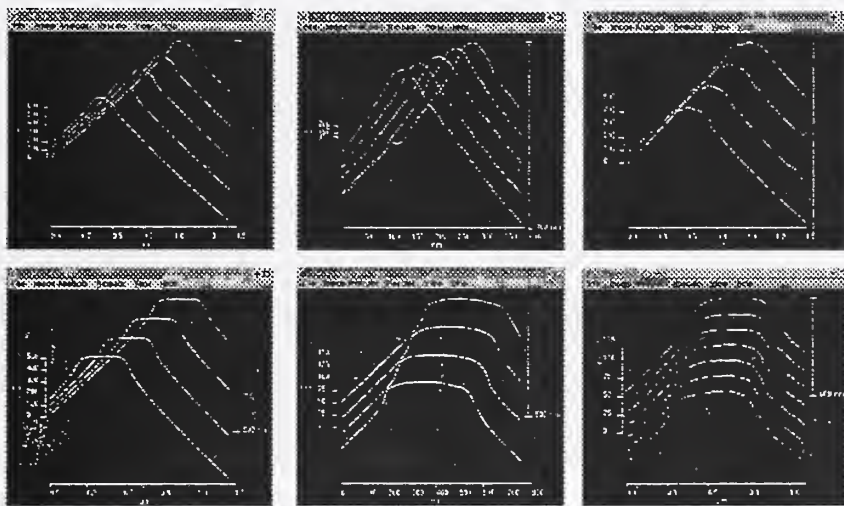


Figure 3: Evolution of a conical AFM probe tip

This information, when combined with an understanding of the relevant sample attributes and a knowledge of the measurement performed, provides an adequate basis for proper interpretation of the measurement results.

The final z dimension measurement capability of the AFM to be discussed with respect to semiconductor applications is the surface roughness measurement. This is measurement for which the AFM garnered its initial notoriety in the industry, for it is the only tool capable of directly (and non-destructively) measuring the nano-scale roughness' typically encountered in semiconductor processing. As more data was collected in this area by industry researchers, the methods for quantification of results, consistency of results over time and between labs and most importantly tip-to-sample interactions, became major issues. Table 1 lists typical RMS roughness values for some of the critical semiconductor films. The capability to accurately measure surface roughness in an in-line, non-destructive fashion enables acquisition of key device performance parameters.

Substrate	Process description	RMS roughness	Reference
Poly Si etch damage	Gate conductor	> 10.0 Å	R. Petri et al J. App. Phys 1994
Poly Si RTCVD	Gate conductor	30 - 157 Å (> 300 Å typ)	Spanos et al J. Vac. Sci Tech A 1994
SiO ₂	Gate dielectric	0.5 - 2.0 Å	J.C. Poles et al J. Vac. Sci. Tech. 1994
TiN	Adhesion and barrier	5.0 - 10.0 Å	T. S. Sriram. Digital Int. Memo1994
Al-Cu(1%)	Conductor	80 - 200 Å	T. S. Sriram. Digital Int. Memo1994
Bare Si	Starting Material	< 1.0 Å	T. S. Sriram. Digital Int. Memo1994

Table 1: RMS roughness for selected thin films

The final example of AFM application to semiconductor manufacturing involves the critical dimension (CD) measurement. As devices continue to be scaled, measurement error budgets are pushed to critical levels. CD measurements, in state-of-the-art manufacturing are performed with automated SEMs. AFMs suitable for CD measurements sense sample interactions from both the apex and the side of the probe tip.

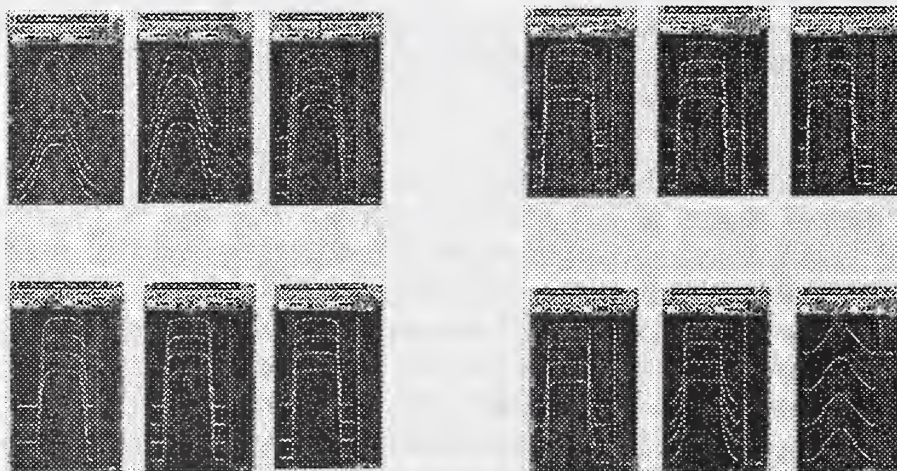


Figure 4: AFM scans of a Focus-Exposure matrix wafer

Specially designed tips and sensor electronics are required. Figure 4 shows results obtained with an AFM used to measure CDs. The sample used in this example was a focus - exposure array wafer which results in samples of varying sidewall angle and width. As can be seen both positively sloped sidewalls and re-entrant sidewalls are sensed by the AFM in this mode of operation. A further correlation of the AFM CD measurements vs. in-line CD-SEM measurements for the Focus Exposure wafer used in Figure 4 is shown in Figure 5. As can be seen in the figure reasonable agreement between methods is achieved and forms a solid basis for further study.

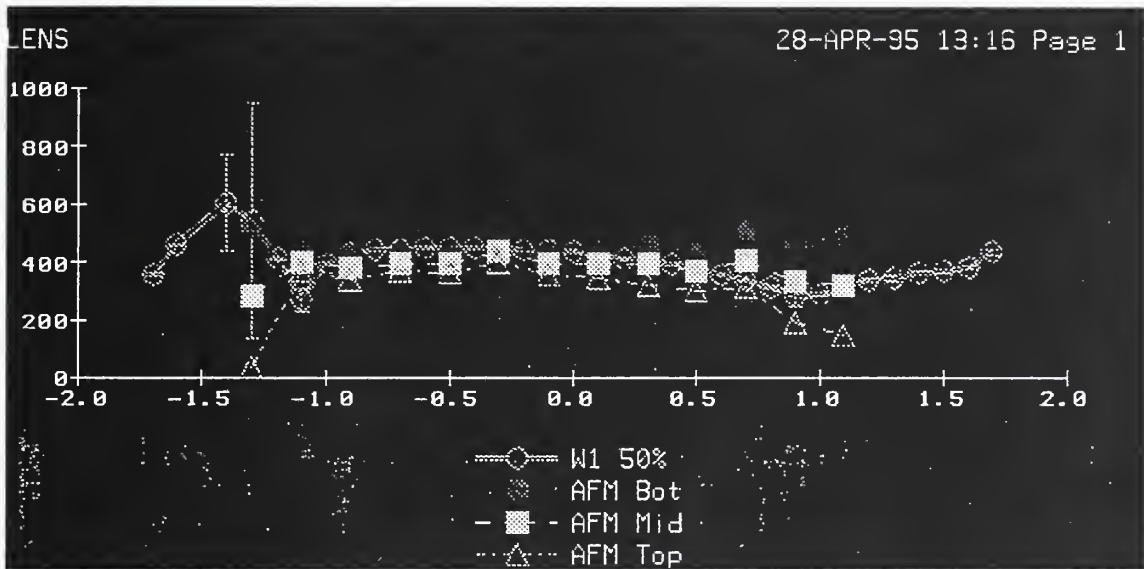


Figure 5: Correlation of AFM and SEM CD measurements

The in-line effectiveness of the AFM for all of the applications discussed is contingent upon the measurement capability, specifically; measurement accuracy and precision as they apply to both 1D (z) and CD measurements. Preliminary correlation of AFM to in-line and off-line measurement SEMs and photolithography simulators demonstrate the high degree of correlation with the AFM. The attached appendix represents a rough outline of AFM performance requirements based upon semiconductor metrology needs. Further study, to fully quantify the performance of the tool from a strict metrology perspective, is essential to the full implementation of the AFM in a production environment.

Appendix: In-Line AFM Performance Requirements

The application specific demands placed upon an in-line AFM in a state of the art semiconductor development / production facility are summarized and used to outline current and future system requirements for successful in-line integration in the following table.

- Measurement Capability
 - Repeatability:
 - » Critical Dimension - < 15 nm (3 sigma)
 - » Z height:
 - 0 - 10 A < 0.2 A (3 sigma)
 - 10 - 100 A < 2.0 A (3 sigma)
 - 100 - 1000 A < 20.0 A (3 sigma)
 - > 1000 A < 100 A (3 sigma)
 - Accuracy:
 - » to designed offsets (CD and Z):
 - b1 (slope) = 1 (w/in 1 sigma)
 - b0 (offset) = 0 (@ 95% CL)
- Software:
 - Auto-measurement routines for; Step height, sidewall angle, CDs, W plug recess, RMS roughness and correlation length,
Capability to select scan parameters for auto-recipe
- Automation:
 - Full cassette to cassette 200mm wafer handling.
 - Fully programmable 200mm wafer stage with 10 um accuracy (mean + 3 sigma).
 - Pattern recognition for all aspects of data acquisition (full “hands off automation”) with 97% success rate.
 - Automatic tip characterization (frequency user selectable) and incorporation of tip into measurement results.
 - Autocalibration / setup of system following service or tip change.
 - SECs / GEM data transport. Ethernet image transport.
- Environmental tolerance:
 - Noise floor < 0.1 A
 - Acoustic threshold > 78 dBc
 - Vibration threshold > 3.0 um peak to peak X, Y, and Z directions.
 -
- ◆ Cleanliness Class 1 compatible (e.g.. < 0.02 part / sqcm) pwp of size > 0.3um.

The Application of Scanning Probe Microscopes to the Defect Review Process

by

Yale E. Strausser
Digital Instruments
Santa Barbara, CA

The process of defect inspection in integrated circuit manufacturing involves using a very expensive machine to rapidly, optically inspect an IC wafer for deviations from the signature expected from a perfect wafer. After the deviations are located the wafer is put through a defect review system, which is again an optical system which allows the defects to be classified according to a system of defect types. This system works well for defects which are large enough to be well resolved by optical microscopy (about $2\mu\text{m}$ and larger). There are second level defect review systems which are also based on optical techniques, this time laser confocal microscopy, which can image and classify smaller defects (about $1\mu\text{m}$ and larger). Integrated circuit processes which run down to $0.35\mu\text{m}$ geometries are impacted by defects which are $0.1\mu\text{m}$ and larger. Thus there is a range of defects which are important but which cannot be imaged well enough for confident classification. These small features, $0.1\mu\text{m}$ and larger, can be made to register on the original defect inspection machine and so there is a desire to classify them.

An atomic force microscope (AFM) is an instrument which measures, in all three dimensions, features on a surface which are in the size range of all of the defects of interest. The resolution of an AFM is much higher than is possible with any optical system, less than an angstrom in the vertical direction and better than 5 nm in the horizontal directions. Thus the features of interest can all be measured and imaged at more than adequate resolution.

The AFM, when operating in TappingMode, is next to the optical probe techniques in terms of not introducing sample damage or modification by the measuring tool. Since the AFM images features on an atomic scale, movement of small numbers of atoms is readily observable. Contact AFM does, at times modify the surface being measured. TappingMode AFM, when operated properly, does not.

Beyond the very valuable measurement of the defects morphology scanning probe microscopy can also measure some of their other properties. For example, lateral force microscopy measures the frictional force between the surface of the defect and the scanning probe. The probe can be coated with specific molecules to detect the chemistry of the defect. Force modulation measures the stiffness of the surface of

the defect and thus can differentiate between softer photoresist residue and the harder metals, silicon, or oxides on which it was left.

AFM defect review systems are now available which have automatic wafer loading and unloading from standard wafer cassettes. The wafers are pre-aligned when placed on the analysis stage. The stage is a precision x, y motion stage which can adapt its motions to any x, y coordinate system which can be registered to fiducial marks on the wafer. It provides precision motion control with 2 μm positioning accuracy, which is more precise, in our experience thus far, than the coordinates which come from the initial defect inspection system. This thus provides a convenient platform for accepting defect coordinate maps from the previously run defect inspection system, even though some manual searching may be required to zero in on the defect. Pattern recognition capability also will help to navigate on the wafer for cases where there are predictable locations of concern.

These systems are fab compatible in that they have been shown to add less than 10 particles (less than 300 nm diameter) per wafer pass to an 8" wafer and they provide the required low noise floor (less than 0.05 nm RMS) even in a clean room environment.

With these systems it becomes possible to see the detailed morphological characteristics of defects from tens of microns in size all the way down to below the 10 nm scale and to measure their sizes and shapes in all three dimensions.

KELVIN PROBE MICROSCOPY FOR DEFECT ANALYSIS

M.P. O'Boyle and H.K. Wickramasinghe
IBM Yorktown Heights
and
T. Hwang
IBM East Fishkill

The Kelvin Probe Force Microscope (KPFM) is a new type of scan probe technology, which has the ability to simultaneously measure surface potentials and surface topography. It has found a home in failures analysis, because of its ability to spatially locate defects in semiconductor devices. This greatly assists in the failure analysis process. It also is able to profile semiconductor implants, providing information about the implantation process.

The Kelvin Probe is a well established technique for measuring the contact potential difference (CPD) between a reference electrode and sample, and this CPD signal is dependent on both the work function and surface conditions of the electrode and sample. Our modified Kelvin technique applies an AC voltage to a cantilever assembly (probe) with a very sharp tip that is 50 Å from a sample. If there is a potential difference between the probe and sample, then the cantilever will vibrate due to the resulting AC electrostatic force. With the addition of a feedback loop that applies a voltage onto the probe that nulls the AC electrostatic force (and also the vibration), the CPD between probe and sample is measured.

The noncontact Atomic Force Microscope (AFM) is a high resolution (lateral resolution = 50 Å and height resolution = 5 Å) nondestructive surface profiler. The technique also makes use of a vibrating probe, but in this case the probe interacts with the surface via the attractive Van der Waals force. The system is set up such that the Van der Waals force reduces the cantilever's vibration and this reduction is kept constant by a second feedback loop and its operation maintains a constant tip to sample spacing.

The KPFM is made by combining the functions of the AFM and Kelvin technique onto one probe and scanning this across the surface of some sample. As a result, both high resolution CPD and surface profile images can be take simultaneously.

Figure a, shows the ability of the KPFM for locating charge in semiconductor devices. This image clearly finds the location of charge which was known to effect the performance of the nearby schottky device.

Figure b, shows how charge, embedded under the corner of a schottky anode, will effect its surface potential.

Figure c, shows how sensitive the KPFM is to different material. In this one can easily distinguish copper precipitates in aluminum metalization.

Figure d, shows a photovoltage image of a n-type (10^{15}cm^{-3}) wafer with p⁺-type ($1.9 \times 10^{19}\text{cm}^{-3}$) regions, is measured. In this case a contrast of 200 mv is measured between the n-type and p⁺-type.

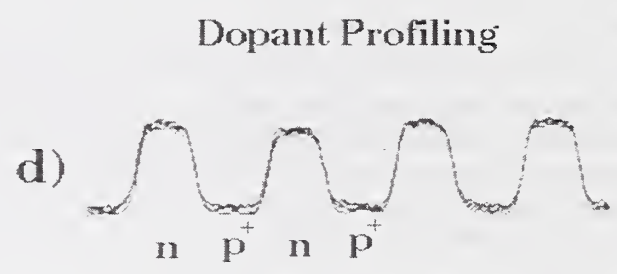
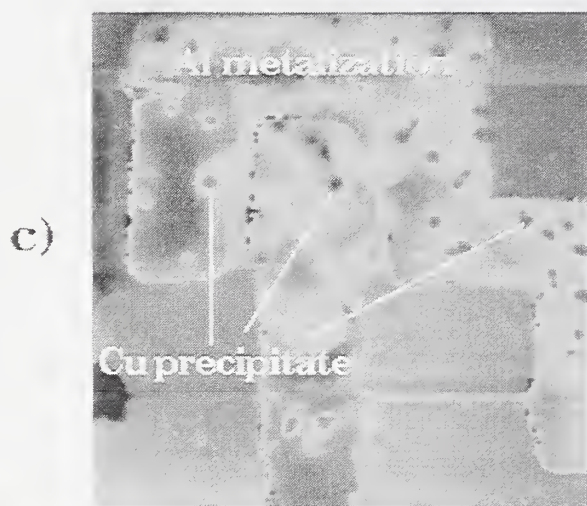
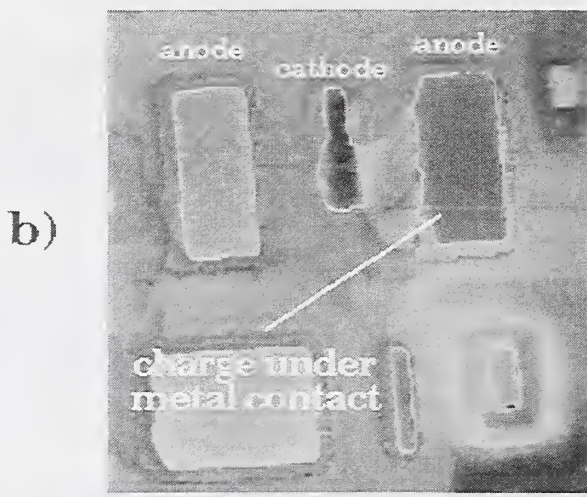
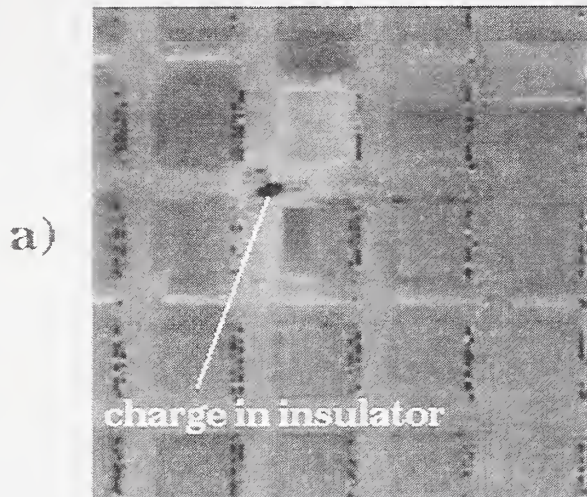
Figure e, shows a cross-sectional view of metalization between M1 and M2. The CPD contrast between the aluminum and tungsten is 600 mv. Close to the expected workfunction difference between these materials.

Figure f. Is a cross-sectional view of a FET test structure. In this case one can obtain dimentional information about dopant structures.

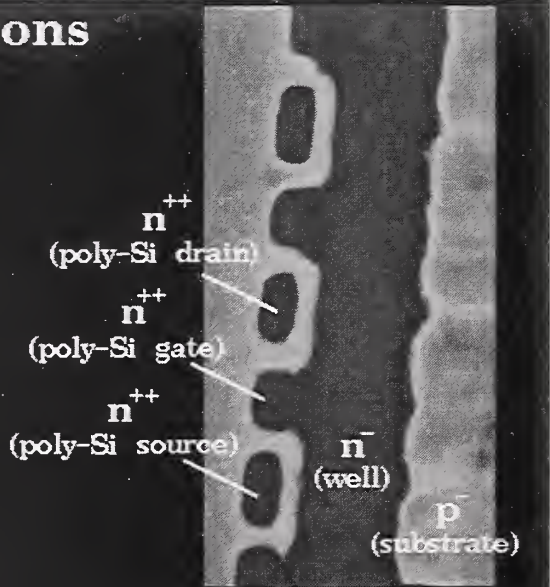
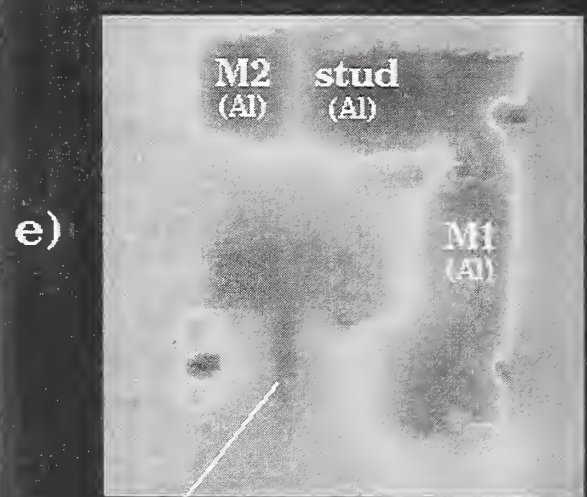
In conclusion, the nondestructive Kelvin Probe Force Microscope has clearly demonstrated its diverse ability in measuring semiconductor surface potentials, spatially locating defects in various technologies and devices along with the capability of measuring with high resolution lateral dopant profiles.

Review of Kelvin Probe Force Microscope

Top views



Cross-sections



AFM Analysis for Planarization, Defects and Other Applications in an Off-Line Laboratory

Henry S. Luftman
AT&T Bell Laboratories
9999 Hamilton Blvd.
Breinigsville, PA 18031

Practical applications of AFM for the micro-electronics industry have been demonstrated for measuring line widths of lithographic patterns and the RMS roughnesses of Si surfaces. This talk will offer several examples of more qualitative but equally critical analyses performed by a service laboratory within a device manufacturing company. The intent is to encourage extension of AFM's application base. The data shown here were taken with a Digital NanoScope III large-stage AFM. "Tapping mode" was used exclusively. All samples were examined as received from the processing engineers.

Examples of attempts to planarize device surfaces include the flowing of spun-on-glass over poly silicon lines and the use of chemical-mechanical polishing (CMP) after the deposition of metal plugs into contact vias. AFM images prove to offer a rapid means of evaluating the success of such techniques, and permit iterative experiments on the same specimens. AFM analysis in support of the optoelectronics industry will then be shown, with the characterization of 0.25 μm gratings used in the manufacture of distributive feedback (DFB) lasers. Required information includes amplitudes, periods and characteristic average line widths from arrays with both rectangular and triangularly shaped cross-sections. While information concerning the shape of the AFM probe is needed to properly derive these values from images, the demand for timely analysis is not consistent with full probe analyses and image deconvolution. A routine, more directed method for this application, using standard gratings of similar geometries, will be discussed.

Returning to Si-based technology, AFM analysis of surfaces often demonstrate morphological issues unanticipated by processing engineers, and difficult to detect or evaluate by any other technique. Voids in submicron metal lines can be characterized for depth and grain characteristics. Nanometer-scale particulate contamination and micro-pits through thin oxide surfaces can be found by quick, routine analyses, and correlated to device problems significantly further down the processing path. Concluding examples will involve the detection of monatomic steps on Si surfaces. Beyond scientific curiosity, the demonstration of monatomic pits or islands have direct bearing on technological issues.

A Near-Field Optical Latent Image Sensor For Linewidth Metrology

Herschel Marchman, Anthony Novembre
AT&T Bell Laboratories, Murray Hill, NJ 07974

and

Ray Eby
Topometrix, Bedminster, NJ 07921

The fabrication of submicrometer devices and structures has presented a new level of difficulty for metrology and process control. The fabrication tolerances for submicrometer devices are typically tens of nanometers, which means the metrology requirements for maintaining suitable process control are on the single nanometer scale. A shift from dimensional metrology of developed features to new in-situ measurement techniques will be required as smaller feature sizes and more control of processes are required. New types of sensors for monitoring features in their various forms at each step of the lithographic exposure and development sequence will aid in this paradigm shift. The monitoring of photoresist after exposure, but before development is known as latent resist metrology. Conventional optical techniques used in the past for latent image detection only sensed scattered intensities from patterns and not spatially resolved images of the latent features. The application of near-field scanning optical microscopy (NSOM) for imaging resist features before (latent) and during development of patterns exposed using advanced optical and X-ray masks will be described.

In near-field scanning optical microscopy (NSOM), a light emitting or collecting aperture at the apex of a sharp probe is brought vertically to within nanometers of a sample surface and then scanned laterally to produce optical images with resolution beyond the classical diffraction limit. The intensity transmitted or collected through the aperture is mainly dependent on the sample properties. Near-field images are also influenced by properties of the microscope itself, such as probe shape or the feedback control system for regulating aperture/tip to sample distance. In the case of latent resist samples, the surface is relatively flat so that artifacts due to the microscope and sample topography are minimized. Variations in the optical properties (i.e. refractive index) on the sample surface affect the amount of intensity transmitted or collected

through the aperture, therefore generating a contrast mechanism for imaging. Topographic data is obtained simultaneously from the distance feedback portion of the system.

The new metrologic applications made possible by highly spatially resolved latent imaging will also be discussed in relation to characterization of lithographic masks, exposure step and repeat systems (steppers), and as a sensor for improving process control.

NEAR FIELD OPTICAL MICROSCOPY OF ELECTRONIC MATERIALS AND DEVICES

Walter M. Duncan
Corporate Research and Development
Texas Instruments, Incorporated
Dallas, Texas 75265

ABSTRACT

Increases in density of integration and concomitant reductions in minimum feature size have driven requirements for spatial resolution in analytical instrumentation to well below the limit set by far field diffraction of visible light. Recent advances in scanned probe and fiber technology have enabled scanning optical measurement to be performed in the near field with spatial resolutions of 20-50 nm, well below the far field limit. Combined near-field scanning optical microscopy (NSOM) and optical spectroscopic capabilities are being investigated as a methodology for chemical and physical analysis of materials and structures with spatial extents in the submicron regime. This work is directed to understanding subdiffraction limited imaging modes appropriate for analysis of microelectronic materials, devices and circuits.

We have combined a near field scanning optical microscope together with spectroscopic capability consisting of a spectrometer, imaging detector and tunable laser. A near field excitation/far field backscattering collection geometry has been employed in this work as dictated by the need to study optically thick and/or opaque structures. Partially fabricated DRAM structures, InGaAs/GaAs and AlGaAs/GaAs heterostructures have been examined as vehicles to elucidate the detail physical mechanisms operative in various near field spectroscopic imaging modes.

We have investigated top-view and cross-sectional sampling of microelectronic structures. Reflected intensity remain the most convenient imaging mode for NSOM due to signal strength. Reflected intensity contrast is sensitive to thin film thickness changes, variation in index of refraction (e.g. compositional changes), and surface topological changes. Reflected intensity contrast has been used to detect thickness variations in dielectric films on Si and to image tungsten vias in interconnect structures. Cross-hatching features due to misfit relaxation (e.g., InGaAs/GaAs) has also been imaged in reflected intensity contrast with a spatial resolution of better than 0.1 μm . Surface topological changes due to particles and thin film contaminants are also evident in the reflected mode imaging.

Fluorescence also provides an imaging mode in NSOM. Our data indicates that in opaque films, carrier diffusion is required to obtain good emission intensity. If carrier diffusion lengths are short then fluorescence will occur under the tip thus reduction collection efficiencies. Fluorescence imaging is being refined with emphasis on AlGaAs/GaAs heterostructures.

Faint, illegible text at the top of the page, possibly a header or introductory paragraph.

Main body of faint, illegible text, appearing to be several paragraphs of a document.

Measurement Issues in Lateral Force Microscopy
Grover C. Wetsel
The University of Texas at Dallas

Scanned-nanoprobe instruments have been developed at the University of Texas at Dallas for fabrication and for topographical, electronic, optical, and tribological characterization of materials and devices^{1,2}. The optical nanoprobe includes an optical fiber oriented with its axis perpendicular to the sample surface; the fiber is vibrated parallel to the surface in order to control the distance between the optical aperture and the sample. The interaction of the surface with the fiber tip affects its lateral motion; monitoring of the motion and comparison with a reference signal enables the distance-regulation. The feedback error signal is used to construct a topographical image based on the lateral force between the fiber tip and the surface. Simultaneous near-field-scanned optical (NSOM) and topographical images can thus be obtained.

In order to evaluate the definition of the simultaneous NSOM and lateral-force-microscope (LFM) images, a nanostructure pattern consisting of Au disks deposited on Si was used to compare images obtained by various nanoprobe techniques. The disks were nominally 0.25 μm in diameter, 0.1 μm in height, and separated by a 0.5 μm center-to-center distance. Scanning electron microscopy (SEM) images indicated a diameter of 0.25 μm and a centerline spacing of 0.52 μm . Images obtained using a commercial scanned-force microscope (SFM) operating in contact mode indicated a diameter of 0.38 μm , a height of 0.10 μm , and a centerline spacing of 0.57 μm . The LFM topographical image indicated a diameter of 0.35 μm , a centerline distance of 0.57 μm , and a height of 0.12 μm . The NSOM image indicated a diameter of 0.28 μm and a centerline distance of 0.57 μm .

The results of the image-comparison study stimulated an effort to better understand the probe-sample interaction in lateral-force microscopy. Understanding of this interaction is important in both tribological investigations and in the interpretation of LFM images of nanoscale materials and devices. A major concern is the effect of the materials and the environment on topographical images of nanostructures. A model of the effect of the lateral force on the fiber's motion has been developed that permits the calibrated measurement of the dynamic force parameters.

One end of the fiber is attached to a piezoelectric scanner tube and vibrated at one of its cantilever resonant frequencies such that the free end moves parallel to the surface. As the probe approaches the surface, the interaction of the surface with the free end of the fiber attenuates the lateral motion of the fiber. A position sensor is used to measure the deflection of a laser beam caused by the fiber motion. The position sensor output is calibrated by moving the stationary fiber through a known distance. Lateral-force measurements are accomplished by measuring the frequency response of the fiber's motion near resonance before and after interaction with the surface.

The dynamics of the fiber is modeled as a continuous elastic cantilever driven at one end and constrained by a lateral force at the other end. Intrinsic losses--due to internal attenuation and (principally) the viscous drag of air--are included; knowledge of the intrinsic loss is important to

determination of the surface interaction and to calculation of the sensitivity of the method. The detailed nature of the model lateral force can be varied to correspond to experimental results.

An example of the determination of lateral force is shown in Figs. 1 and 2 for a quartz fiber and a quartz surface in air. The top curve in Fig. 1 represents the measured frequency response of the fiber before interaction with the surface; this result is compared with the model to determine the intrinsic loss factor α . The measured frequency response when the fiber interacted with the surface is represented by the discrete data in Fig. 1. The solid curve through the experimental data represents a theoretical fit assuming that the lateral force is a frictional force proportional to the particle velocity at the end of the fiber; the proportionality (frictional) factor η is determined from the fit. The lateral force calculated from the data of Fig. 1 is shown as a function of frequency in Fig. 2.

Applications of this method to the determination of lateral-force interactions for a variety of surface materials are in progress.

FIBER FREQUENCY RESPONSE FROM MADN6RES40, QUARTZ/AMORPHOUS C
 COMPARED WITH LATERAL-FORCE-PROBE MODEL
 $L=9.5265$ mm, $Z_m=2.1$ mm, $\alpha=7.45E-7$, $\eta=2.35E-7$

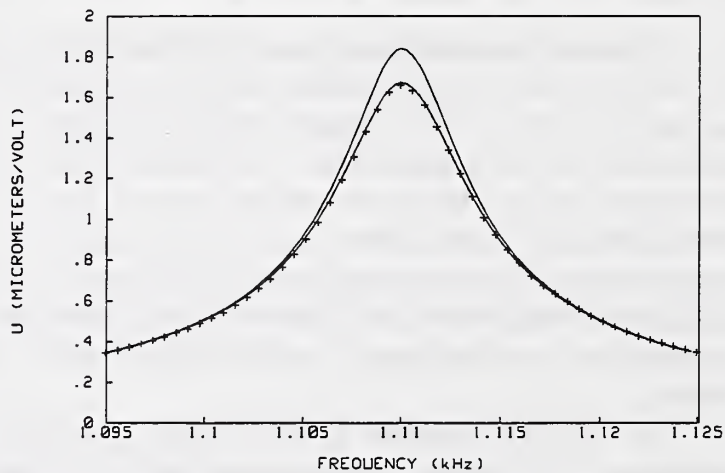


Figure 1

FORCE VS FREQUENCY FROM MADN6RES40, QUARTZ/AMORPHOUS C
 COMPARED WITH LATERAL-FORCE-PROBE MODEL
 $L=9.5265$ mm, $Z_m=2.1$ mm, $\alpha=7.45E-7$, $\eta=2.35E-7$

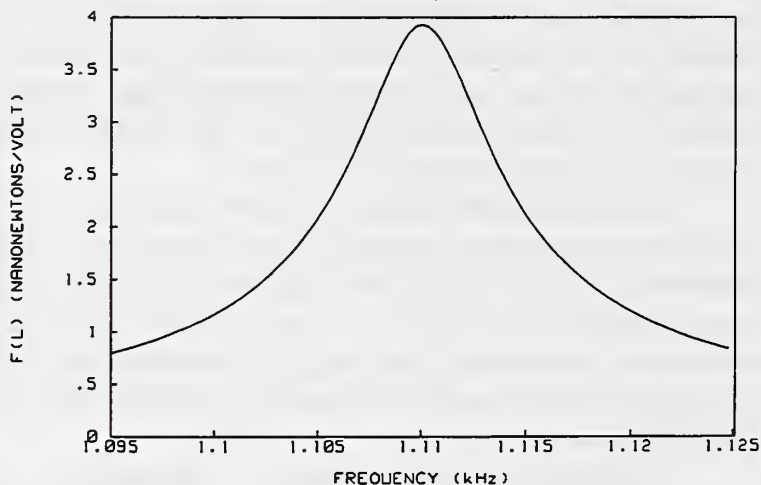


Figure 2

1. G.C. Wetsel, Jr., S.E. McBride, and H.M. Marchman, "Fabrication and Characterization Using Scanned Nanoprobes", pp. 268-288, *Technology of Proximal Probe Lithography*, C. Marrian, Ed., SPIE Press, Bellingham, WA (1993).
2. G.C. Wetsel, Jr., M.D. Taylor, and C.Y. Wang, "Nanoscale Topographical, Electronic, Optical, and Thermal Characterization Using Scanned Probes", *Proceedings of the St. Petersburg Technical University Materials Characterization Workshop* (1994).

PROGRESS ON APPLICATIONS IN NEAR-FIELD SCANNING OPTICAL MICROSCOPY (NSOM)

Patrick J. Moyer, Li Zhou, and Paul West
TopoMetrix Corporation, 5403 Betsy Ross Drive, Santa Clara, CA 95054

Near-field scanning optical microscopy (NSOM) is an optical microscopy and spectroscopy technique that allows for optical characterization and modification on a scale of dimension not previously realizable because of the effects of far-field diffraction. Diffraction limits the spatial resolution of conventional optical techniques to roughly $\lambda/2$, where λ is the wavelength of light. NSOM overcomes this limitation by placing a subwavelength-sized light source within 10 nm of a surface and uses scanning probe microscopy instrumentation to scan the sample and collect data. Resolution of many applications routinely exceeds 50 nm, with some experiments providing better than 15 nm resolution.

As might be expected, light levels transmitted through a subwavelength aperture are very low. With no more than about 10 nW cw power at visible wavelengths transmitted through a 50 nm diameter aperture, some limitations presently exist for simply transposing all current optical characterization techniques to the near-field with better than 50 nm resolution. This report will deal in detail with the limitations and solutions to experimentally overcome some of these barriers.

This report will include a brief description of NSOM operation, discussion regarding a sample standard for NSOM testing and resolution determination, and applications of the instrument to scientific problems of significance. Applications to be discussed include single molecule detection, liquid crystal investigations, and semiconductor failure analysis. Single molecule fluorescence spectroscopy provides a characterization of the NSOM probe, indicates the sensitivity achievable with NSOM, and allows ensemble averaging to be eliminated when probing fluorescent samples. Studies on the air-liquid (free) surface of liquid crystal samples show the ability to optically write and subsequently read information from the LC with lateral spatial resolution of better than 60 nm. Finally, with current integrated circuit failure analysis tools limited to the diffraction limit of spatial resolution, NSOM has shown some promise for defect analysis of semiconductor chips.

Industry Needs for SPM Standards: The View from NIST

Dennis A. Swyt

Chief, Precision Engineering Division, NIST

With its extremely high spatial resolution and inherent 3D capability, scanned probe microscopy (SPM) is beginning to fulfill its promise of becoming a major addition to the array of measurement tools used by U.S. manufacturing industries for characterization and control of the dimensions of features such as those of next-generation microelectronic and magnetic memory devices. With its mission to provide generic technology, measurement and standards support to U.S. industry - including practical access to the national and international standards of length at accuracies industry determines it requires, NIST is working with industry to develop means to achieve industry-sought accuracy and traceability in industrial SPM measurements. These means include fundamental understanding of SPM processes, methods for quantifying errors and uncertainties in SPM measurements, and physical standards for the calibration of SPMs used for measurements of different types and scales of dimensional features.

UPDATE ON ASTM E42.14 ACTIVITIES

Alain C. Diebold
SEMATECH

Joe Griffith
AT&T Bell Laboratories

Approximately two years ago, ASTM subcommittee E42.14 on STM/AFM was formed. The goal of E42.14 is to promote the developments of standards for surface characterization by scanning probe microscopy (SPM). The entire SPM community is invited to participate in ASTM E42.14 activities, and we will update our work in this presentation. E42.14 is presently working on several documents. One describes techniques for probe tip characterization, the second describes scan artifacts arising from probe-sample interactions, and a new NIST effort on height calibration has begun. E42.14 plans on using the definitions of the new subcommittee on Surface Texture of ASTM F1 on Electronics.

Steps Toward Accuracy in Linewidth Measurements by Two-Dimensional Scanning Force Microscopy

Mark D. Lagerquist

IBM Microelectronics Division
Essex Junction, VT 05452

The advent of scanning probe microscopy (SPM) has brought new opportunities in dimensional measurements by allowing high-resolution, three-dimensional, non-destructive measurements. Linewidth measurement capability of SPM has been extended with the new technology of two-dimensional scanning force microscopy (2D-SPM). The unique capabilities of 2D-SPM for dimensional metrology are outlined, citing advantages and disadvantages in meeting semiconductor device linewidth measurement needs. Particular focus is given to initial concerns and actions required to improve 2D-SPM measurement accuracy.

An important element in the fabrication of submicron semiconductor devices is the ability to perform dimensional measurements on the critical device features. Accurate and repeatable linewidth, or critical dimension (CD), measurements are essential in developing new processes and controlling existing ones. As minimum dimensions and measurement tolerances of these semiconductor devices decrease, the challenge of maintaining a viable dimensional metrology strategy increases. Furthermore, as lithographic features shrink, geometry becomes an even more important factor in the CD measurement. We have demonstrated that a 2D-SPM can perform scans on a variety of semiconductor photoresist and etch features, exhibiting unique capabilities in providing sidewall profile information. In order to achieve accuracy in these measurement scans, we implemented a series of procedures on reference samples to properly characterize the probe shape and size, and calibrate the scanners. We tested performance by checking tool repeatability on control samples and comparing the measurements to SEM measurements on cross-sectioned, or cleaved, features.

Investigations and discussions on using conventional scanning force microscopy for dimensional measurements have been presented in the past[1,2]. A limitation to conventional (1D) SPM is that probe shape interaction with steep-sloped features obscures the sidewall detail. Since sidewall slopes and details are becoming more important to semiconductor processing, much effort has been given to probe characterization and removing the probe influences in the measurements. However, there will always be sidewall detail that is non-reconstructible because it was never measured.

2D-SPM differs from conventional SPM in essentially two ways: it uses a boot-shaped probe and has two-dimensional feedback on the scan[3,4]. As such, the instrument can adjust its scan direction on reaching sharp sidewalls, detailing sidewall topography -- even

recursive slopes. Depending on probe geometries, the proper sidewall profiles can be measured nondestructively on multiple cross-sectional planes, and with high data-point resolution.

Issues of initial concern were scan calibration (traditionally considered magnification calibration), and characterization of probe shape and size. Of additional concern was removing any asymmetries in the two feedback directions by setting them orthogonal to each other. We found it necessary to first address the orthogonality issue to better characterize the probe shape and size. The reference sample used consisted of an anisotropically etched silicon grating, exhibiting the desired attributes of depths in the range of product measurements, near vertical and linear sidewalls, and minimal sidewall and edge roughness. Repeat scans were performed on the sample, which was oriented along one axis, and then rotated 180 degrees, in order to determine the asymmetry and correct for it. Probe shape and size was determined by scanning two samples, a highly recursive ridge-like structure, and a vertical knife edge structure. The former consists of a highly recursive structure at a height greater than the length of the probe, giving the effective length of the probe and the amount of recursiveness it is capable of measuring. The latter is used to measure the effective width of the tip.

Once the initial probe characterization and system calibration steps have been accomplished, we turned our focus toward tool repeatability on certain reference samples. We used repeat measurements to create statistical process control (SPC) charts to monitor tool performance and to give random error inputs into overall tool measurement uncertainty.

References:

- [1] J. Griffith and D. Grigg, "Dimensional metrology with scanning probe microscopes," J. Appl. Phys., 74 (9), R83, Nov 1993.
- [2] J. Griffith, H. Marchman, et al., "Dimensional metrology of phase-shifting masks with scanning probe microscopes," SPIE, vol. 2087, 107 (1993).
- [3] D. Nyyssonen, L. Landstein, and E. Coombs, "Two-dimensional atomic force microscope trench metrology system," J. Vac. Sci. Technol. B9 (6), 3612 (1991).
- [4] Y. Martin and H.K. Wickramasinghe, "Method for imaging sidewalls by atomic force microscopy," Appl. Phys. Lett. 64 (19), 2498, 9 May 1994.

Progress in Tip Modeling

J.S. Villarrubia

National Institute of Standards and Technology, Gaithersburg, MD 20899

Feature geometries are distorted in SPM topographs due to the finite size of the tips used to image them. This is particularly problematical for surface microroughness measurements, where spacial wavelengths comparable to or even smaller than the tip radius are of interest, and for width measurements on lithographically produced features, where high relief is the complicating factor. For these reasons, models of the tip/specimen interaction are required 1) to correct for geometric distortions where possible, 2) to identify regions where correction is not possible, thereby making explicit the limitations of a measurement, and 3) to facilitate the estimation of tip geometry required to carry out the first two requirements. The importance of these issues was highlighted at the first IASPM workshop, where the topics of “certifiable tip geometry” and “tip characterization structures and software” were each flagged as among the top three in importance by five of the seven discussion groups[1].

There exist numerically stable methods which permit surface reconstruction from images if the tip shape is known[2-4], and which do not require the tip shape to be expressible in a simple functional form. These methods may also be inverted to determine the tip shape from images of specimens (tip characterizers) whose shape is known. Hence the interest at the first IASPM on tip characterization structures, which would not only enable estimation of tip geometry, but would in principle render this sufficiently routine that one could periodically recheck tips to insure against errors due to wear or damage.

A significant issue for tip characterizers is illustrated in Figure 1a. Here, a calibration uncertainty of only $\pm 2\%$ in the width of the tip characterizer (very optimistic by current capabilities) leads to significant uncertainty in the reconstructed tip shape (inset). Accordingly, proposed tip characterizers tend to be restricted to the simplest and most easily measurable shapes, and it is not clear that even these shapes can be measured with sufficient accuracy.

I will discuss a new method for reconstructing tips from images of characterizers which does not require that the true characterizer geometry be independently known[5]. The result is an application of mathematical morphology, and is expressible in set notation as an iteration formula:

$$P_{i+1} = \bigcap_{x \in I} [(I - x) \oplus P_i'(x)] \cap P_i. \quad (\text{EQ } 1)$$

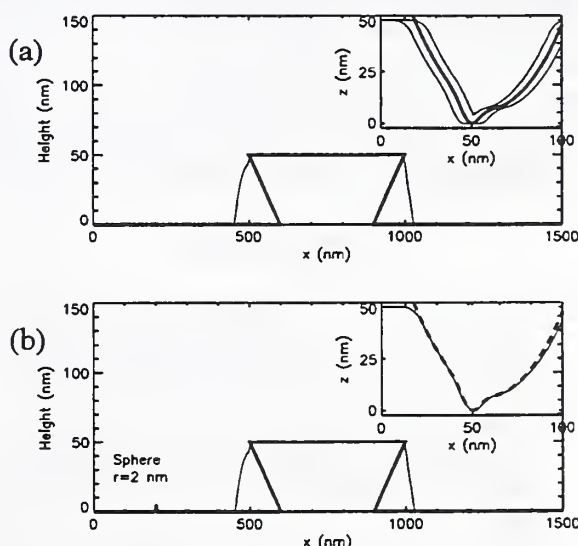


FIGURE 1. Tip reconstruction: (a) from “known” characterizer (bold line) and its image (thin line). The inset shows results for calibration errors of 0 and ± 10 nm. (b) Same problem using method described in text, and an uncalibrated modified characterizer. The inset shows the result (solid) and the true (dashed) tip shape.

Here P_i and I are sets of points contained within the tip estimate (at the i 'th iteration) and the image, respectively. The iteration scheme allows an initial outer bound estimate of the tip shape, P_0 , to be successively refined. Note that only the image and tip shapes, and not the characterizer shape, appear in the equation.

There is a simple explanation of Equation 1 which serves to provide an intuitive rationale. Practitioners of SPM are well aware that image protrusions are broadened replicas of those on the specimen. However, it is only convention which determines which of the two objects being scanned across one another is the tip and which the specimen. We are equally entitled to regard features on the image as representing broadened replicas of the tip. In particular, for example, it is not possible for the radius of the tip at the apex to be larger than the smallest top radius encountered in the image, since this would imply that the corresponding specimen feature had a negative lateral dimension. A similar consideration applies to parts of the tip away from the apex and corresponding parts of the image to which they give rise. Since tips are chosen to be slender and sharp, it can safely be assumed that they do not interact with surface objects that are sufficiently far away. In this way, sufficiently separated subsets of the image may be regarded as *independent* images, each of which places an outer bound on the tip shape. The true tip shape must be inside of the envelope which is at each point equal to the tightest of all these bounds. Figure 1b shows a reconstruction using this method. The characterizer of Figure 1a has been modified by the addition of a small particle. No information about the characterizer is assumed other than that available within its image. The reconstructed tip shape is quite close to the actual one, as shown in the inset. The outer bound on the tip can be used to place a lower bound (to be paired with the image/upper bound) on the unknown specimen surface.

Besides saving the time and expense of calibrating tip characterizers there are at least two other significant potential advantages of this method. 1) Instability of characterizer geometry (e.g. through contamination or oxidation) becomes a less serious issue. 2) It lifts the measurability constraint, to which I alluded above, from tip characterizers, permitting more flexibility that may be used to satisfy other constraints. The two characterizers shown in Figure 2, for instance, are equally good from the point of view of Equation 1, but the one on the right would in practice be significantly more robust, and it is likely to be easier to fabricate something approximating it.

References

1. J.A. Dagata et al., "Workshop Summary Report: Industrial Applications of Scanned Probe Microscopy," NISTIR 5550, 1994, p. 10.
2. H. Gallarda and R. Jain, in: Proc. Conf. on Integrated Circuit Metrology, Inspection, and Process Control, V, SPIE Vol. 1464 (1991) p. 459.
3. G.S. Pingali and R. Jain, in: Proc. IEEE Workshop on Applications of Computer Vision (1992) p. 282.
4. D.J. Keller and F.S. Franke, Surf. Sci. 294 (1993) 409.
5. J.S. Villarrubia, Surf. Sci. 321 (1994) 287.

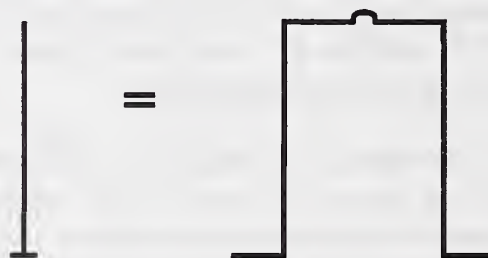


FIGURE 2. At left is an ideal tip characterizer, a spike of width 0. Anything approximating this would in practice be fragile and compliant. The efficacy of the characterizer at right (a small radius sphere and a cylinder with vertical sidewalls) is as good, but without the fragility or compliance.

Calibration and Use of a Waffle Pattern Step Height SPM Artifact

J. Schneir¹, T.H. McWaid¹, V.W. Tsai², and R. Dixon¹

¹National Institute of Standards and Technology, Gaithersburg, MD 20899.

²Dept. of Material Engineering, University of Maryland, College Park, MD 20742-4111.

Waffle pattern step height artifacts (fig. 1) are widely used as X, Y, and Z calibration standards for SPM. NIST traceable calibrated waffle pattern artifacts are available commercially. The calibration is performed by using a stylus profilometer to measure the height of a feature located near, but not on, the waffle pattern. The stylus profilometer is calibrated using a step height artifact calibrated using the NIST step height calibration service. This service is not capable of calibrating AFM waffle pattern artifacts directly.

NIST has developed a metrology AFM which can perform the X, Y, and Z calibration of an AFM waffle pattern artifact.¹ We call this instrument the calibration AFM (C-AFM). The C-AFM uses interferometers to monitor the X, Y sample position. The Z position is monitored using a capacitance gauge. The capacitance gauge is calibrated using an interferometer before and after each sample is imaged. Fig. 2 shows the calibration curve for the capacitance gauge.

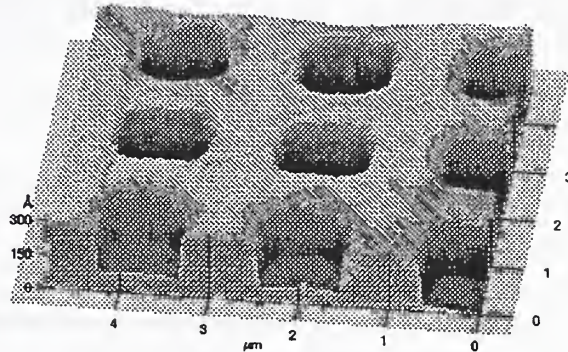


Figure 1 C-AFM image of a VLSI Standards waffle pattern artifact. The nominal pitch is 1.8 μm and the nominal height is 18 nm.

There exists no standard practice for reducing AFM images of waffle pattern standards to a Z calibration value. In lieu of a consensus standard practice we have developed our own method. Fig. 3 diagrams the method we use to determine AFM step height values from a C-AFM line scan. The transition regions are ignored. A least squares line is fit to the upper left, lower middle, and upper right surfaces. The best fit lines are then extrapolated into the transition region. The step is located laterally in the transition region. The height of the left step is assessed perpendicularly from the upper left line to the lower middle line. The height of the right step is assessed perpendicularly from the upper right line to the lower middle line. The choice of the two step locations and the size of the transition region is left to the user.

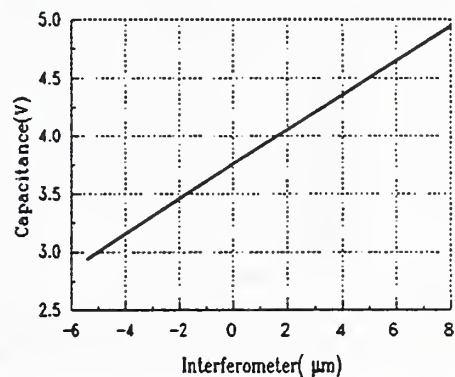


Figure 2 Calibration curve for the Z capacitance gauge determined using laser interferometry.

¹ J. Schneir, T.H. McWaid, J. Alexander, and B.P. Wilfley, "Design of an atomic force microscope with interferometric position control", *J. Vac. Sci. Technol.* **12** (6), 3561-3566 (1994).

As part of our program to validate the metrology on the C-AFM we have measured the same 18 nm step height at 3 different positions using the C-AFM and the NIST metrology stylus profilometer. All U.S. step height standards are traceable to the NIST metrology stylus profilometer. Ten C-AFM traces were performed at each position and the results were averaged to give a single step height value. Averaging reduced the random errors from 0.3 nm (1σ) to 0.1 nm (1σ). The step height values obtained using the C-AFM and the NIST metrology stylus profilometer are plotted in fig. 4. The average step height value determined using the stylus profilometer is 17.3 ± 0.6 nm (2σ) in good agreement with the C-AFM average of 17.3 ± 0.5 nm (2σ). The uncertainty specified does not include any effects due to nonuniformity of the step calibrated.²

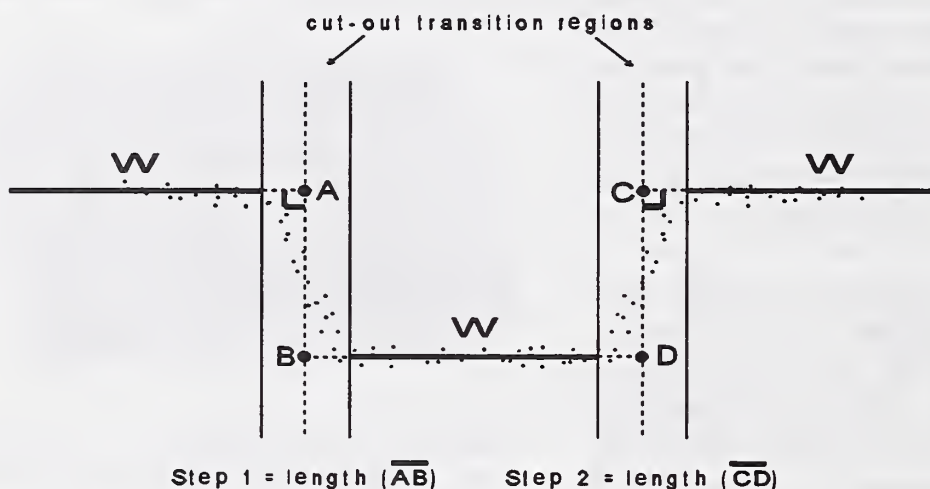


Figure 3 Step height calculation method used at NIST in lieu of a consensus standard practice.

Step Height Measurement Intercomparison

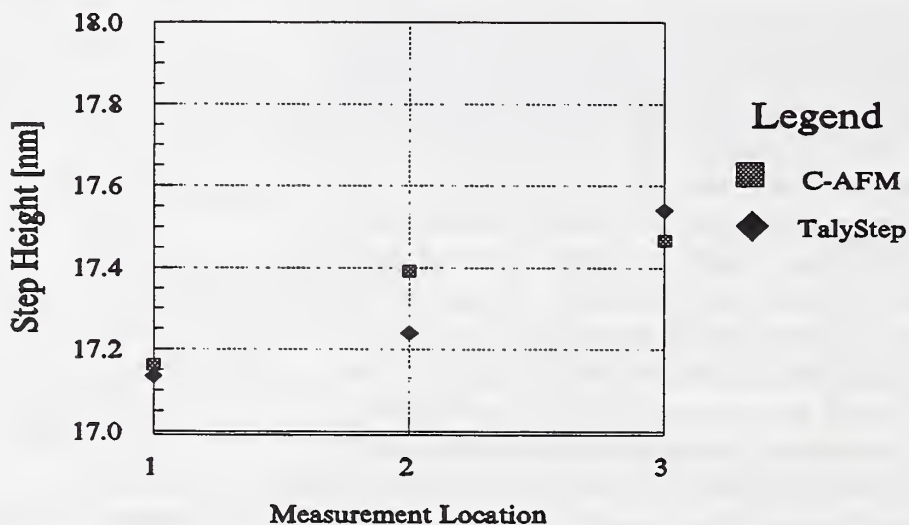


Figure 3 The NIST metrology stylus profilometer (TalyStep) and the C-AFM were used to measure the same step.

² This work was supported in part by the National Semiconductor Metrology Program (NSMP) at NIST.

Advances of SPM Lithography with New Resist Material

Sun-Woo Park*, Mike Kirk, and Sang-il Park

Park Scientific Instruments, 1171 Borregas Avenue, Sunnyvale, California 94089

ABSTRACT

We have used a Spin-On Glass (SOG) polymer as a resist layer on a Si substrate and performed SPM lithography to alter the reactivity of the SOG polymer resist layer to etching. The patterned SOG layer was developed by wet chemical etching. The patterning speed was over 1 mm/sec and obtained line width was below 0.1 μm .

INTRODUCTION

A continuing objective in silicon wafer processing technology is the reduction of pattern sizes. The minimum pattern size that can be produced by conventional optical lithography is mainly limited by the wave length of the light source used to pattern the resist layer. There has been a need for a technique which can further reduce the pattern size achieved in silicon wafer processing. Many attempts have been made with SEM and X-rays to produce line widths of 0.1 μm and below. However serious proximity effects and complexity of providing vacuum environment prevented these technique from becoming practical tools.

Recently, SPM has gained significant attention as a strong candidate of the next generation lithography technology. The probe tip of SPM can produce highly localized strong electric field and electron beam. Since the electron beam was produced by low voltage and it does need to be focused, there are no proximity effects and secondary electron effects in SPM lithography. In addition, SPM lithography does not require vacuum environment.

SPM lithography experiments have been performed on various materials. Dobisz at NRL used self-assembling organic monolayer [1] and very thin e-beam resists [2]. Earlier, Pease at Stanford used ultrathin PMMA [3]. However, these conventional resist materials have high dielectric strength and, therefore, the field emission can occurs only through a very thin layer of such materials, generally on the order of 10 nm. Such thin layer is not suitable for use in silicon wafer fabrication processes since it will not survive through etching process. Snow at NRL used hydrogen-passivated Si as resist film [4]. The intense E-field produced by SPM tip breaks the hydrogen bond and oxidize the silicon. Quate at Stanford used similar method on hydrogen-passivated poly-Si to fabricate a working FET with a gate length of 0.1 μm [5]. However, this oxidation process is rather slow, which imposes significant limitations.

There has been a need for a resist layer material which can be effectively used to perform SPM lithography. In particular, a resist layer material is needed which has sufficiently high exposure speed and which has low dielectric strength such that it does not prevent field emission through the resist layer of sufficient thickness.

SOG : A NEW RESIST MATERIAL FOR SPM LITHOGRAPHY

We have used a Spin-On Glass as a new resist material for SPM lithography. Spin-On glass, also commonly referred to as "SOG," refers to a process for forming a silicon based polymer dielectric film. Since SOG forms a very flat and uniform surface, it has been used for planarization in integrated circuit fabrication. We have proved that a siloxane SOG polymer has a positive resist properties, where exposed

region by strong E-field or sufficient electron beam becomes more sensitive to etch by a factor of at least 20. Siloxane SOG polymer has the formula $[R_YSiO_{(2-0.5Y)}]$ where R is C_NH_{2N+1} organic compound. The positive resist properties of the siloxane SOG polymer is believed to be due to the decomposition of the SiO_2-R bond of the siloxane when exposed to electric field and electron beam. The partial decomposition of the siloxane polymer renders the SOG into porous SiO_2 which is prone to etching.

EXPERIMENTS

The schematic diagram of the system used in this experiment is shown in Fig. 1. A 97 nm thick film of the methylsiloxane SOG polymer film ($R = CH_3$) [6] was made on a silicon wafer by spinning the wafer at 5,000 rpm. The film was then cured at 280 °C for ten minutes. A bias voltage is applied between sample and AFM tip. The amount of dosage and electric field on the sample was controlled by changing the DC voltage applied. Experiments verified that the field emission currents generated by this setup closely follow Fowler-Nordheim behavior (I/V^2 versus $1/V$). The actual voltage applied between the SPM tip and the sample was 40 - 60 V. The resulting field emission current was measured at 12 nA. The scan speed was about 1mm per second.

After exposure, the sample was developed by wet chemical etching with a 1:100 Buffered Oxide Etcher (BOE) solution. Only a dilute BOE solution was employed due to the highly porous nature of the exposed resist film. The etching time of the exposed region was measured to be 5 seconds, the etching rate being calculated to be around 20 nm/sec.

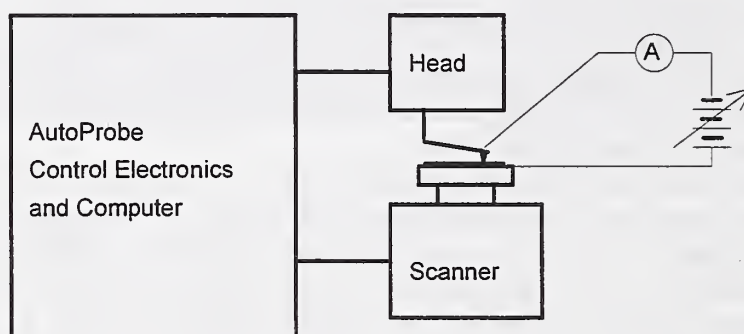


Fig. 1 Schematic diagram of SPM lithography. Only an external DC power supply was added to standard AutoProbe CP system.

RESULTS AND DISCUSSION

Fig. 2 and Fig. 3 show AFM images of a SOG resist film after development. The dark lines represent regions which were exposed by SPM. The line widths are about 0.1 μm in Fig. 2, and about 0.05 μm in Fig. 3. Slight deviation at the corners is due to the tracking error of ScanMaster, our closed loop servo scan system. ScanMaster is critically needed in lithography because the creep and hysteresis of piezoelectric scanner cannot be corrected by software in vector graphics.

SOG polymer films are particularly useful as resist layer materials in that these films have low dielectric strength and can be altered to have sufficiently different etch rate with high exposure speed. SOG polymer films are able to form a continuous crack resistance film which undergoes a low degree of shrinkage upon curing. In addition, these polymer films may be used to perform high resolution

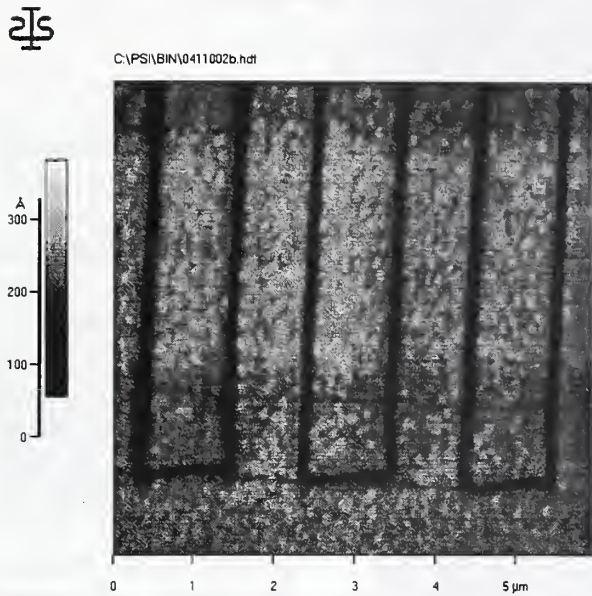


Fig. 2. AFM image of SOG film after lithography.

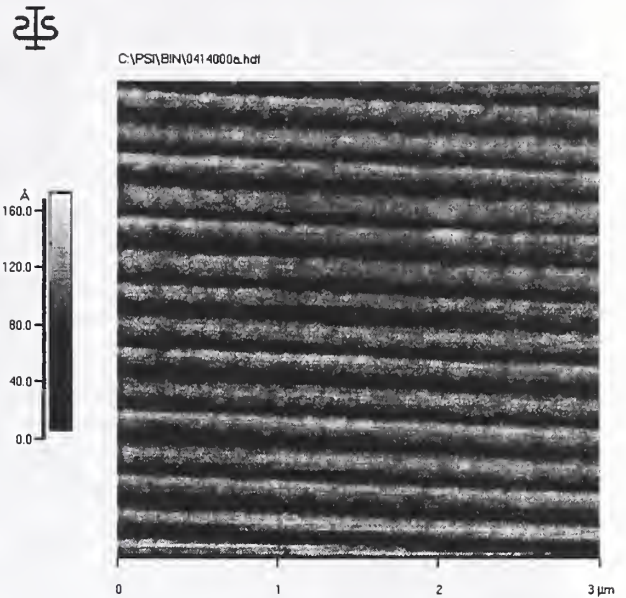


Fig. 3. AFM image of SOG film with finer line width and pitch.

patterning by a dry patterning and etching process, thereby avoiding difficulties associated with wet processes.

Since SPM lithography does not need electron focusing lens nor accelerator, SPM lithography can produce much smaller patterns without proximity effects. Since the surface of SOG is very flat, the probe of SPM can be scanned over the SOG layer with a little or no feedback control in the vertical direction, thus improving the writing speed. Combined with the advantages of SOG as a resist layer, SPM lithography will become very powerful technology for next generation semiconductor process, especially when parallel exposure technology is fully developed [7].

*Permanent address: Seoul City University, Seoul, Korea.

- [1] C. R. K. Marrian, F. K. Perkins, S. L. Brandow, T. S. Koloski, E. A. Dobisz, and J. M. Calvert, *Appl. Phys. Lett.* **64**, 390 (1994).
- [2] C. R.K. Marrian and E. A. Dobisz, *J. Vac. Sci. Tech.* **B10**, 2877 (1992).
- [3] H. Zhang, L. S. Hordon, S. W. J. Kuan, P. Maccagno, and R. F. W. Pease, *J. Vac. Sci. Tech.* **B7**, 1717 (1989).
- [4] E. S. Snow and P. M. Campbell, *Appl. Phys. Lett.* **64**, 1932 (1994).
- [5] S. C. Minne, H. T. Soh, Ph. Flueckiger, and C. F. Quate, *Appl. Phys. Lett.* **66**, 703 (1995).
- [6] ACCUGLASS 111 from Allied Signal.
- [7] S. C. Minne, Ph. Flueckiger, H. T. Soh, and C. F. Quate, *J. Vac. Sci. Tech.* **B** (1995 May/June to be published).

AFM analysis of Photoresist Test Structures for use in SEM as in-house Linewidth Standards

Donald A. Chernoff, Advanced Surface Microscopy, Inc.,
6009 Knyghton Rd., Indianapolis, IN 46220

Producing the desired linewidth is one of the major responsibilities of lithography engineers. Photoresist linewidths are presently controlled by inspecting wafers in plan view with a 'metrology SEM'. We outline some of the problems with this procedure and propose a methodology for overcoming them. Proprietary algorithms convert signal intensity to a pseudo-topographic profile and place markers at the inferred foot of the photoresist. The algorithms attempt to account for the complexities of electron scattering. No standard reference materials exist for checking this measurement. We show the feasibility of creating an in-house quasi-standard for this purpose. Using a modern i-line stepper (0.54 N.A.) with a range of defocus conditions, we produced three specimens of 0.5- μm wide photoresist line test patterns which presented both aberrated and good line shapes. We cleaved die from the wafer so that the cleaved face was normal to the photoresist line. We examined each cleaved face using the AFM (giving the cross-section view) and then re-examined the same specimens in plan view using the metrology SEM, at a location adjacent to the cleaved face.

Figures 1 and 2 show typical SEM and AFM images of a good resist line. The AFM images had crisp edges defining the line profile, showing the Si substrate and the foot, sidewall and top of the photoresist. Pitch, line width, and slope angles were measured from the AFM images and compared with the pitches and line widths reported by the SEM. For both the AFM and SEM data, we normalized the linewidths to the pitch, using the 1.00 μm pattern pitch as an internal length standard. Table 1 summarizes the quantitative results and includes qualitative remarks about lineshape based on the AFM images.

Table 1: Linewidth, Sidewall Slope and Lineshape

<u>Specimen</u>	<u>Linewidth (μm)</u>		<u>Sidewall Slopes($^{\circ}$)</u>	<u>Lineshape</u>
	<u>SEM</u>	<u>AFM</u>	<u>Left/Right</u>	<u>Sidewall/Top</u>
A2	0.558	0.530	87/85	Concave/Flat
B3	0.567	0.568	87/84	Straight/Flat
C1	0.595	0.550	87/78	Convex/Curved

Note the excellent agreement of the SEM and AFM linewidths for specimen B3, which had an ideal lineshape, with straight, steep sidewalls. However, the SEM results disagreed significantly with AFM for the other two specimens. It seems that the metrology algorithm was fooled by those more complex shapes.

This work has shown that the AFM can directly examine resist line profiles and provide images of useful precision, without adding a conductive coating as is customarily done when a high resolution SEM is used to examine cleaved cross-sections to check the metrology SEM. Furthermore, the uncoated specimens examined by AFM can be re-examined by the metrology SEM, an examination which would not be meaningful if a metal coating had been applied. Therefore, it ought to be possible to utilize AFM-measured specimens to check the metrology SEM repeatedly over a period of time.

Acknowledgement. The author thanks Dennis Schrope for the initial concept of this research and for supplying the specimens and SEM images, and AT&T Bell Laboratories for financial support.

Figure 1. SEM measurement of linewidth of 'good' specimen B3 (plan view). The SE intensity profile is superimposed on the image. Electron scattering from the substrate is enhanced near the resist wall, so the inferred foot location is part way up the curve.

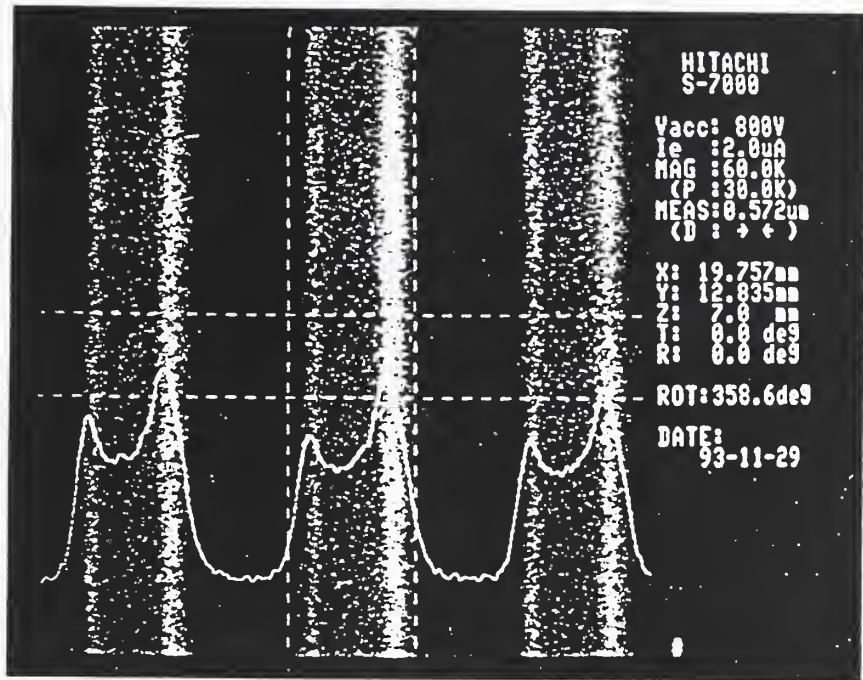
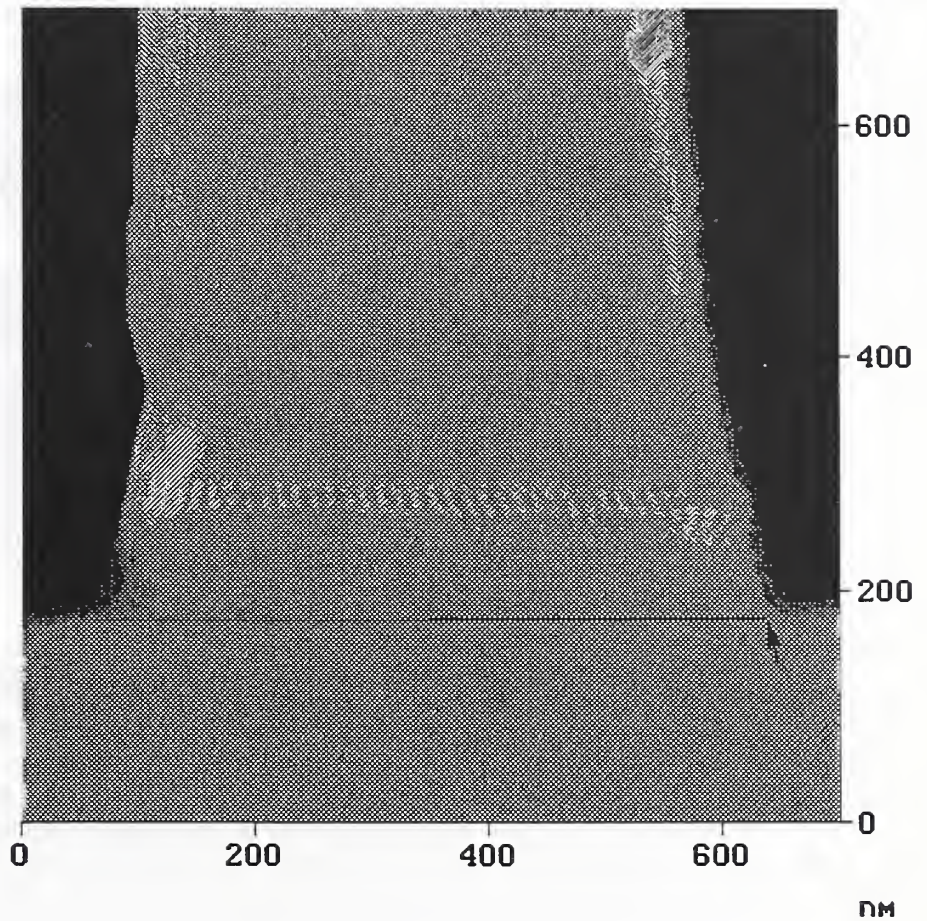


Figure 2. AFM measurement of linewidth of specimen B3 (cleaved face). The AFM images the foot of the resist directly.





[Faint, illegible text or graphics on the right side of the page]

Study of VLSI Step Height Standards on the Veeco AFM

Ruby Raheem

Advanced Micro Devices, Sunnyvale, CA

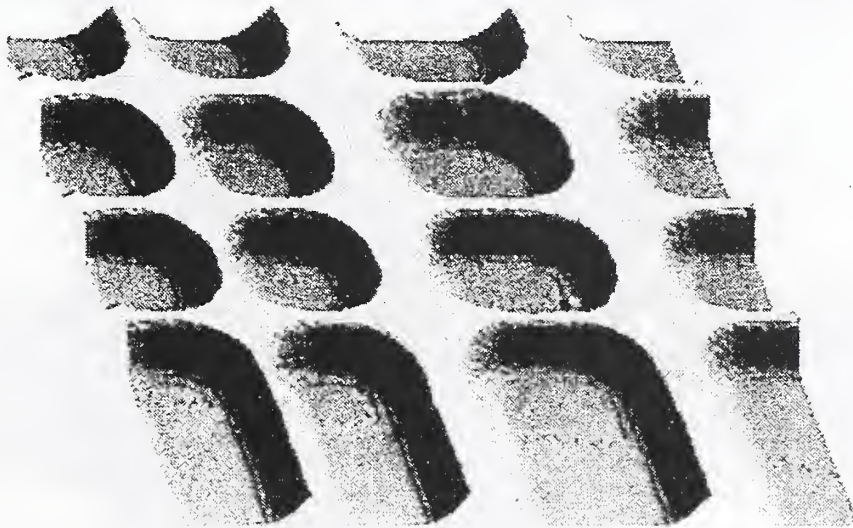
and

Michael Young

Sloan Technology, Santa Barbara, CA

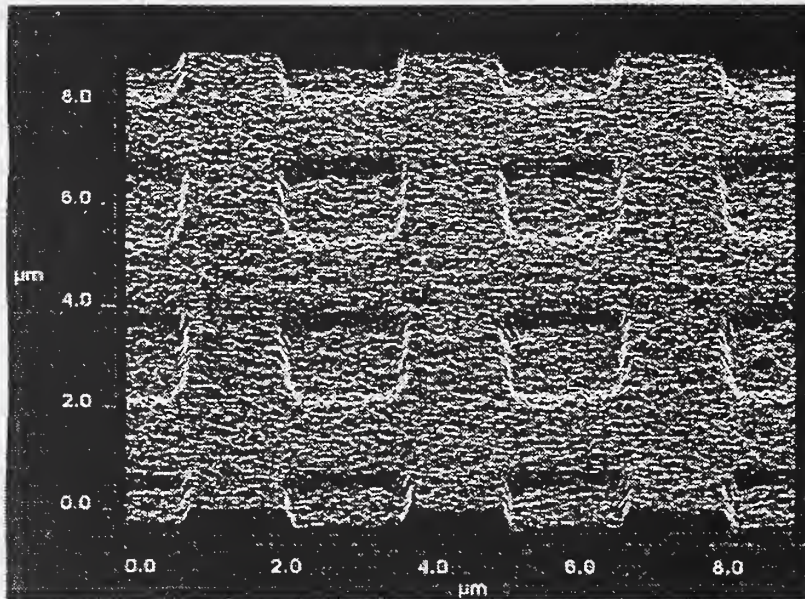
This study is a statistical analysis of the reproducibility of VLSI z-heights on the Veeco AFM. The Dektak SXM AFM developed by IBM is used for non contact, nondestructive nanometer scale measurement of submicron structures. The VLSI Standards are traceable to NIST for step height and meets MIL-STD-45662A.

Three step heights of 180Å, 9400Å and 1.8µm are used to study the effect of the z range and reproducibility. Three dimensional and Top View images of the Standards along with statistical data will be included.



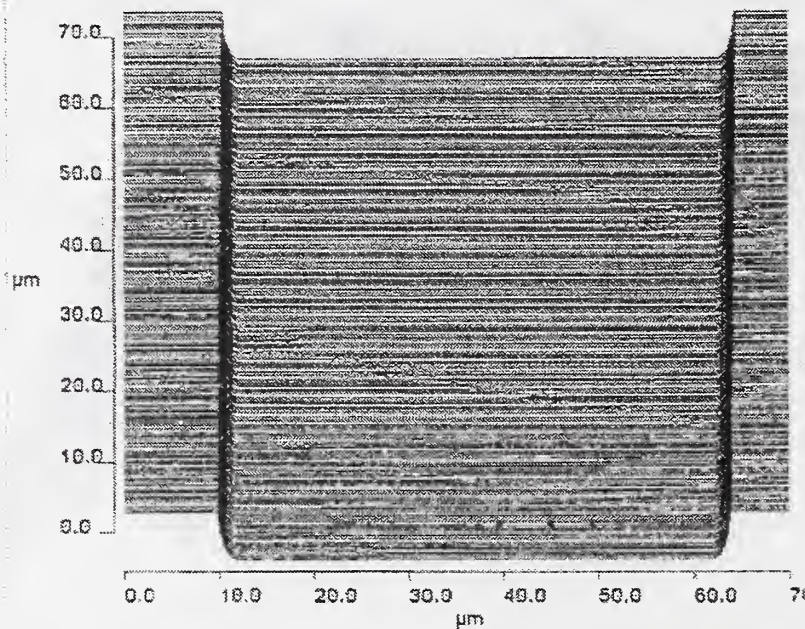
SHS -9400 Thin Step Height Standard
17µm x 17µm Scanning Atomic Force Image

VLSI calibration data: - 9391Å ± 59Å @ 21°C & 49% Humidity
Measured data 9367Å (std dev 36Å) @ 27°C



STS-180 Surface Topography Standard
8μm x 8μm Scanning Atomic Force Image

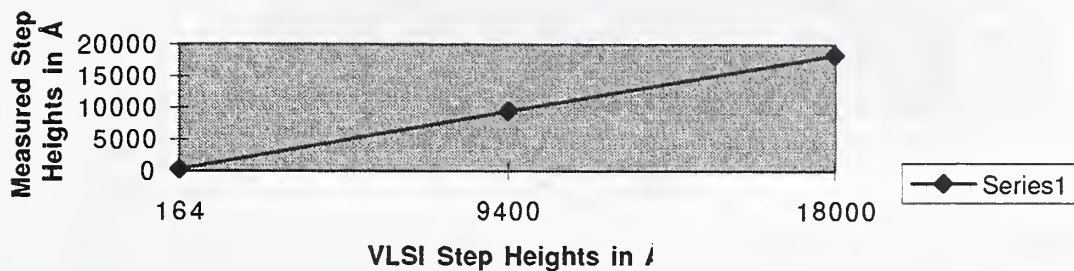
VLSI calibration data :- $164\text{\AA} \pm 27\text{\AA}$ @ 22.4°C & 48% Humidity
Measured data 167.7\AA (std dev = 6.7\AA) @ 27°C



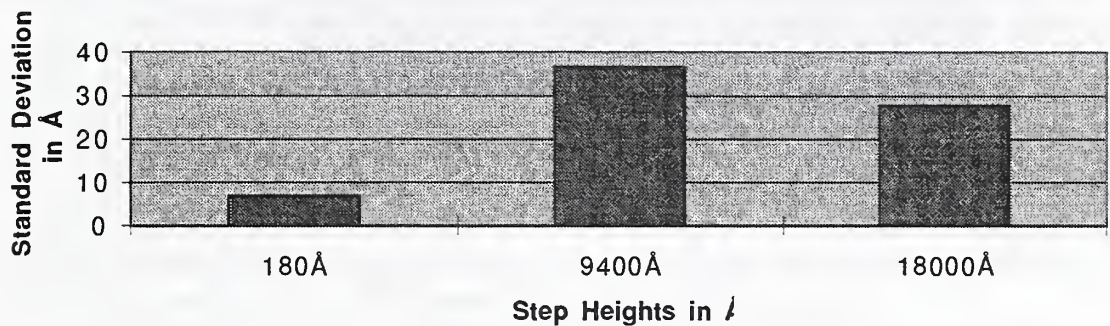
SHS - 1.8 Thick Step Height Standard
70μm x 70μm Scanning Atomic Force Image

(VLSI calibration data :- $1.798\mu\text{m} \pm 0.011\mu\text{m}$ @ 21°C & 47% Humidity)
Measured data $1.8306\mu\text{m}$ (std dev = $0.003\mu\text{m}$) @ 27°C

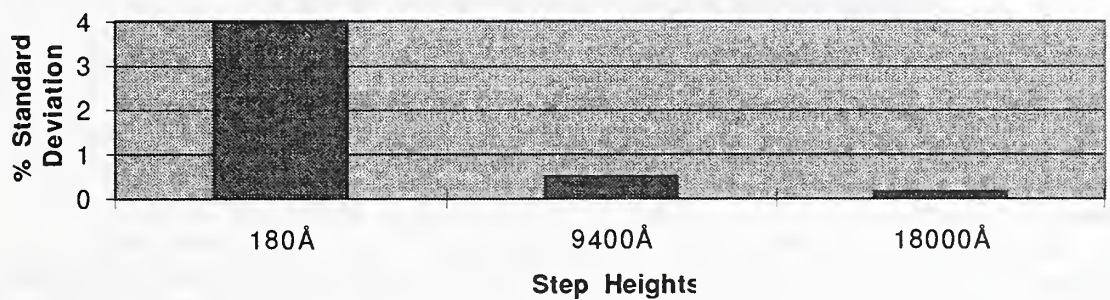
Plot of measured Step Heights Versus VLSI Step Height



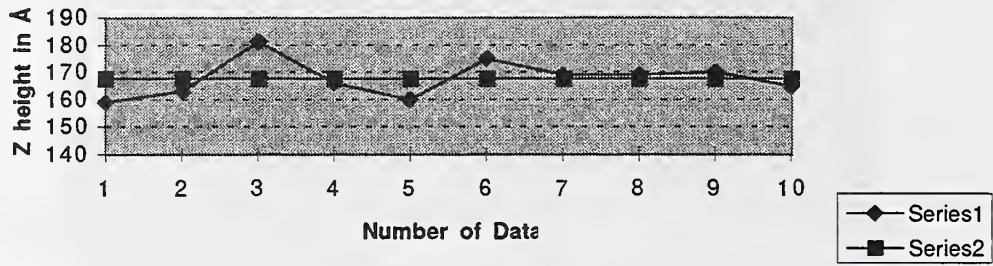
Standard Deviation Versus Step Height



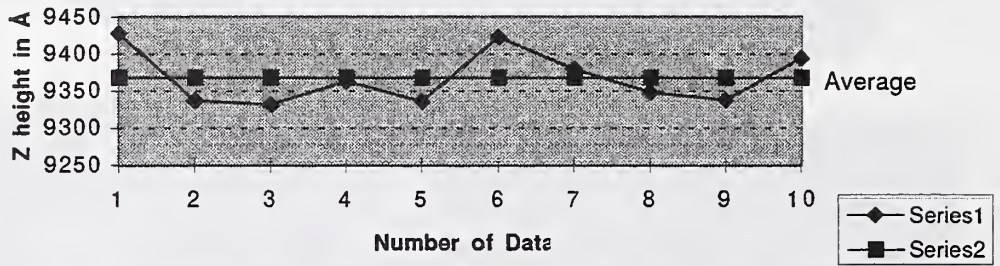
Percent Standard Deviation Versus Height



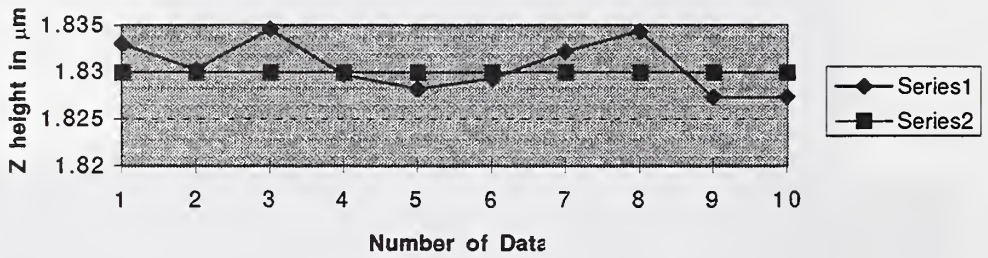
Plot of 10 Z heights on STS-18



Plot of 10 Z heights on the SHS 940



Plot of 10 Z heights on the SHS 1.



Dimensional Metrology with AFM

T. McWaid¹, J. Schneir¹, R. Dixon¹, V.W. Tsai², N. Sullivan³, S.H. Zaidi⁴, S.R.J. Brueck⁴, E.D. Williams⁵, and E. Fu⁵

¹*National Institute of Standards and Technology, Gaithersburg, MD 20899.*

²*Dept. of Matls. Engr., University of Maryland, College Park, MD 20742-4111.*

³*Digital Equipment Corporation, Hudson, MA 01749-2895.*

⁴*Center for High Technology Materials, University of New Mexico, Albuquerque, NM 87131.*

⁵*Dept. Of Physics, University of Maryland, College Park, MD 2074-4111.*

ABSTRACT

Accurate dimensional metrology with atomic force microscopy (AFM) requires accurate control of the tip position, an estimate of the tip geometry and an understanding of the tip-surface interaction forces. We describe recent progress toward the realization of accurate AFM dimensional metrology. The National Institute of Standards and Technology (NIST) has developed a calibrated AFM (C-AFM) that performs highly-resolved measurements that are directly traceable to the wavelength of light in all three axes of motion [1].

Our goals for the C-AFM system are: (1) the capability of calibrating sub-micrometer pitch artifacts with an expanded uncertainty (2σ) of three nanometers; and (2) the capability of calibrating sub-micrometer height artifacts with an expanded uncertainty (2σ) of 0.3 nm plus 1% of the height [2]. We are quantifying the performance of the C-AFM by comparing step height measurements made with a Talystep stylus profiler; the Talystep is used to perform NIST's step height calibrations. The pitch measurement capability of the C-AFM will be quantified by comparing pitch measurements made with the C-AFM and NIST's linescale interferometer, respectively. The pitch measurements (nominally 0.2 μm) are being made on a prototype Standard Reference Material 2090 scanning electron microscope magnification standard [3]. We plan to begin performing calibrations by the end of calendar year 1995.

The first AFM calibration artifact calibrated with the C-AFM will be a combined two-dimensional pitch and height standard (i.e., an X,Y,Z calibration artifact). Suitable X,Y,Z calibration standards are essential to the use of AFM in metrological applications, and several AFM calibration standards are commercially available. One series of artifact contains pitch values ranging from 1.8 μm to 20 μm , and heights ranging from 180 nm to 18 nm [4,5]. The pitch of this standard is calibrated optically; the height is calibrated using a stylus profiler.

Ideally, this family of standards should be expanded to include artifacts with pitch values down to 0.1 μm and step heights below 10 nm. These standards should be calibrated with an AFM. As the height and pitch are reduced, optical pitch calibrations become increasingly difficult. Moreover, even where the optical and stylus techniques can be used, methods divergence between these calibration techniques and AFM could introduce uncertainty into the calibration of a force microscope. The impact of methods divergence on the measurement of sub-micrometer features is discussed in a recent publication [6].

Researchers at the University of Maryland have developed methods of fabricating atom-based silicon artifacts with controlled distributions of terrace widths and heights [7]. At one end of the spectrum, artifacts consisting of single atomic steps separated by some controlled distance might make a valuable addition to the family of step height standards available to industry. Alternatively, such a standard might constitute a valuable resolution standard for surface height measuring instruments. At the other end of the spectrum, artifacts consisting of relatively wide, but characterized, distributions of step heights and terrace widths might make a valuable roughness artifact. We are investigating the feasibility and utility of both types of atomic silicon-based artifacts.

Industrial applications of SPM often include the accurate measurement of feature widths or surface microroughness. Because probe geometry affects feature width and surface microroughness measurements,

the availability of magnification standards does not enable industry personnel to perform these types of measurements accurately. Methods and/or standards for tip characterization also need to be developed. If the tip shape can be determined, and it is geometrically stable during imaging, it can be “deconvolved” (eroded) from an image to obtain some or all of the actual specimen geometry. Of course, the actual specimen geometry can only be determined in those areas where the tip interacted with the specimen surface.

Most commercial AFMs cannot image the sidewalls of vertical or near-vertical features: the feedback from the force sensor (probe) is unidirectional (nominally perpendicular to the scan plane); moreover, the geometry of most tips precludes their use for sidewall imaging. There is, however, at least one instrument, the Sloan SXM, which has been developed for imaging the sidewalls of features [5,8,9].

We are working to develop a technique for making width measurements with AFM. The strategy is to use the C-AFM to measure the feature’s top width, and a SXM owned by Digital Equipment Corporation to measure the feature’s sidewall angles. The results of these measurements will be compared with width measurements obtained using scatterometry and cross-sectional transmission electron microscopy (X-TEM).

The metrological capabilities of the SXM will be evaluated using artifacts calibrated with the C-AFM. An uncertainty budget will be generated based on the findings of these studies. As mentioned above the goal is to measure a feature’s sidewall angles using the SXM. Figure 1 presents profile data obtained with the C-AFM and the SXM, respectively. Both measurements were made on the same artifact, though not over the same feature. The artifact was fabricated out of silicon using a preferential etch procedure [10]. It contains a set of nominally 800 nm high, 0.3 μm wide lines on a 1.1 μm pitch. The limitations of the C-AFM for feature width measurement are evident from the figure; however, the potential of the C-AFM for top width measurement is also apparent. The SXM measurement illustrates both the difficulty of obtaining an absolute measurement of a width (the probe width must be eroded from the raw data), and the potential of obtaining an accurate sidewall angle measurement.

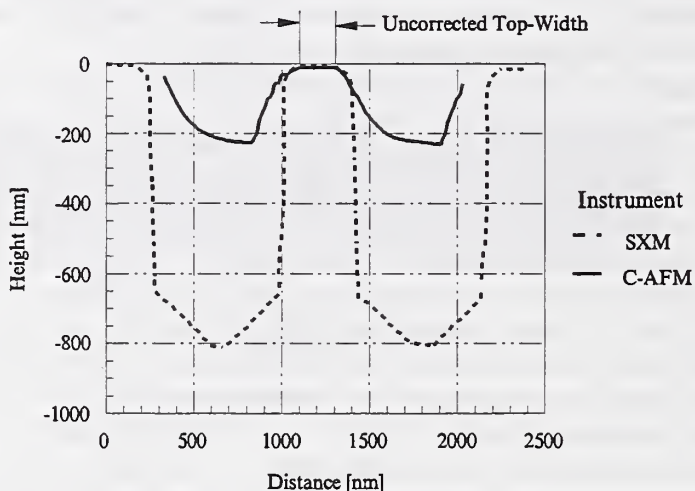


Fig. 1. Line profiles obtained with Sloan SXM and C-AFM.

We define the top width to be the width 5 nm to 50 nm below the top of the feature; we have not yet concluded what the optimal offset from the top should be. In order to accurately measure the top width of a line using the C-AFM we must know our tip dimensions over at least the bottommost 5 nm - 50 nm. Images of colloidal gold particles have been used to estimate the geometry of our tip [11,5]. The colloidal gold particles are incompressible, monodisperse and spherical. We have used the C-AFM to image both the 5.7 nm and the 28 nm diameter gold spheres deposited on mica. Thus far, we have only been able to image

the spheres using non-contact and intermittent contact (“tapping”) imaging modes; the tip pushed the particles aside when we attempted to image the specimens in contact mode.

Our plan is to image the spheres before and after imaging a line on our specimen. This will enable us to both determine the size of the tip, and ensure that the tip geometry did not change while imaging the line. Thus far, we have only followed this procedure with the 5 nm spheres. We have not yet been able to obtain indistinguishable images of the 5 nm spheres before and after imaging our artifact. Fig. 2 shows our most encouraging (best agreement of before and after images) results so far. We do not know whether the observed lack of reproducibility is due to the tip being damaged, the tip adsorbing and desorbing contaminants during imaging, or some other phenomenon. The uncertainty of our top-width measurements will have to include the geometric changes of the sphere images.

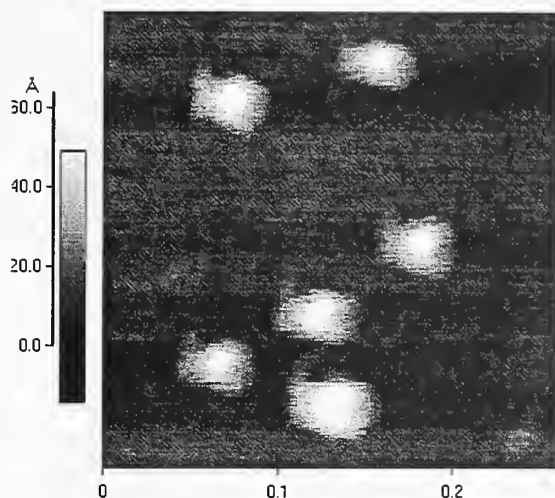


Fig. 2a. Image of Au spheres prior to imaging width artifact.

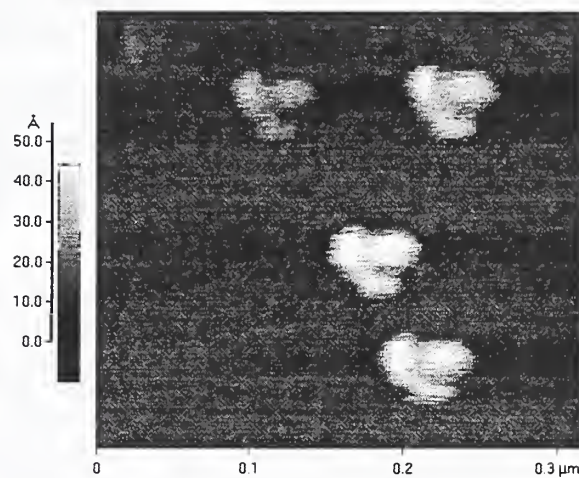


Fig. 2b. Image of Au spheres after imaging width artifact.

ACKNOWLEDGMENTS

This work was supported in part by SEMATECH and the National Semiconductor Metrology Program at NIST.

REFERENCES

1. Schneir, J., McWaid, T.H., Alexander, J. and Wilfley, B.P., *J. Vac. Sci Technol. B*, **12**(6), 3561(1994).
2. Taylor, B.N. and Kuyatt, C.E., *Guidelines for Evaluating and Expressing the Uncertainty of NIST Measurement Results*, NIST Tech. Note 1297, 1994.
3. Newell, B.L., Postek, M.T. and van der Ziel, J.P., Proc. SPIE, In Press.
4. VLSI Standards, Incorporated, San Jose, CA 95134-2006.
5. Certain commercial equipment is identified in this report in order to describe the experimental procedure adequately. Such identification does not imply recommendation or endorsement by NIST, nor does it imply that the equipment identified is necessarily the best available for the purpose.
6. McWaid, T.H., Vorburger, T.V., Fu, J., Song, J.F. and Whinton, E., *Nanotech.*, **5**, 33(1994).
7. E.D. Williams, R.J. Phaneuf, J. Wei, N.C. Bartelt, and T.L. Einstein, *Surf. Sci.*, **294**, 219(1993).
8. Veeco Instruments Inc., Milpitas, CA 95035.
9. Y. Martin and H.K. Wickramasinghe, *Appl. Phys. Lett.* **64**(19), 2498(1994).
10. A.S. Chu, S.H. Zaidi, and S.R.J. Brueck, *Appl. Phys. Lett.*, **63**, 905(1993).
11. Ted Pella, Inc., Redding, CA 96049-2477.

Faint, illegible text at the top of the page, possibly a header or introductory paragraph.



Main body of faint, illegible text, appearing to be several paragraphs of a document.

Precision nanometer-scale 3-D and Z-only Calibration Standards

Douglas Hansen
James Thorne
Wang Qui*

MOXTEK, Inc
Orem, Utah

*Brigham Young University
Provo, Utah

MOXTEK Inc. intends to produce calibration standards designed to meet the needs of scanning probe microscopy. Standards suitable for use by scanning tunneling, scanning force, scanning capacitance, and other probe microscopies will be produced. The methods used to produce these standards are derived from technologies developed to serve MOXTEK's primary market in x-ray analytical instruments.

The three-dimensional standards we will present are derived from research on soft x-ray diffraction grating fabrication and measurement. These techniques have been used to produce a two-dimensional grid with a periodicity in X and Y under 300 nm. Standards for scanning electron microscope applications produced using these techniques have demonstrated a three-sigma accuracy of 1%, or about 3 nanometers. We expect to achieve similar levels of accuracy for an SPM standard. The height, or Z dimension of the calibration standard is established by fabrication of a thin film into which the grid pattern is transferred. The thickness of this film is measured using ellipsometry or other accepted thin film measurement techniques before the pattern is transferred. The processing necessary to transfer this pattern does not alter the thickness of the initial thin film. We do not yet know the final accuracy of the Z dimension.

We have made Z-only standards by cleaving mica to reveal steps that are all integral numbers of layers thick. The layer thickness (about 0.5 nm) has been measured to 4-significant figures using x-ray diffraction. The same mica mineral (e.g. muscovite) will have slightly different layer thicknesses, depending upon its geologic history. A typical mica standard shows a dozen or so steps with heights from 4 to 300 layers thick. We have developed techniques to restrict this range (say 4 to 20 layers) for certain applications. The standard error of the slope of the calibration curve on these standards has consistently been less than 0.5%. The mica standard currently is applicable to AFM but not STM calibration. We are investigating metal coatings to extend its usefulness.

The poster paper will present images (SEM and AFM) of these standards in various stages of fabrication as well as completed prototypes. Other forms of data demonstrating the performance characteristics will also be provided.

Effect of Interface Roughness on Mobility of Si/SiGe Heterostructures

M.A. Lutz and R.M. Feenstra *

IBM Research Division, T. J. Watson Research Center
P.O. Box 218, Yorktown Heights, NY 10598

Atomic force microscopy (AFM) is used to measure surface morphology of modulation doped Si/SiGe heterostructures, and computed mobility limits due to this roughness are found to correlate with observed device mobilities. Layers are grown by ultra-high-vacuum chemical vapor deposition, at temperatures in the range 450–560°C. Step graded $\text{Si}_{1-x}\text{Ge}_x$ buffer layers are grown, reaching 30–40% Ge composition. Strained Si channels with thickness of 10 nm are grown on top of this buffer layers, and growth of a 15 nm thick spacer layer, n-type supply layer, and 4 nm thick cap layer complete the structures. Measured electron mobilities, at 0.4 K, are in the range 100,000–500,000 cm^2/Vs , depending on the details of the buffer layer growth.

AFM measurements are performed on the top surface of the structure. Quantitative roughness information is obtained over lateral length scales ranging from 50 Å to 10 μm , and is presented in the form of Fourier spectra. Three distinct components are found in the roughness spectra: (1) At the μm -scale, undulations in the surface topography (cross-hatch) arising from misfit dislocations formed to relieve strain, give rise to a large spectral peak. Figure 1(a) shows an AFM image of this cross-hatch topography. (2) At the 50–100 Å scale, atomic roughness on the surface is seen in the spectra, with amplitude which does not vary from film to film. (3) Finally, at the 500 Å scale, an intermediate scale roughness is observed as shown in Fig. 1(b). This roughness component is associated with 3-dimensional growth of the strained high-mobility channel layer. This feature in the roughness spectra shows amplitude variations of 0–15 Å from film to film and from different locations on the same film.

The roughness spectra are incorporated into a scattering computation for the mobility, where both the effect of the geometrical roughness, as well as the effect of the resulting strain inhomogeneities at the interface, are included. The results are compared with mobility limits arising from remote ionized impurities and from misfit dislocations at the bottom interface of the channel. The conditions are discussed under which roughness scattering is the mobility limiting mechanism.

* In collaboration with Frank Stern, K. Ismail, J.O. Chu, and B.S. Meyerson

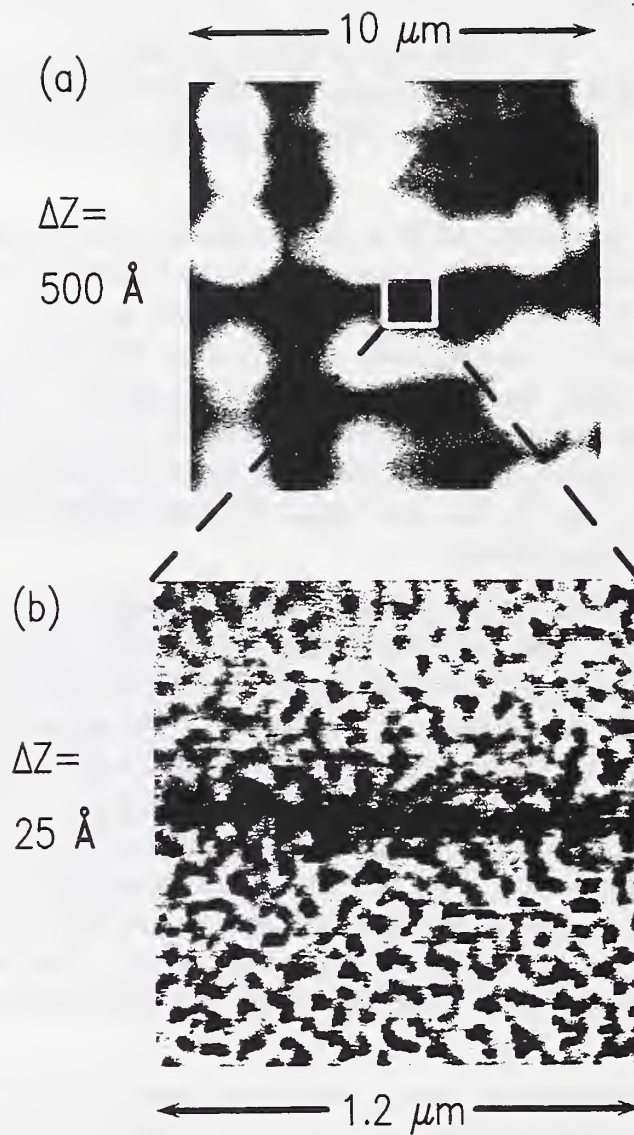


FIG. 1. AFM images of Si/SiGe structure showing (a) the cross-hatch morphology arising from misfit dislocations relieving strain in the buffer layer, and (b) intermediate scale roughness arising from 3-dimensional growth of the strained channel. The range of the grey-scale is denoted by ΔZ .

SCANNED PROBE MICROSCOPY OF MIXED CHAIN LENGTH LANGMUIR-BLODGETT FILMS

D.D. Koleske^a, W.R. Barger, and R.J. Colton

Chemistry Division, Naval Research Laboratory, Code 6177, Washington DC 20375-5342.

Studies of friction and adhesion are presented using scanning probe techniques. Since both friction and adhesion depend strongly on the chemical and structural properties of the contacting surfaces, understanding how these properties influence friction and adhesion at the nanometer scale will aid in reducing these forces in applications such as micromachined mechanical devices. Recently, several groups¹ have concentrated on the chemical aspects related to tip-surface adhesion, by correlating the magnitude of the lateral cantilever twist (friction) or pull-off adhesion force to a chemically patterned region on a surface. In these studies, the ability to distinguish changes in the local chemical environment was demonstrated¹. However, general application of SPM techniques to chemically identify unknowns on surfaces is complicated by the structural properties of the film (i.e. thermodynamic phase, modulus) and the interaction of the tip to the surface (i.e. contact area, surface/tip compliance) which are not measured directly. Using two alkanolic acids with different chain lengths to cover the surface with the same chemical endgroup, we measure two discrete adhesion levels which are related to the differences in modulus and contact area over the molecularly segregated areas of the mixed film.

The surfaces studied consisted of a mixed Langmuir-Blodgett (LB) film composed of 50% $C_{15}H_{31}COOH$ (C_{16}) and 50% $C_{23}H_{47}COOH$ (C_{24}) deposited on mica. The film was deposited at a film pressure of 30 mN/m, with the pressure vs. area isotherm indicating that the mixed film was in the 2-D solid state. Compressional moduli of pure C_{16} and C_{24} films were calculated from the pressure vs. area isotherm and were 110 mN/m for C_{16} and 150 mN/m for C_{24} . Silicon nitride cantilever tips with a nominal radius of 20 nm were used. Probe tips silanized using octadecyltrichlorosilane give similar results to the silicon nitride tip which over time adsorbs some of the LB film. The adhesion of the tip to the surface was studied using force curves, where the cantilever deflection is measured vs. the tip/surface separation (see Figure 1).

Three points are examined for each force curve measured. These three points are labeled in Figure 1 and correspond to A) the point where the tip contacts the surface or pull-on force, B) the point of maximum preset load applied between the tip and surface, and C) the point where the tip separates from the surface or pull-off adhesion. Maps (see Figure 2) which represent the surface topography, adhesion force, and lateral (friction) force and are constructed from the z-piezo distance at point B), the normal cantilever deflection at point C), and lateral cantilever deflection at point B), respectively.

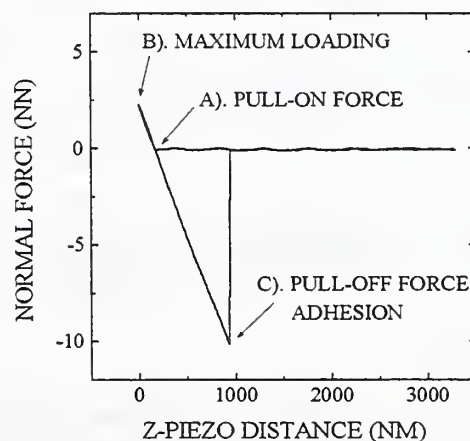


Figure 1. Example force curve measured over the C_{16} region of the surface

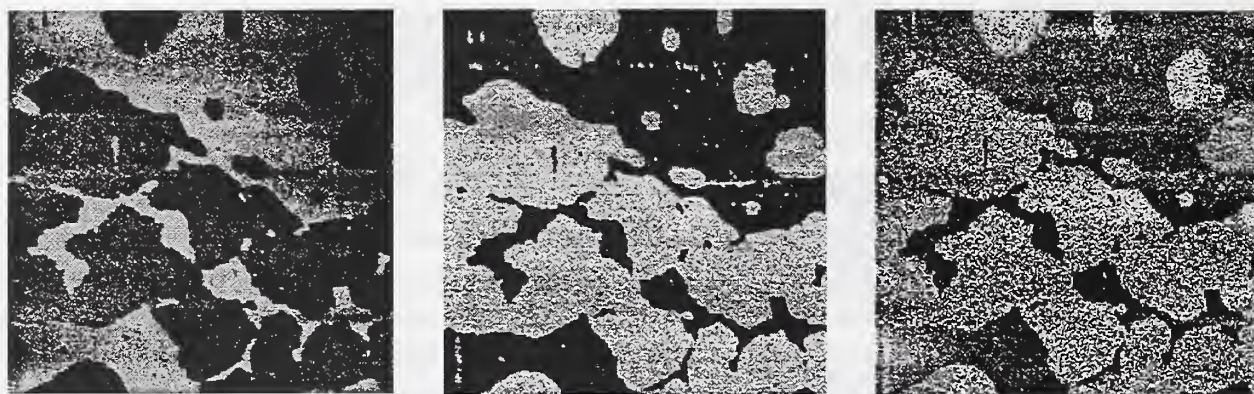


Figure 2. Topography (left), adhesion (middle), and lateral force (right) maps constructed from a 256 x 256 array of force curves over a 2 μm x 2 μm area of the mixed C₁₆ and C₂₄ film.

Maps constructed from an array of force curves measured over the mixed C₁₆ and C₂₄ film are shown in Figure 2. The surface topography is shown in the left image and was measured at point (B) at an est. maximum preset load of 2.6 nN. The topographic image has two discrete levels resulting from the phase segregation of the mixed hydrocarbons. The lighter (higher) level corresponds to the C₂₄ phase region and the darker (lower) level corresponds to the C₁₆ phase region. A height difference of ≈ 2.0 nm is measured between the C₁₆ and C₂₄ regions which is twice the expected height difference of 1.0 nm between the C₁₆ and C₂₄ acids. This difference in film height is in good agreement with previous measurements² and depends on tip penetrating more deeply into the C₁₆ regions which have a lower modulus than the C₂₄ regions.

Two distinct levels are also shown in the adhesion map (middle) measured at point (C) which inversely correlate with the levels shown on the topography map. In the adhesion map the pull-off force is 20% larger (lighter level in image) on the C₁₆ regions than on the C₂₄ regions (darker level in image). The increased adhesion over the C₁₆ regions is a consequence of the increased contact area compared to the C₂₄ regions. Using the compressional moduli, this increase in the contact area is estimated to be 21% larger over the C₁₆ regions compared to the C₂₄ regions in good agreement with the measured adhesion difference.

The lateral force map (right) measured at point (B) corresponds to the maximum degree of cantilever twisting during the force curve. The cantilever twists during the force curve because the cantilever tip axis is not perfectly normal to the surface plane. The two levels shown in the lateral force map correlate with the two adhesion levels, supporting the notion that the lateral signal measured during contact scanning is a combination the frictional and adhesion forces. Measurements where the C₂₄ acid is replaced with perfluorostearic acid will also be presented to explore chemical influences on the measured adhesion levels.

References

- a. NRC/NRL postdoctoral research fellow.
1. T. Nakagawa, *et al*, J. Vac. Sci. Technol. B **12**, 2215 (1994); C.D. Frisbie, *et al*, Science **265**, 2071 (1994); R.C. Thomas, *et al*, J. Phys. Chem. **98**, 4493 (1994).
2. L. Wolthaus, A. Schaper, and D. Möbius, J. Phys. Chem. **98**, 10809 (1994).

Characterization of Metallic Thin Film Growth by STM[†]

A. Davies, J. A. Stroscio, D. T. Pierce, J. Unguris, M. D. Stiles, and R. J. Celotta
National Institute of Standards and Technology, Gaithersburg, MD 20899

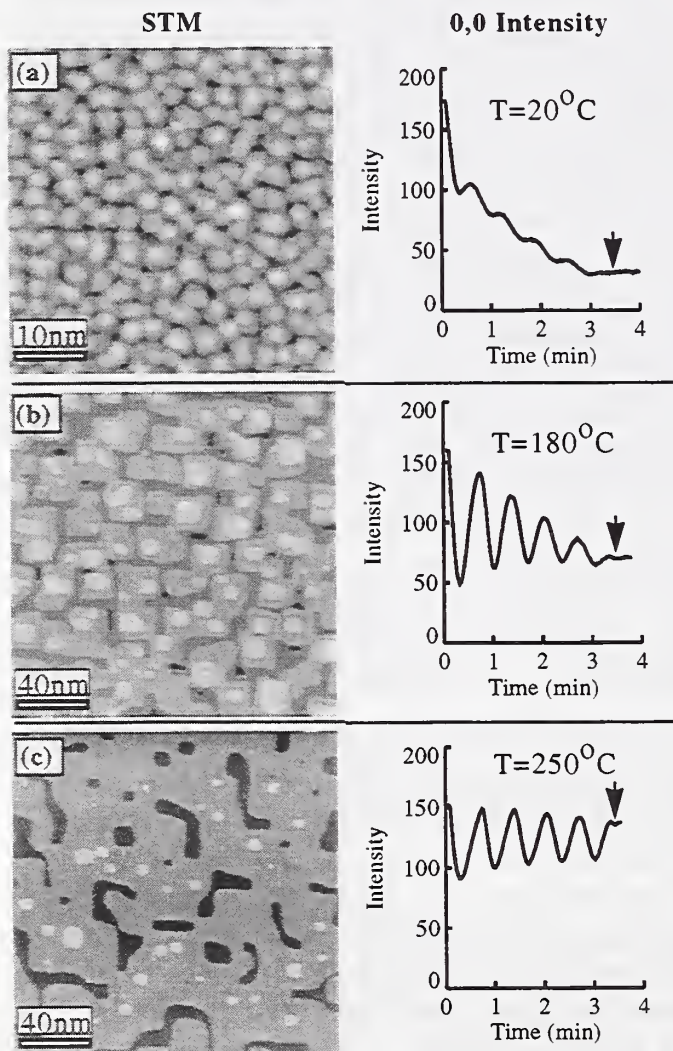
Over the past several years, metallic multilayer systems have emerged as an important new area of research from the perspective of both fundamental science and technology. For example, magnetic multilayer systems exhibit a giant magnetoresistance (GMR) which is currently being exploited to develop superior read heads for magnetic recording. From the fundamental science viewpoint, a basic understanding of this phenomenon is lacking and represents both an experimental and theoretical challenge. A significant aspect of the challenge is that the final properties of multilayer systems depend strongly on structural details such as layer uniformity and interfacial structure, and therefore an understanding of the magnetic properties requires detailed characterization of and control over thin film growth. Scanning tunneling microscopy (STM) can be used to directly evaluate thin film morphology and is an ideal tool for determining growth processes in these systems. By using STM to study the growth of both Fe and Cr on Fe(001) substrates, we have made significant progress in the determination of fundamental growth processes in metallic systems. We have also correlated STM-determined details of the Cr/Fe interface with the magnetic properties of Fe/Cr/Fe multilayer systems to understand the relationship between magnetic properties and structure.

In the fundamental growth studies, we have characterized the temperature dependence of Fe(001) homoepitaxy from the nucleation of atomic-layer islands through the evolution of the growth of a thin film. In the early stages of growth, the density of the atomic-layer islands is found to be a strong function of temperature [1]. This results from the temperature dependence of the adatom diffusion and the critical atomic size of stable island formation, both of which can be determined from a statistical analysis of the 2-d nucleated islands [2]. As growth proceeds, we have shown that the film morphology is determined by step-edge barriers for diffusing adatoms [3]. At low temperatures where adatoms have insufficient energy to overcome the step-edge barriers, additional islands nucleate on existing islands resulting in a film morphology determined by the island density in the early stages of growth. This leads to rough surfaces with several layers in the growth front and damped RHEED intensity oscillations measured during growth as shown in Fig. 1 (a) and (b). Layer-by-layer growth is achieved at higher temperatures where the adatom thermal energies are sufficient to overcome the step-edge barriers. The characteristic persistent RHEED intensity oscillations measured during layer-by-layer growth are shown in Fig. 1 (c) along with the STM image of the surface after growth was stopped. To gain a full theoretical understanding of the growth process, a simulation of film growth has been achieved in a continuum growth model.

To correlate the STM-determined structure of Cr/Fe thin film systems with the magnetic properties, we use scanning electron microscopy with polarization analysis (SEMPA) to evaluate the exchange coupling in similarly prepared Fe/Cr/Fe multilayers [4]. In this system, the magnetic coupling of the two Fe layers oscillates between ferromagnetic and antiferromagnetic coupling with increasing thickness of the Cr spacer layer. The thickness dependence of the coupling is evaluated by depositing a wedge of Cr for the spacer layer and then exploiting the spatial resolution of SEMPA to determine the magnetization of the top Fe film along the wedge. Two periods of oscillation with thickness are observed in the Fe/Cr/Fe(001) system. The dominant period is found to depend on the Cr growth temperature. By using STM to evaluate

the temperature dependence of the Cr film morphology, the observed strengths of the oscillation periods in the exchange coupling are seen to be a result of the roughness, or thickness fluctuations, of the Cr spacer layer.

Another consequence of the structural details of the Fe/Cr/Fe(001) system is seen in the exchange coupling measurements in the thin-Cr layer limit. The exchange oscillations with Cr thickness are not seen for thicknesses less than ~ 5 monolayers and the sign of the first oscillation is opposite to expectations. STM investigations of the early stages of Cr growth on Fe(001) show that the Cr alloys with the Fe substrate and that this interdiffusion persists for several layers of Cr deposition. For Cr coverages less than a monolayer, the alloy is seen as a low concentration of single impurity atoms embedded in the surface layers. The dominant element at the surface can be identified as Fe and the impurity atoms as Cr by using tunneling spectroscopy; a surface state near the Fermi energy on the Fe(001) surface leads to narrow peak in the tunneling conductance spectra and this conductance peak is seen on the alloyed surface between the single impurity atoms. As the initial Cr coverage is increased, the Fe concentration in the surface layers decreases. Chromium becomes the dominant element in the surface layers only after deposition of somewhere between 5 to 10 monolayers of Cr.



† Supported in part by the Office of Naval Research

[1] J. A. Stroscio, D. T. Pierce and R. A. Dragoset, Phys. Rev. Lett. **70**, 3615 (1993).

[2] J. A. Stroscio and D. T. Pierce, Phys. Rev. B **49**, 8522 (1994).

[3] To be published.

[4] D. T. Pierce, J. A. Stroscio, J. Unguris and R. J. Celotta, Phys. Rev. B **49**, 14564 (1994).

FIG. 1. STM and RHEED (0,0) beam intensity measurements of Fe on Fe(001) growth obtained on the same samples. All of the films were grown for five RHEED oscillations, at which time the Fe flux was turned off, indicated by the arrows in the RHEED plots. Sample temperatures during growth are (a) 20 °C, (b) 180 °C and (c) 250 °C. STM images are shown in a grey scale with black corresponding to the lowest height level. The major changes in grey level indicate monatomic steps.

Surface Studies with the Scanning Kelvin Force Probe

Todd Hochwitz, Albert K. Henning, Chris Levey, and Charles Daghljan

Dartmouth College Hanover, NH

James Slinkman, James Never, Phil Kaszuba, Robert Gluck,
Randy Wells, Ronald Bolam, and Peter Coutu

IBM Microelectronics Essex Junction, VT

A novel combination of atomic force (AFM) and electrostatic force based scanning Kelvin probe microscope (SKPM) has been used to examine a variety of fabrication related defects in integrated circuits (IC) on a sub-micron scale [1-3]. Research also indicates that the SKPM is capable of imaging dopant profiles in ICs of technological interest [4-10]. The poster will present some of the successful surface studies we have made with the SKPM.

The force-based SKPM shown in Figure 1 was developed upon a non-contact AFM originally built at IBM's Thomas J. Watson Research Center [11]. We have added the necessary electronics to convert the system to the force-based SKPM [12]. The AFM is used to maintain a constant spacing between a sample and tip of a force-sensing probe as the probe is scanned over the sample's surface. The feedback signal needed to maintain this spacing yields an estimate of the surface topography. We refer to measurements with this loop as the van der Waals (vdW) signal.

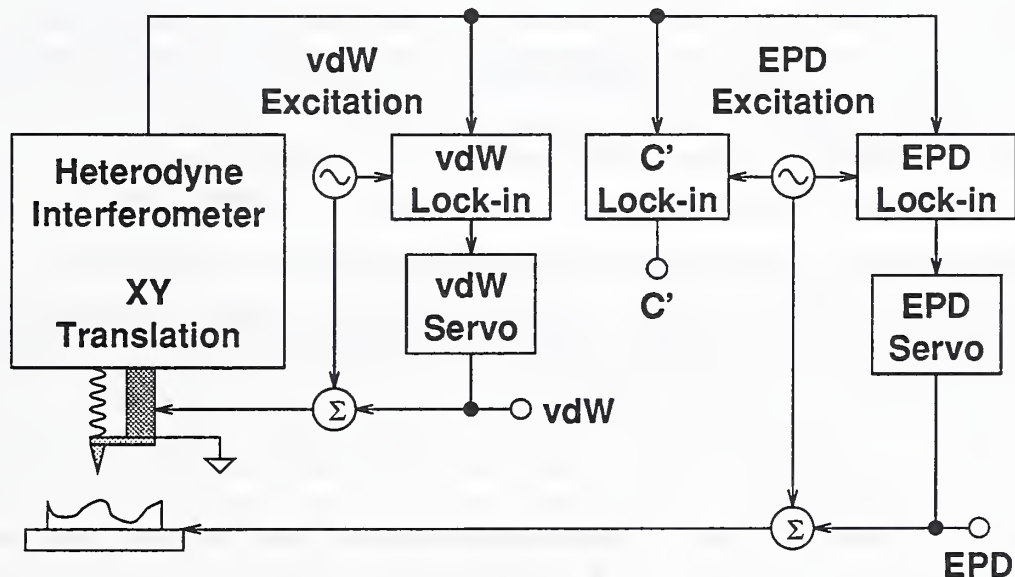


Figure 1: The force-based SKPM system.

A second detection and control loop is used to monitor spatial inhomogeneities in the surface work function (WF) of the sample under study. The variations in measured WF are directly attributable to material properties, from which we are able to infer the measurements we present in the poster. There is an

additional electrical signal obtained that is directly proportional to the total capacitance between the probe and electrical connections to the back of the sample. Thus, we are additionally able to map out spatial variations in the bulk capacitance of the sample. We refer to the electrical measurements as the electrical potential difference (EPD) and C' signals.

The system consistently achieves lateral resolutions under 100 nm, a closed loop vdW noise level of $0.5 \text{ \AA}/\sqrt{\text{Hz}}$ measured in a 100 Hz bandwidth, and a closed loop EPD noise level of $5 \text{ mV}/\sqrt{\text{Hz}}$ measured in a 160 Hz bandwidth. The system has achieved lateral resolutions of 25 nm, a closed loop vdW noise level of $0.1 \text{ \AA}/\sqrt{\text{Hz}}$, and a closed loop EPD noise level of $1 \text{ mV}/\sqrt{\text{Hz}}$. Further details about the system operation may be found elsewhere [10].

The poster will include results of measurements upon surface cracks and dislocations on silicon substrates; bird's beak stress due to field oxide at the edges of poly-silicon gates; the presence of surface charge on oxide; dopant profiles, including lightly doped drains and p/n junctions; ionic contaminants in the dielectric of DRAM cells; cracks in and contact vias missing from aluminum lines due to electromigration; and boron doped NiAl grains.

References

- [1] T. Hochwitz, A. K. Henning, C. Levey, C. Daghljan, J. Slinkman, J. Never, P. Kaszuba, R. Gluck, S. Hoffmann, and M. O'Boyle, in *1994 Fall Meeting of the IBM Failure Analysis Technical Exchange* (IBM Microelectronics, Burlington, Vt, 1994).
- [2] T. Hochwitz, A. K. Henning, C. Daghljan, R. Bolam, P. Coutu, R. Gluck, and J. Slinkman, in *Proc. Int. Reliability Physics Symp.* (IEEE, New York, NY, 1995).
- [3] Martin O'Boyle and Tom Hwang, private discussions.
- [4] Y. Martin, D. W. Abraham, and H. K. Wickramasinghe, *Appl. Phys. Lett.* **52**, 1103 (1988).
- [5] D. W. Abraham, C. C. Williams, J. Slinkman, and H. K. Wickramasinghe, *J. Vac. Sci. Technol. B* **9**, 703 (1991).
- [6] J. M. R. Weaver and D. W. Abraham, *J. Vac. Sci. Technol. B* **9**, 1559 (1991).
- [7] J. M. R. Weaver and H. K. Wickramasinghe, *J. Vac. Sci. Technol. B* **9**, 1562 (1991).
- [8] M. Nonnenmacher, M. O'Boyle, and H. K. Wickramasinghe, *Ultramicroscopy* **42-44**, 268 (1992).
- [9] T. Hochwitz, A. K. Henning, C. Levey, C. Daghljan, J. Slinkman, J. Never, P. Kaszuba, R. Gluck, R. Wells, J. Pekarik, and R. Finch, in *Proceedings of the Third Intl. Workshop on the Measurement and Characterization of Ultra-Shallow Doping Profiles in Semiconductors* (American Vacuum Society, New York, NY, 1995), pp. 47.1-47.8.
- [10] A. K. Henning, T. Hochwitz, J. Slinkman, J. Never, S. Hoffmann, P. Kaszuba, and C. Daghljan, *J. Appl. Phys.* **77**, 1888 (1995).
- [11] Y. Martin, C. C. Williams, and H. K. Wickramasinghe, *J. Appl. Phys.* **61**, 4723 (1987).
- [12] M. Nonnenmacher, M. P. O'Boyle, and H. K. Wickramasinghe, *Appl. Phys. Lett.* **58**, 2921 (1991).

Measurement of the Absolute Nanoscale Mechanical Properties of Polymer Surfaces using the AFM

D.M. Schaefer¹, C.F. Draper², R.J. Colton¹, B.M. DeKoven³, G.F. Meyers³, T. Ho⁴, K. J. Wynne⁴, Stephen C. Webb⁵, and S.M. Hues¹

¹ Code 6170, Naval Research Laboratory, Washington, D.C. 20375-5342

² Dept. of Mechanical Engineering, Vanderbilt University, Nashville, TN

³ The Dow Chemical Company, Midland, MI

⁴ Office of Naval Research, Arlington, VA

⁵ Wilson Instruments/Instron Corporation, 100 Royall Street, Canton, MA 02769

Indentation is used to measure specific material properties of a surface such as elastic modulus, hardness, or creep by monitoring the penetration of an indenter tip into a material. This may be done as a function of load at a constant loading rate or of time at a constant load. Nanoindentation involves performing indentation with either a contact diameter or penetration depth on the nanometer scale. Nanoindentation may be performed either on a single point of the surface to characterize the material properties of homogeneous surface layers or as a series of indentations in a raster scan pattern thereby probing both the lateral and in-depth property distributions of the sample. The nanoscale mechanical properties of surfaces are of particular importance in industrial applications as they dominate critical parameters such as friction, wear, and adhesion. With the advent of nanoindentation using the atomic force microscope, we now have the ability to directly measure the mechanical properties of surface layers having only nanometer thicknesses.

Quantitative mechanical property measurement involves the precise and accurate measurement of the relative differences in mechanical properties between two volumes, e.g., volume A is 2.2 times stiffer than volume B. Quantitative measurements may also be absolute in that the measurement may be measured without regard to a reference volume, e.g., volume A has a modulus of 6.4 GPa. In industrial applications, absolute measurements are preferable as results may then be compared with those from different laboratories, standard reference materials, or industry standards.

A critical factor in absolute measurement is the determination of the contact area between the tip and the surface. In previous studies, we have used diamond indentors to probe surface oxide coatings on metal [1] and silicon [2] single crystals. These indenter tips were fabricated by growing diamond crystals onto tungsten wire by chemical vapor deposition. By using the apexes of the diamond crystals as indentors, contact diameters as small as 10 nm have been achieved at penetration depths of 20 nm. The exact contact area is, in practice, very difficult to determine. Pointed tips all have some finite bluntness at the end which may be characterized by some method such as apex imaging with an atomic force microscope. These methods, however, provide the non-loaded tip contour. The tip will flatten under load unless the surface is extremely compliant with respect to the tip. In addition, the extent of this deformation will differ depending upon the relative modulus of the tip and the sample. When dealing with such small contact areas even deformations of a few atomic dimensions will affect the derived material properties. While the uncertainties in the contact area determination precluded absolute measurements in these earlier studies, quantitative information of surface mechanical properties was obtained on these surfaces using the diamond tips. Work at NRL is currently in progress to investigate tip/surface contact dynamics through both experiment and

simulation.

When measuring the properties of homogenous thin films or coatings, where high lateral resolution is not required, spherical indentors have several advantages [3]. Among these is a larger and more easily defined contact area with the surface. Spherical indentors are commonly used to examine mechanical properties as a function of strain in that, unlike indentors of other geometries (e.g., flat punches, pointed tips), they generate a changing strain as a function of penetration depth. We have used a similar approach in that we maintain a constant penetration depth (20 nm in Fig. 1) and increase the strain by decreasing the sphere diameter (2000 μm - 15 μm). While this approach may be used with other geometry tips they do not have the well-defined shape, and hence contact area, as do the spheres. The spherical indentors in our instrument are fabricated using glass spheres and have been used to obtain *absolute* measurements of surface elastic modulus and hardness in materials such

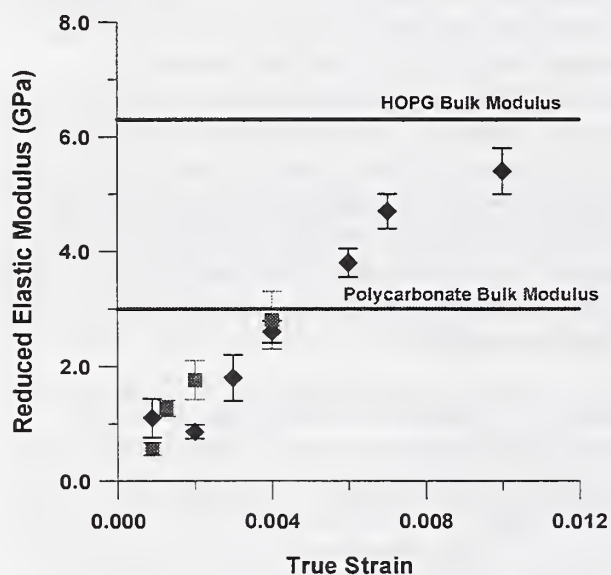


Fig. 1: ■ Polycarbonate
▲ HOPG

as highly-orientated pyrolytic graphite (HOPG) [4], and polycarbonate, Fig. 1. Measurements obtained at the highest strains accessible with our instrument have shown excellent agreement with the bulk elastic modulus measured via indentation at much higher strains using commercial instrumentation (UMIS-2000). This is the first example of absolute nanoscale mechanical property measurements that have been verified by an independent technique. As the strain is reduced, interesting material-dependent effects are seen. For example, while polycarbonate quickly reaches its bulk elastic modulus as the strain is increased (the initial softening being ascribed to the semibounded nature of the surface), HOPG shows a much more extensive softened region. This effect we attribute to residual tensile strain between the surface basal plane layers produced by

the exfoliation of the sample prior to analysis. Because of their larger contact areas, however, these spheres do not have the lateral resolution required to measure mechanical property variations about such features as interfaces or different phase regions in a nanoscale composite. Because of these limitations our work is continuing on the application of small contact area probes to absolute nanoindentation measurements.

- [1] S.M. Hues, C.F. Draper, and R.J. Colton, *J. Vac. Sci. Technol.*, **B12**, 1 (1994).
- [2] S.M. Hues, C.F. Draper, and R.J. Colton, *Forces in Scanning Probe Microscopy*, NATO ASI Series E: Applied Sciences, edited by H.J. Güntherodt, D. Anselmetti, and E. Meyer, Kluwer Academic Publishers, in press.
- [3] J.S. Field and M.V. Swain, *J. Mater. Res.*, **8**, 297 (1993)
- [4] C.F. Draper, D.M. Schaefer, R.J. Colton, S.C. Webb, and S.M. Hues, *J. Mater. Res.*, submitted.

Pneumatic Scanning Force Microscopy - A Methodic Approach of Membrane Characterization

H. Kamusewitz, M. Keller and D. Paul

*GKSS Research Centre Geesthacht GmbH, Institute of Chemistry,
Kantstrasse 55, D-14513 Teltow, Germany*

1. Introduction

The growing significance of membranes as an efficient component for industrial applications is based on their excellent separation performance. Using the common NanoScope and siliconitride tip, pores with a diameter larger than 50 nm can be visualised. Pores of smaller diameter are not measurable, in particular if the membrane is very rough. Pores smaller than 20 nm were not found in the literature.

The poster describes a new application of Scanning Force Microscopy, called Pneumatic Scanning Force Microscopy (PSFM), which has been developed especially for porous materials. The PSFM utilized a pressure difference between the downstream and the upstream side of a porous material. Therefore the common SFM on these samples is a special case of the PSFM without pressure. The purpose of PSFM is to obtain more specific information about the properties of individual pores by observing the influence of the pores on a gas streaming through them.

2. Experimental details

All PSFM images were obtained at normal temperatures, by means of common NanoProbe (registered trademark) using a NanoScope III, Digital Instruments. PSFM requires an additional special chamber to investigate flat membranes. The chamber is sealed hermetically with the object of interest. The maximum pressure difference between the interior of the chamber and the exterior was $\Delta p = 1.5$ bar and constant during the whole scan time. Pure nitrogen was used in all experiments, but normal pressurized air should work just as well. A platinum electron beam diaphragm with a well defined single hole (diameter 5 micron) and a broad spectrum of practically relevant membranes made from polymeric and ceramic material were selected in order to demonstrate the possibilities and limitations of this special SFM application.

3. Results

Using the diaphragm with an extended single hole (diameter 5 micron) the image shows that the whole cantilever interact with the nitrogen stream. In contrast, the gas stream through a smaller pore (diameter smaller than a half micron) interacts only with the pyramidal tip. Therefore, a real image of the membrane surface around the pores is available. Additionally, the gas stream gives well defined cones above the pores. Both the volume and the estimated height of an average gas cone (approximately 26 nm) are a function of the pressure differential.

The investigation of a ceramic membrane shows that the very small and apparently rather closely packed gas channels were no longer detected individually by the tip and as a result the probe only detected a compound effect of the constituent gas jets. The local forces are great enough to separate the tip from the sample across extended areas of the membrane. The stronger the individual streams are and the more of them exist within a small area, the more extended are the regions of separation between tip and sample. As the pressure increases, more and more pores take part in the transport of gas, and as a result the areas streamed through by the gas start to dominate the image.

This new technique enables us to obtain more specific information about the actual volume, the diameter and the distribution of pores through which the gas is streaming.

NIST Industrial Fellows Program: Magnetic Force Microscopy at Maxtor Corp.

Paul Rice and Jim Potter*

National Institute of Standards and Technology, Boulder, CO

*Maxtor Corporation, Longmont, CO

The Superconductor and Magnetic measurements group at the National Institute of Standards and Technology, Boulder CO has developed a strong program in magnetic force microscopy (MFM). Previously we have established several collaborations with Maxtor Corporation of Longmont CO to use MFM to image samples of current concern. To further our understanding of disk drive technology and help Maxtor develop their own MFM capabilities we have entered into a cooperative research agreement that will benefit both NIST and Maxtor. This is a new program of NIST called the Industrial Fellows Program. The goal of the Industrial Fellows Program is to help American industry compete in a world wide market by transferring technical knowledge directly to industry and to help direct NIST research towards solutions of technically challenging industry problems.

Several projects are currently being developed under this program at Maxtor. Among these projects are imaging the magnetic field profiles of thin-film recording heads. Test procedures for thin-film heads consist of writing data on a disk and then reading back this previously written information. The comparison of the write and read data signals determine the quality of the head. Also, the magnetic "bit" structure written to the disk is analytically described by applying the calculated write field profile of the recording head to the disk. This is assuming that the head is manufactured exactly as specified, but due to manufacturing variables this is not always consistent. It would be useful to have a magnetic image of the head fields to correlate these data.

Fig. 1 is an image of a thin-film head taken with ac MFM. This head is from a disk drive currently in production. The magnetic force image (left) and the topographic image (right) were taken simultaneously. The tip used was a commercially coated CoCr, Si tip. The MFM image shows that the tip responds as if coated with a magnetically hard coating. This is indicated by the bright and dark pole pieces corresponding to opposite polarities. The steep gradient across the pole pieces in the MFM image corresponds to the width of the recording gap in the topographic image. Notice the dark areas trailing from the pole pieces in the MFM image¹. These correlate to the transition in the alumina overcoat. This could be caused by a concentration of magnetic flux in a seed layer of Ni-Fe alloy that was left after the deposition process for the pole pieces or it could be caused by stray field from the yoke of the receding pole piece located within a few microns of the air bearing surface².

Other projects focus on magnetization of the data written on the disk, such as measuring the dimension of the magnetic transitions of bit patterns and the static field interactions between the bits on the disk. We have used near-field MFM to image bit patterns on a glass substrate hard disk. This disk is used in one of the small drives for laptop computers. Fig. 2 is a 10 μm X 10 μm scan of the disk. The magnetic force image on the left shows the bit patterns on the disk. The right image is the topography of the disk. Notice the mottling of the background in the magnetic image. This mottling corresponds to topographic features and is not present when imaging with a

non-magnetic tip indicating that there could be a correlation between surface features and magnetic domain size.

These images show the viability of MFM for qualifying disk drive components. Since the MFM is a non-destructive technique the recording heads and media can be reused after imaging to provide additional information. We plan to explore further applications of scanned probe microscopy to disk drive components.

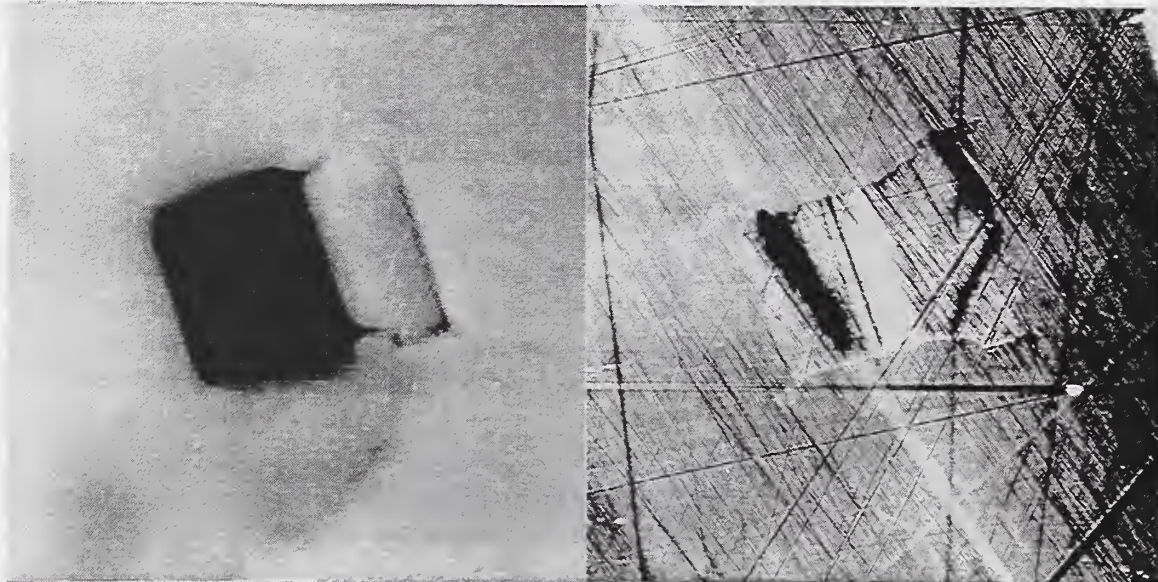


Fig. 1 Magnetic force image (left) and topographic image (right) of a thin-film head.

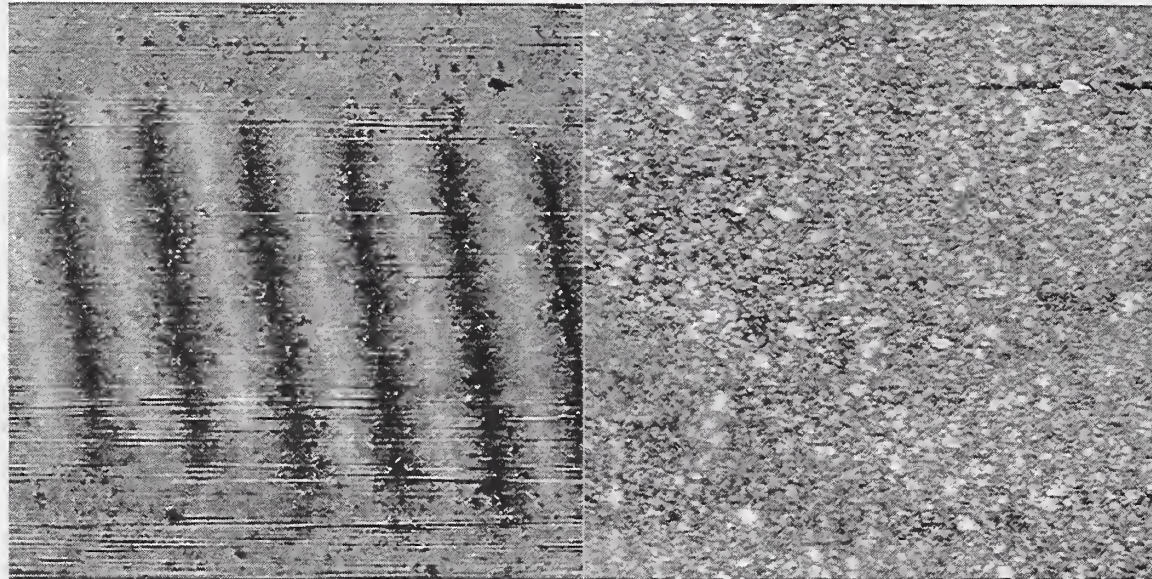


Fig. 2 Magnetic force image (left) and topographic image (right) of a glass substrate hard disk.

1. P. Rice, J. Moreland, and A. Wadas, "dc magnetic force microscopy imaging of thin-film recording head," *J. Appl. Phys.*, Vol. 75, No. 10, pp 6878-6880, 15 May, 1994.
2. P. Rice, B. Hallett, and J. Moreland, "Comparison of magnetic fields of thin-film heads and their corresponding bit patterns using magnetic force microscopy," *IEEE Trans. Mag.*, Vol. 30, No. 6, pp. 4248-4249, Nov. 1994.

Automated calibration of scanning probe microscopy by image processing

J.F. Jørgensen

National Institute of Standards and Technology, Bld. 220, Rm A117, Gaithersburg MD 20899

Danish Institute of Fundamental Metrology

Email: JJorgen@Pyrolusite.NIST.Gov

1 Introduction

The continuing drive within high technology industries to push dimensional tolerances to still smaller values motivates the use of scanning probe microscopy (SPM), which has the ability to resolve surface structures with atomic resolution. The types of measurements that can be addressed by SPM are, step heights, displacements and micro roughness by direct topographical measurements and micro hardness by analysis of hardness indentations. Such measurements are becoming important for quality control of motor parts, smooth optical surfaces, coatings and micro electronics.

Inspired by the new opportunities given by SPM we have, in a project for the European Union [1], recently developed a number of calibration and measuring techniques based on image processing and we have defined a set of roughness and hardness parameters for three dimensional topographic images. This presentation will focus on the calibration aspects.

2 Calibration

The practical value of an instrument depends strongly on its user friendliness and reliability. Commercial microscopes are software based with an easy-to-use human interface. The calibration, however, is not always easy to accomplish, and the calibration procedures typically do not measure all the factors that can produce distorted surface images. There are, therefore, intrinsic errors in the calibration typically performed on SPM instruments. At the Danish Institute of Fundamental Metrology (DFM) we have developed new, automated techniques for accurate calibration of SPM microscopes [2, 3, 4]. The techniques are based on the imaging of repeated surface structures with known characteristics.

The calibration analyses are carried out off-line on a workstation computer on which the images can also be corrected if desired. Some of the calculated calibration factors may afterwards be entered into the SPM instrument, while other parameters still can not be handled by the instruments.

There are many factors that may cause distorted SPM images. Here we will address only the most important ones X-, Y- and Z-sensitivities, nonorthogonality and hysteresis.

2.1 Hysteresis

To produce correct images it is necessary to sample the surface height values at equidistant locations. Since the scanning elements are usually nonlinear due to hysteresis effects, it is necessary to apply some correction mechanism. Certain instruments have built-in electromechanical sensors, *e.g.*, capacitive sensors for control of the lateral displacement. This may improve the linearity of the images significantly, but the sensors may have residual nonlinearities and they are not suitable for all scanning devices. Most other SPM instruments have some correction procedures integrated in the software. However, these procedures do not always precisely fit the scanning element actually used and are difficult or impossible to adjust by the user.

Our approach to the problem has therefore been to use advanced image processing techniques to characterize the hysteresis effects and to define correction algorithms, which may either be used off-line or incorporated in the SPM instrument. One of the techniques we have developed is based on Fourier analysis of images acquired from calibration artifacts that have periodic structures. The goal is to find the hysteresis model that enables the reconstruction of the image such that local periodicities are uniform over the entire image. Such a situation will be reflected in the Fourier domain by high and narrow peaks. The hysteresis model can therefore be found iteratively by adjusting the hysteresis model and correcting the spatial image such that the peaks in the Fourier space image are maximized.

2.2 Lateral calibration

Most SPM instruments have a provision for lateral calibration. However, this calibration can only be done by the user, who must define the length between selected points on the image. Such procedures are not very accurate and can give different results depending on the orientation of the sample. The accuracy is also limited because angular distortions caused by drift or asymmetric scanning elements are not estimated.

We have therefore developed a new method for automatic and accurate calibration that accounts for angular distortion. The technique is based on recorded images of calibration artifacts with well known periodic structures and subsequent Fourier analysis. Fourier transforms of periodic patterns exhibit peaks corresponding to the periodicities of the surface. These peaks are suitable for automatic recognition by image processing software, thus enabling the calculation of the unit cell, *i.e.*, the periodic distances and angles, can be calculated. By comparing the measured unit cell with the known structure of the surface it is possible to calculate the calibration factors for the X and Y directions along with a skewness angle, which is the deviation from the ideal 90° between the X-Y axes.

2.3 Vertical calibration

The vertical calibration of SPM microscopes has until recently been a difficult task because no suitable calibration artifacts have been available. Now calibration objects with certified step height values can be obtained, [5]. For many of the other 3D measurements however, there are still no standards for calibrating height. A given step height may be measured locally, but due to local variations of the surface structure and noise in the image, repeated measurements can give quite different results. Step height measurements should therefore be based on average values.

We have been using a "correlation averaging technique" [4, 1] for calculating the average topographic image of a repeated step structure. In this technique one of the repeated structures is selected as a template. The

calculated cross correlation function of the template and the original image will reveal the positions of the areas most similar to the template. By aligning these areas an average image for the repeated structure can be calculated. The advantage of the technique is that the averaged image has a much better signal to noise ratio so that the step height can be detected easily and robustly from the height distribution histogram.

Acknowledgment

This study work has been supported by the Commission of the European Communities (contract no. 3423/1/0/184/91-BCR-DK-30).

References

- [1] G. Barbato, K. Carneiro, D. Cuppini, J. Garnaes, G. Gori, G. Hughes, C. P. Jensen, J. F. Jørgensen, O. Jusko, S. Livi, McQuoid, L. Nielsen, G. Picotto, and G. Wilkening. Synthesis report on the bcr project: "*Scanning tunneling microscopy methods for roughness and micro hardness measurements*", contract no 3423/1/0/184/4/91-bcr-dk(30), 1994.
- [2] J.F. Jørgensen, L.L. Madsen, J. Garnaes, and K. Carneiro. Calibration, drift elimination and molecular structure analysis. *J. Vac. Sci. Tec.-B*, 12(3):1698-1701, 1994.
- [3] J.F. Jørgensen, K. Carneiro, L.L. Madsen, and K. Conradsen. Hysteresis correction of scanning tunneling microscope images. *J. Vac. Sci. Tec.-B*, 12(3):1702-1704, 1994.
- [4] J.F. Jørgensen. *Scanning Probe Microscopy Image Restoration and Analysis*. PhD Thesis, ISBN 87-88306-14-3, IMSOR, DTH Denmark, 1993.
- [5] VLSI Calibration objects of VLSI Standards Incorporated, 2660 Marine Way, Mountain View, CA, 94043, USA.

MAGNETIC FORCE MICROSCOPY USING Fe-SiO₂ COATED TIPS^a

P. F. Hopkins and J. Moreland

National Institute of Standards and Technology, Boulder, CO 80303

S. S. Malhotra and S. H. Liou

Dept. of Physics and Astronomy, University of Nebraska, Lincoln, NE 68588

We report the first magnetic force microscopy (MFM) images obtained with batch micromachined tips coated with nanocomposite Fe-SiO₂ thin films and compare these images to those obtained with commercial MFM tips. Nanocomposite Fe-SiO₂ films consist of small (3-16 nm) size Fe crystallites in an amorphous SiO₂ matrix and have been shown to have both high corrosion and wear resistances. In addition, the magnetic properties can be favorably engineered by controlling the microstructure during the deposition process [1]. In the presented poster, we show that Fe-SiO₂ coated Si₃N₄ and Si cantilevers/tips can be used to obtain high resolution MFM images of bit tracks on a hard disk and on a metal-evaporated tape. We show that the magnetic tip coating can be engineered to give bit track MFM images characteristic of either magnetically soft or hard tips, depending on the Fe-SiO₂ film thickness used.

Commercial cantilevers/tips were magnetron sputter-coated at 300 K using a homogeneously mixed composite Fe-SiO₂ target [1]. Magnetic force (DC mode) MFM images were taken using Fe₇₀(SiO₂)₃₀ coated Si₃N₄ cantilevers with spring constants $k = 0.06$ N/m. A Fe₇₀(SiO₂)₃₀ film grown simultaneously on a glass substrate was 70 nm thick and showed a room temperature saturation magnetization M_s approximately that of bulk Fe and a coercivity $H_c = 1.4 \times 10^4$ A/m (176 Oe). Force derivative (AC mode) MFM images were taken using Fe₈₀(SiO₂)₂₀ coated Si cantilevers with spring constants $k = 1-5$ N/m, resonant frequencies $f_0 = 81-89$ kHz, and quality factors of $Q \sim 100$ in air. Two batches of 6 tips with different Fe₈₀(SiO₂)₂₀ film thicknesses, 36 nm and 100 nm, were used. Previous film thickness studies of Fe₈₀(SiO₂)₂₀ sputtered onto glass substrates suggest that the 36 nm and 100 nm films should have different coercivities, $H_c = 1.0 \times 10^4$ A/m (130 Oe) and $H_c = 2.7 \times 10^4$ A/m (340 Oe), respectively [2]. MFM images taken with these tips were compared to images taken with similar AC MFM Si tips commercially available with magnetic coatings of Co-Cr (30 nm) and permalloy (15 nm).

The tips were mounted on a commercial MFM which detects cantilever deflections by reflecting a laser spot off the back of the cantilever into a split photodiode detector. Three samples were studied. Sample 1 was a formatted (16 Mbit/cm², 0.1 Gbit/in²) thermally textured glass substrate magnetic recording hard disk. Sample 2 was a specially written aluminum substrate magnetic recording hard disk [3]. The magnetic layer was 40 nm thick and had a magnetization $M_s = 6.5 \times 10^5$ A/m (8125 G) and coercivity $H_c = 1.4 \times 10^5$ A/m (1800 Oe). Sample 3 was a piece of written particulate media analog video tape supplied with our SPM. Imaging the small magnetic features of the particulate media provided a crude test of the resolution of our MFM tips.

Figure 1a shows a 10 $\mu\text{m} \times 10 \mu\text{m}$ force derivative MFM image of Sample 2 using a nominally 36 nm thick Fe₈₀(SiO₂)₂₀ coated tip. Figure 1b shows a similar image taken with a 100 nm Fe₈₀(SiO₂)₂₀ coated tip. Both tips were not intentionally magnetized. Simultaneous topography (not shown) and magnetic force derivative images were obtained in tapping mode and AC lift mode, respectively. The lift height L was 30 nm and the change in resonant frequency was

measured without feedback using FM detection. The most striking difference between the two figures is the different contrast for bit transitions. Fig. 1a is characteristic of a magnetically soft tip, with all bit transitions appearing as dark lines as the tip magnetization rotates to always give an attractive tip-sample interaction. Fig. 1b, however, is characteristic of a magnetically hard tip, as bit transitions give alternating light and dark contrast as the tip magnetization remains fixed. The thicker coated tip gave considerably higher sensitivity, as evidenced by the contrast scale (100 Hz vs 15 Hz full scale). Resolution of the thinner coated tip was at least a factor of 2 better than the thicker tip, in agreement with Babcock et al. [4]. We compared images of Sample 3 and found that the 36 nm thick $\text{Fe}_{80}(\text{SiO}_2)_{20}$ coated tips gave comparable resolution to commercial Co-Cr (30 nm) and permalloy (15 nm) coated tips.

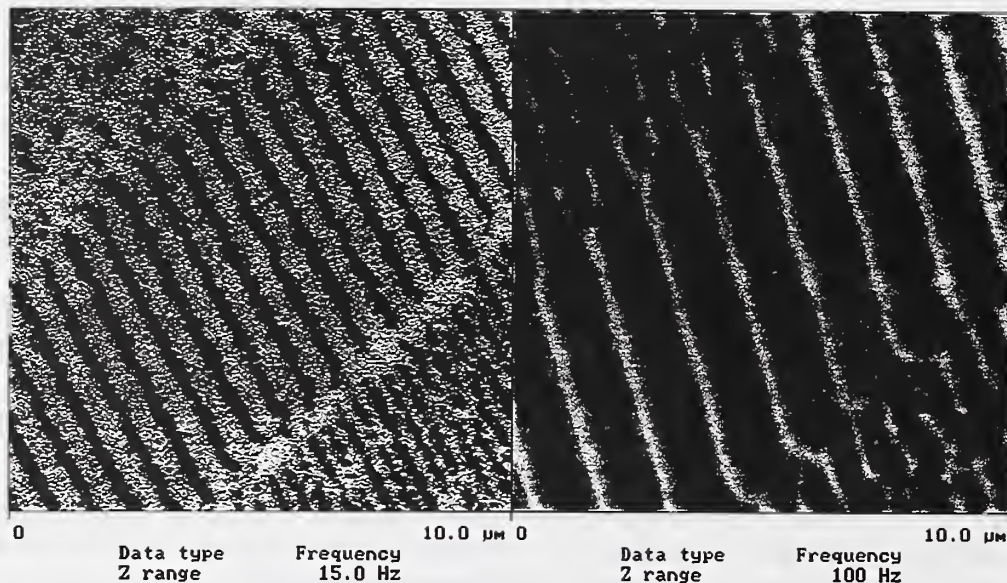


Fig. 1. 10 μm \times 10 μm force derivative MFM image of Sample 2 using $\text{Fe}_{80}(\text{SiO}_2)_{20}$ coated tips with nominal thicknesses of: a) 36 nm, b) 100 nm.

By lowering the Fe volume fraction we hope to make magnetically softer tip coatings, consisting of more completely isolated superparamagnetic Fe particles. Thin (20-40 nm) magnetically hard $\text{Fe}(\text{SiO}_2)$ tip coatings might also be possible by reducing the Fe volume fraction while increasing the particle size [1]. These corrosion and wear resistant tips would be useful for high resolution MFM imaging of hard magnetic samples which require tip coatings with high coercivities. In addition, the Fe volume fraction could be reduced further, allowing the possibility of having a single isolated small dipole near the apex of the tip and improving current MFM resolution limits.

References

- [1] S. H. Liou and C. L. Chien, *J. Appl. Phys.* **63**, 4240 (1988).
- [2] S. S. Malhotra, Y. Liu, J. X. Shen, S.H. Liou, and D.J. Sellmyer, *J. Appl. Phys.* **76**, 6304 (1994).
- [3] same hard disk studied by Paul Rice, Bill Hallett, and John Moreland, *IEEE Trans. Magn.* **30**, 4248 (1994).
- [4] K. Babcock, V. Elings, M. Dugas, and S. Loper, *IEEE Trans. Magn.* **30**, 4503 (1994).

^a Contribution of the National Institute of Standards and Technology, not subject to copyright.

Work at the University of Nebraska supported by NSF grant OSR-9255225.

An Atomic Force - Scanning Tunneling - Scanning Electron Microscope with a Novel Electron Beam Cantilever Deflection Sensor.

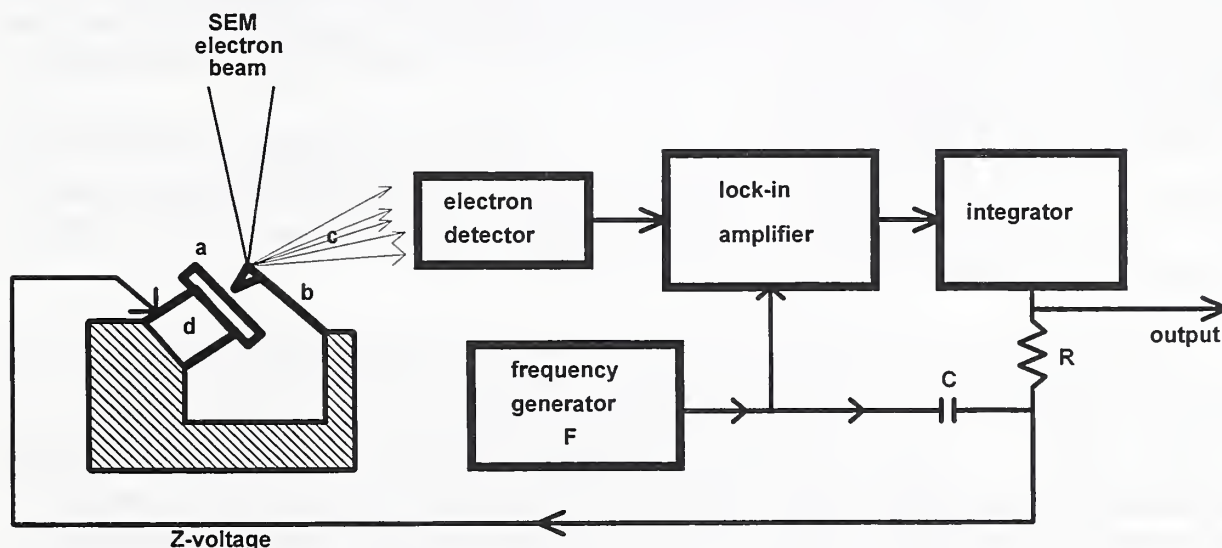
A.V. Ermakov, E.L. Garfunkel

Rutgers University, Dept. of Chemistry, Piscataway, NJ 08855-0939

An SEM, an STM and an AFM all yield a topographic image of a surface. The former differs from the latter two in their useful ranges and magnification. Our combination AFM/STM/SEM allows us to image a surface by scanning an area greater than 1 cm^2 by SEM, then zooming in to analyze this area by AFM or STM with resolution of several angstroms.

Conventional devices for measuring AFM cantilever deflection (e.g. optical methods) are somewhat complicated to use inside an SEM, and can readily degrade. Use of our novel method is an excellent solution to this problem providing both facile operation of the AFM inside an SEM and a constant and rapid method for tip inspection. Cantilever force and position are determined by using the focused electron beam and secondary electron detector of the SEM. The tip deflection is monitored by the secondary electron current using a lock-in method slightly off-resonance. Our method does not require any additional equipment such as laser optics or a capacitance position sensor.

The system consists of an SEM, an AFM/STM, their associated electronics, a frequency generator, a lock-in amplifier, and an integrator to provide AFM/STM feedback. The STM operates in a conventional mode. The block-diagram of AFM feedback is shown below:



The sample (a) is attached via a sample holder to an XYZ piezoelectric positioner, which, in turn, is rigidly connected to the base. An AC potential at the cantilever resonant frequency F (10-100 kHz) is applied through capacitor C to the Z piezoelectric translator (of the sample). The oscillating potential on the piezoelectric translator enhances the amplitude of the cantilever

oscillation because of mechanical coupling through the base and direct (through space) tip-sample interactions. The amplitude of the tip oscillation is about several angstroms. The SEM electron beam is focused on the edge of the cantilever, such that any deflection of the cantilever causes a change in the number of scattered electrons. Both static and dynamic changes in cantilever behavior are detected by the SEM electron detector. Decreasing the tip-sample distance increases the attractive tip-sample interaction (prior to contact), causes a measurable decrease in the cantilever resonant frequency and shifts the phase lag of the cantilever oscillation backward. The signal from the electron detector is sent to a lock-in amplifier, locked at a frequency F' . A phase-shift is chosen such that the output signal is zero when the distance between tip and sample is at a desired value. Any signal is thus an error signal, and this is the signal used for feedback. The error signal after filtering and integrating is applied through resistor R to the Z-piezoelectric translator. If the error signal is not zero, the integrator varies the output voltage until the tip-sample distance increases or decreases to the desired value. Thus the feedback loop, including the electron detector, lock-in amplifier, frequency generator and integrator, is intended to maintain a constant AFM tip resonance frequency, hence tip-sample separation.

The system has been experimentally tested on a variety of sample surfaces in both AFM and STM modes.

There are variety of fundamental and practical aspects of our design that limit the ultimate resolution. In the STM mode we are limited by vibrational noise - we obtain atomic resolution on graphite because our head is reasonably rigid. We have not yet incorporated sophisticated vibrational isolation needed to obtain atomic resolution on most elemental surfaces. We believe we are also vibrationally limited in the AFM mode. Ultimate resolution in the AFM mode may be limited by statistical noise. This can be estimated as follows: for a 300Å electron beam diameter, 1 nA e-beam current, and 1 kHz feedback bandwidth, the number of electrons hitting the cantilever during 10^{-3} sec is:
 $n = 10^{-9} \text{Amp} \cdot 10^{-3} \text{sec} / 1.6 \times 10^{-19} \text{coul.} = 6.25 \times 10^6$. The statistical uncertainty of the number of electrons is $\delta n = \sqrt{n}$. Thus the statistical uncertainty of cantilever position signal is $\delta s = (\delta n / n) \cdot 300 \text{ \AA} = 0.12 \text{ \AA}$. Some improvement may be gained by better focusing or higher currents, but care should be taken to avoid local heating.

Our system allows both an AFM or an STM to be used in combination with an SEM, thus providing a microscope with an extremely large dynamic range: $\sim 10^{-2} - 10^{-8} \text{m}$ SEM and $10^{-5} - 10^{-10} \text{m}$ AFM/STM. This system is of more general use than either a conventional AFM/STM or SEM. It offers an extremely powerful new microscopic imaging tool for a variety of diverse uses including semiconductor manufacturing process control and biological imaging. Images of a gold surface with nanometer resolution in the AFM mode, and graphite with atomic resolution in STM mode have been presented. Also we have estimated the ultimate resolution of our method (which may be limited by statistical noise), to be better than 1Å.

PART IIC: PARTICIPANTS LIST

FINAL PARTICIPANTS LIST

Second Workshop on Industrial Applications of Scanned Probe Microscopy National Institute of Standards and Technology Gaithersburg MD

May 2-3 1995

Phillip Abel
NASA-Lewis Research Ctr.
21000 Brookpark Rd.
MS 23-2
Cleveland, OH 44135
216-433-6063
FAX: 216-433-5170
msabel@lerc.nasa.gov

Ken Babcock
Digital Instruments, Inc.
520 E. Montecito St.
Santa Barbara, CA 93103
805-899-3380

William Barger
NRL
Chem. Div., Code 6177
Washington, DC 20375
301-767-3573
FAX: 301-767-3321

Winthrop Baylies
Baytech Group
30 Winsor Way
Weston, MA 02193
617-893-9919
FAX: 617-893-0313
75530.3553@compuserve.com

Greg Blackman
E.I. DuPont de Nemours, Inc.
Experimental Station,
E323/110B

Wilmington, DE 19880-0323
302-695-2415

Rene Blanquies
VLSI Standards, Inc.
3087 North First St.
San Jose, CA 95134-2006
408-428-1800 x.116
FAX: 408-428-9555

Susan Brandow
Naval Research Laboratory
4555 Overlook Ave.
Code 6900
Washington, DC 20375
202-404-6020
i:brandow@cbmse.nrl.navy.mil

Robert Brizzolara
NSWC-White Oak
10901 New Hampshire Ave.
Silver Spring, MD 20903
301-394-1394
FAX: 301-394-4472
brizzola@oasys.dt.navy.mil

Robert Celotta
NIST
Bldg. 220, Rm. B206
Gaithersburg, MD 20899-0001
301-975-3710
FAX: 301-926-2746
celotta@epg.nist.gov

Wei Chen
Motorola, Inc.
2200 W. Broadway Rd.
MD MD360
Mesa, AZ 85202
602-655-3766
FAX: 602-655-5013

Donald Chernoff
Adv. Surface Microscopy, Inc.
6009 Knyghton Rd.
Indianapolis, IN 46220
317-251-1364
FAX: 317-254-8690
echernof@ucs.indiana.edu

David Chung
Howard Univ.
Washington, DC
202-806-7903

Richard Colton
NRL
Code 6177
Washington, DC 20375-5342
202-767-0801
FAX: 202-767-3321
rcolton@stmz.nrl.navy.mic

John Dagata
NIST
Bldg. 220, Rm. A107
Gaithersburg, MD 20899-0001
301-975-3597
FAX: 301-869-0822
dagata@enh.nist.gov

Dan Dahlberg
Univ. of Minnesota
Dept. of Physics
116 Church St., SE
Minneapolis, MN 55455
612-624-3506

Angela Davies
NIST
Bldg. 220, Rm. B206
Gaithersburg, MD 20899-0001
301-975-3743
FAX: 301-926-2746
davies@epg.nist.gov

Gary DiBiase
Veeco Instruments, Inc.
Terminal Dr.
Plainview, NY 11803
516-349-8300 x.331

Alain Diebold
SEMATECH
2706 Montopolis Dr.
Austin, TX 78731
512-356-3146
FAX: 512-356-7640
alain_diebold@sematech.org

Ronald Dixon
NIST
Bldg. 220, Rm. A117
Gaithersburg, MD 20899-0001
301-975-4399
FAX: 301-869-0822
rdixon@enh.nist.gov

Walter Duncan
Texas Instruments, Inc.
P.O. Box 655936, MS 147
Dallas, TX 75265
214-995-3134
FAX: 214-995-7785
duncan@resbld.csc.ti.com

Alexel Ermakov
Rutgers Univ., Dept. of Chem.
P.O. Box 939
Piscataway, NJ 08855
908-445-2689
FAX: 908-445-5312
ermakov@rutchem.rutgers.edu

Chris Evans
NIST
Bldg. 220, Rm. A107
Gaithersburg, MD 20899-0001
301-975-3484

Joseph Fine
NIST
Bldg. 222, Rm. B248
Gaithersburg, MD 20899-0001
301-975-2545
jfine@enh.nist.gov

Joseph Fu
NIST
Bldg. 220, Rm. A117
Gaithersburg, MD 20899-0001
301-975-3495
FAX: 301-869-0822
jofu@enh.nist.gov

Andrew Gilicinski
Air Products and Chemicals, Inc.
7201 Hamilton Blvd.
Allentown, PA 18195-1501
610-481-5958

Joe Glancy
Digital Instruments
520 E. Montecito St.
Santa Barbara, CA 93103
805-899-3380
FAX: 805-899-3392
jglancy@di.com

Cynthia Goh
Univ. of Toronto
Dept. of Chem.
80 St. George St.
Toronto, Ontario, M5S 1A1
CANADA
416-978-6254

Richard Goodheart
Digital Instruments

501 E. Montecito St.
Santa Barbara, CA
800-873-9750

Joseph Griffith
AT&T Bell Labs.
Rm. 6F225
Murray Hill, NJ 07974-0636
908-582-5222
FAX: 908-582-2950

Gus Gurley
Digital Instruments
520 E. Montecito St.
Santa Barbara, CA 93103
805-899-3380
FAX: 805-899-3392
ggurley@di.com

Douglas Hansen
MOXTEK, Inc.
452 West 1260 North
Orem, UT 84057
801-225-0930
FAX: 801-221-1121
hansend@physcl.byu.edu

M.G. Heaton
Digital Instruments
520 E. Montecito St.
Santa Barbara, CA 93103
805-899-3380

Todd Hochwitz
Dartmouth College
Thayer School of Engineering
HB 8000
Hanover, NH 03755
603-650-1337
FAX: 603-646-3856
todd.hochwitz@dartmouth.edu

Peter Hopkins
NIST/Boulder
325 Broadway

MS 814.05, EEEL
Boulder, CO 80303
303-497-7894
FAX: 303-497-3725
hopkins@boulder.nist.gov

Steven Hues
NRL
Code 6170
Washington, DC 20375-5342
202-767-2671
FAX: 202-767-3321
hues@stm2.nrl.navy.mil

Richard Jackson
NIST
Bldg. 220, Rm. B322
Gaithersburg, MD 20899-0001
301-975-3401
FAX: 301-948-5668
jackson@nist.gov

Mark Johnson
Univ. of Maryland
Dept. of Physics
College Park, MD 20742
301-405-5985

Jan Jorgensen
NIST
Bldg. 220, Rm. A117
Gaithersburg, MD 20899-0001
301-975-3102
jjorgen@pyrolusite.nist.gov

Jay Jun
NIST
Bldg. 220, Rm. A117
Gaithersburg, MD 20899-0001
301-975-3516
jjun@enh.nist.gov

Michael Kahn
Tencor Instruments
3231 Scott Blvd.

Santa Clara, CA 95054
408-654-2349

M. Kamusewitz
GKSS Research Centre
GKSS Institute of Chemistry
Kantstrasse 55, D-14513
Teltow
GERMANY

Kenneth Kehrer
Armstrong World Industries, Inc.
R&D
P.O. Box 3511
Lancaster, PA 17604
717-396-5172

M. Keller
GKSS Research Centre
GKSS Institute of Chemistry
Kantstrasse 55, D-14513
Teltow
GERMANY

Daniel Koleske
Naval Research Lab.
9555 Overlook Ave.
Code 6177
Washington, DC 20375-5342
202-404-7547
FAX: 202-767-3321

Joe Kopanski
NIST
Bldg. 225, Rm. A305
Gaithersburg, MD 20899-0001
301-975-2089
FAX: 301-948-4081
kopanski@sed.eeel.nist.gov

John Kramar
NIST
Bldg. 220, Rm. A117
Gaithersburg, MD 20899-0001
301-975-3447

jak@enh.nist.gov

Mark Lagerquist
IBM Microelectronics Div.
D/B57, B/967-1
1000 River St.
Essec Jct., VT 05452-4299
802-769-1720
FAX: 802-769-3255
mlagerquist@vngt.ibm.com

Eric Liu
Gillette
One Gillette Park
Boston, MA 02127
617-463-3942
FAX: 617-463-4448

Jan Lorincik
NIST
80 B Bureau Dr., #327
Gaithersburg, MD 20899-0001
301-975-2345
lorincik@magpost.nist.gov

Henry Luftman
AT&T Bell Labs.
9999 Hamilton Blvd.
Rm. 2C-208
Breinigsville, PA 18031
610-391-2254
FAX: 610-391-2761

Lan Sueng Luo
Univ. of Minnesota
MINT
Minneapolis, MN
612-626-7781

Joe Luo
Texas Instruments
12203 SW Freeway
MS 733
Stafford, TX 77477
713-274-3492

FAX: 713-274-3555
jl原因@lead18.micro.ti.com

Martin Lutz
IBM Research Division
T.J. Watson Research Ctr.
P.O. Box 218
Yorktown Heights, NY 10598
914-945-3201
FAX: 914-945-2556
malutz@watson.ibm.com

David Mansur
OPTRA, Inc.
461 Boston St.
Topsfield, MA 01983-1240
408-887-6600

Herschel Marchman
Texas Instruments, Inc.
P.O. Box 655012
MS 944
Dallas, TX 75265

Mathew Mate
IBM Almaden Research Ctr.
650 Harry Rd.
MC K64
San Jose, CA 95120
408-927-2372
FAX: 408-927-2100

Tom McWaid
NIST
Bldg. 220, Rm. A117
Gaithersburg, MD 20899-0001
301-975-3466
FAX: 301-869-0822
mcwaid@enh.nist.gov

Brian Medower
Optex Communications
7 Research Ct.
Rockville, MD 20850
301-840-0011

FAX: 301-840-8917
brian@optex.com

Gregory Meyers
The Dow Chemical Co.
Analytical Sciences
1897 F Bldg.
Midland, MI 48674
517-636-4149

Howard Mizes
Xerox Corp.
800 Phillips Rd.
MC 113-23D
Webster, NY 14580
716-422-5079
FAX: 716-422-2126
mizes@wrc.xerox.com

John Moreland
NIST
Electronic & Electrical Eng. Lab.
325 Broadway, MS 814.05
Boulder, CO 80303
303-497-3641
moreland@boulder.nist.gov

Thomas Neal
DOD/MRI
9231 Rumsey Rd.
Columbia, MD 21045
410-964-0610
FAX: 410-964-0619

Martin O'Boyle
IBM
IBM, TJ Watson Research Ctr.
Rt. 134
Yorktown Hgts., NY 10598
914-945-3395
FAX: 914-945-2141
marty@watson.ibm.com

Sang-il Park
Park Scientific Instruments

1171 Borregas Ave.
Sunnyvale, CA 94089

D. Paul
GKSS Research Centre
GKSS Institute of Chemistry
Kantstrasse 55, D-14513
Teltow
GERMANY

Michael Perez
NIST
Bldg. 223, Rm. A256
Gaithersburg, MD 20899-0001
301-975-3670

Dan Pierce
NIST
Bldg. 220, Rm. B206
Gaithersburg, MD 20899-0001
301-975-3711
FAX: 301-926-2746
pierce@epg.nist.gov

Michael Postek
NIST
Bldg. 225, Rm. A347
Gaithersburg, MD 20899-0001
301-975-2299
postek@sed.eeel.nist.gov

Jim Potter
Maxtor Corp.
2190 Miller Dr.
Longmont, CO 80501
303-678-2330
FAX: 303-678-2125
jim_potter@maxtor.com

J. Jerry Prochazka
VLSI Standards, Inc.
3087 North First St.
San Jose, CA 95134-2006
408-428-1800 x.123
FAX: 408-428-9555

Carol Rabke
Burleigh Instruments, Inc.
Burleigh Park
Fishers, NY 14453
716-924-9355
FAX: 716-924-9072

Ruby Raheem
Advanced Micro Devices
MS 32, One AMD Place
P.O. Box 3453
Sunnyvale, CA 94086
408-749-3508
FAX: 408-749-8812
ruby.raheem@amd.com

B.L. Ramakrishna
Arizona State Univ.
SPM Facility
Ctr. Solid State Science
Tempe, AZ 85287-1604
602-965-6560
FAX: 602-965-2747
ramakrishna@asochm.la.asu.edu

Paul Rice
NIST/Boulder
MS 814.05
325 Broadway
Boulder, CO 80303
303-497-3841
FAX: 303-497-3725
ricep@boulder.nist.gov

Mark Rodgers
Digital Instruments
520 E. Montecito St.
Santa Barbara, CA 93103
805-899-3380
FAX: 805-899-3392
rodgers@di.com

Amin Samsavar
Tencor Instruments
3231 Scott Blvd.

Santa Clara, CA 95054
408-654-2465
FAX: 408-982-9654

Joyce Sapjeta
AT&T Bell Labs.
600 Mountain Ave.
Rm. 1A142
Murray Hill, NJ 07974
908-582-4750
FAX: 908-582-3999
joyce@allwise.att.com

David Schaefer
NRL
Chem. Div., Code 6170
Washington, DC 20375-5342
202-767-2671
FAX: 202-767-3321
dschaefer@stm2.nrl.navy.mil

Jason Schneir
NIST
Bldg. 220, Rm. A117
Gaithersburg, MD 20899-0001
301-975-3486
FAX: 301-869-0822
schneir@enh.nist.gov

Rick Schultz
Burleigh Instruments, Inc.
Burleigh Park
Fishers, NY 14453
716-924-9355
FAX: 716-924-9072

Allen Schultz
Seagate Technologies
7801 Computer Ave., S.
Minneapolis, MN 55435
612-844-7939

J. Sharma
Naval Surface Warfare Ctr.
Carderock Div.

Silver Spring, MD 20903-1394
301-394-1394
FAX: 301-394-4472

C.K. Shih
Univ. of Texas at Austin
Dept. of Physics
RLM 5.208
Austin, TX 78712

Tom Silva
NIST
MS 814.05
325 Broadway
Boulder, CO 80303
303-492-7826
FAX: 303-492-5316
silva@boulder.nist.gov

Rick Silver
NIST
Bldg. 220, Rm. A107
Gaithersburg, MD 20899-0001
301-975-5609

David Stadden
Armstrong World Industries, Inc.
R&D
P.O. Box 3511
Lancaster, PA 17604
717-396-5109

Joseph Stoscio
NIST
Bldg. 220, Rm. B206
Gaithersburg, MD 20899-0001
301-975-3716
FAX: 301-926-2746
joestro@epg.nist.gov

R. Marshall Stowell
IBM
1798 NW 40 Street
MC 2105
Boca Raton, FL 33432

407-443-9202

Yale Strausser
Digital Instruments
520 E. Montecito St.
Santa Barbara, CA 93103
805-899-3380
FAX: 805-899-3392
yale@di.com

Timothy Stultz
Sloan Technology
602 East Montecito St.
Santa Barbara, CA 93103
805-963-4431
FAX: 805-965-0522

Paul Sullivan
NIST
Bldg. 220, Rm. A117
Gaithersburg, MD 20899-0001
301-975-6386
sullypj@enh.nist.gov

Neal Sullivan
Digital Equipment Corp.
77 Reed Rd.
HC02-31N08
Hudson, MA 01749-2895
508-568-6876
FAX: 508-568-4681
nsullivan@astg.enef.doc.com

Dennis Swyt
NIST
Bldg. 220, Rm. A107
Gaithersburg, MD 20899-0001
301-975-3463
swyt@micf.nist.gov

E. Clayton Teague
NIST
Bldg. 220, Rm. A117
Gaithersburg, MD 20899-0001
301-975-3488

ecteague@enh.nist.gov

James Thorne
MOXTEK, Inc.
452 West 1260 North
Orem, UT 84057
801-225-0930
FAX: 801-221-1121

Vincent Tsai
NIST
Bldg. 220, Rm. A117
Gaithersburg, MD 20899-0001
301-975-4459
FAX: 301-869-0822
chieh@enh.nist.gov

David Turner
Naval Research Lab.
4555 Overlook Ave., SW
Code 6930
Washington, DC 20375
202-404-6021
FAX: 202-767-9594
dturner@cbmse.nrl.navy.mil

John Unguris
NIST
Bldg. 220, Rm. B206
Gaithersburg, MD 20899-0001
301-975-3712
FAX: 301-926-2746
unguris@epg.nist.gov

John Villarrubia
NIST
Bldg. 220, Rm. A117
Gaithersburg, MD 20899-0001
301-975-3958
FAX: 301-869-0822
villar@enh.nist.gov

Andras Vladar
NIST
Bldg. 225, Rm. A347

Gaithersburg, MD 20899-0001
301-975-2399
vladar@sed.eeel.nist.gov

Theodore Vorburger
NIST
Bldg. 220, Rm. A117
Gaithersburg, MD 20899-0001
301-975-3493
FAX: 301-869-0822
tvtv@enh.nist.gov

Michael Weber
Tencor Instruments
3231 Scott Blvd.
Santa Clara, CA 95054
408-654-2465
FAX: 408-982-9654
mikew@mtv.ten.com

Paul West
TopoMejrix
5403 Betsy Ross Dr.
Cupertino, CA 95054
408-982-9700
FAX: 408-982-9751

Grover Wetsel
The Univ. of Texas at Dallas
P.O. Box 830688
Richardson, TX 75083-0688
214-690-2974

Stan Yarboro
Park Scientific Instruments
1171 Borregas Ave.
Sunnyvale, CA 94089
408-747-1600

Michael Young
Veeco Instruments
602 E. Montecito St.
Santa Barbara, CA 93103
805-963-4431
FAX: 805-965-0522

Russell Young
NIST
Bldg. 220, Rm. A117
Gaithersburg, MD 20899-0001
301-975-3155

G.W. Zajac
Amoco Research Ctr.
P.O. Box 3011
MC B-5
Naperville, IL 60566-7011
708-961-7722
FAX: 708-961-6250
zajac@nap.amoco.com

